7-1-2010

Biological and Physical Analysis of Currents and Water Masses Off the Coast of Southeast Florida

Stephanie Healey
Nova Southeastern University

Nova Southeastern University Oceanographic Center

Biological and Physical Analysis of Currents and Water Masses Off the Coast of Southeast Florida

By

Stephanie Healey

Submitted to the Faculty of Nova Southeastern University Oceanographic Center in partial fulfillment of the requirements for the degree of

Master of Science with a specialty in:

Marine Biology and Coastal Zone Management

Nova Southeastern University

July 2010

Abstract

Biological and physical sampling of a 10km long, east-west transect was performed during 2007, off the coast of southeast Florida. Temperature and salinity measurements were recorded using a conductivity-temperature-depth (CTD) sensor, and current direction and magnitude measurements were recorded using an acoustic Doppler current profiler (ADCP). Zooplankton samples were collected, during the daytime, using a Tucker multiple net mid-water trawl, with 760μm mesh, at intended depths of ~25m and ~200m, at three stations along the transect. Laboratory analysis indicated that several currents and water masses influenced the density distribution of calanoid copepods and chaetognaths. During April and September 2007, a Subsurface Counter Current existed in conjunction with an offshore meander of the Florida Current. Physical data confirmed the presence of Continental Edge Water and Yucatan Water occupying different spatial and temporal scales, and the boundary between these two water masses existed as the western boundary of the Florida Current. Temperature and salinity profiles confirmed that the Subsurface Counter Current was composed of Continental Edge Water and not Yucatan Water. Therefore, the Subsurface Counter Current observed during the transect was not a cross section of a passing eddy caused by the meandering front of the Florida Current. Densities of both taxa were highest in the Subsurface Counter Current and the Intermediate water, while the lowest densities are found in the Florida Current. Calanoid copepod and chaetognath densities exhibited typical zooplankton trends for tropical and subtropical coastal waters. Densities were highly influenced by the physical parameters of each month. Highest densities were observed in April and the lowest in July/September, typically the nutrient limited season. Analysis by location showed that

the calanoid copepod and chaetognath densities were highest inshore and decreased offshore. The Florida Current exhibited the lowest densities for both taxa, while the Subsurface Counter Current and Intermediate water had higher densities. Previously documented southward flow had been associated with an offshore meander of the Florida Current, but during May and July there was a Subsurface Counter Current and an onshore meander of the Florida Current. Densities of both taxa were still lowest in the Florida Current. The stable isotope values of the zooplankton were skewed because of the preservation media and it was not possible to determine if the currents and water masses were isotopically different, and thus creation of a correction factor for the preservation effect was not possible. The $\delta^{13}C$ values were variable in magnitude and direction from the control for each taxon. The $\delta^{15}N$ values were less variable, but increased from the control, rather than decrease, as was expected for each taxon.

Keywords

zooplankton, Florida Current, stable isotopes, $\delta^{13}C$, $\delta^{15}N$, preservation

Acknowledgements

This project was funded by Calypso LN, LLC and GDF Suez Energy North America. Thanks to the crew of the R/V Walton Smith, of the University of Miami Rosenstiel School of Marine and Atmospheric Science, for the use of their equipment and their time and efforts during our sampling period. Thank you to the volunteers from the Florida Institute of Technology and Nova Southeastern University for their time and effort collecting the biological and physical data. Thank you to the Alaska Stable Isotope Facility at the University of Alaska Fairbanks and the Smithsonian Institution OUSS/MCI Stable Isotope Mass Spectrometry Facility for their processing of our stable isotope samples. A special thanks to my Advisor, Dr. Amy Hirons, for giving me an opportunity to participate in these research cruises, and for giving me an opportunity to work with these samples. Also, thank you for taking the time to help me work through those difficult moments when I was losing confidence in myself. Thank you to my committee members. Dr. Jonathan Shenker, thank you for your guidance on my project ideas at the beginning of this thesis project, and your helpful edits along the way. Dr. Alex Soloviev, thank you for your help with the synthesis of my physical data and for your helpful edits along the way. A special thanks goes out to my lab mates, Jessica Bostock, Madhura Mokashi, and Gabriela Wisniewski for their help with the zooplankton analysis and analysis of the physical data. Also, thanks for their unending emotional support throughout this whole project. A most special thanks to my family and friends for their unending support and confidence in my ability to complete my degree.

Table of Contents

List of Tables

List of Figures

1. Introduction

1.1. North Atlantic Ocean and the Gulf Stream

1.1.1. Current Transport

The water of the Florida Current originates in the low latitude North Atlantic/South Atlantic Ocean and joins the Gulf Stream to become part of the global thermohaline circulation, known as the Meridonal Overturning Cell (MOC). The Gulf Stream is western boundary current along the east coast of the United States. It is about 100km wide and velocities can exceed 2m/s, in contrast to currents on the eastern side of the gyre, which are over 100km wide and have velocities only reaching 0.25m/s. Its properties, in the northern hemisphere are due to the cyclonic rotation of the earth and the resulting Coriolis force that creates this anticyclonic gyre. Water from the North and South Atlantic oceans travel westward in the North Equatorial Current and divides into two parts. One part travels along the western edge of the Bahamas to join the Florida Current north of Bimini, Bahamas, and in full at Cape Hatteras. The other part enters the Caribbean Sea through the Windward Islands Passages and Leeward Islands Passages (The Lesser Antilles) and the Greater Antilles Passages (Stommel, 1966; Schmitz and McCartney, 1993; Johns et al., 2002; Colling, 2004). Johns et al. (2002) proposed a model that suggested the transport of water into the Caribbean was equally partitioned between these passages, ~10 Sv, ~8 Sv, and ~10 Sv, respectively (1 Sverdrup (Sv) = 10^6 m^3/s). The model also suggested that the seasonal transport variability of the Florida Current closely resembled that of the transport through the Windward Islands Passages, with the maximum during June/July and the minimum during October/November, having

an amplitude of 4 Sv (Johns et al. 2002). Flow through the Old Bahama Channel, Santaren Channel and Northwest Providence Channel add to the total transport of the Florida Current through the Florida Straits (Figure 1) (Atkinson et al. 1995; Lee et al. 1995; Wang and Mooers 1997; Johns et al. 2002). At Jupiter, Florida these passages provide direct connections between the Florida Straits and the subtropical gyre that flows northwest past the passages of the Lesser Antilles (Atkinson et al. 1995).

1.1.2. Water Masses

Potential vorticity, the angular momentum of water masses, as well as temperature and salinity, are acquired at the source of water mass formation and are assumed to be a conservative property as the water mass spreads and moves throughout the ocean basin. These variables are used to distinguish a certain water mass from another flowing along with it (Stommel, 1966). A variety of conservative and non-conservative water properties have been used to identify water masses. The most often used conservative measurements are temperature and salinity, but some semi-conservative tracers used are dissolved oxygen, nitrate and phosphate, dissolved inorganic carbon, and $\delta^{13}C_{(DIC)}$, $\delta^{13}C_{(sw)}$, and $\delta^{18}O_{(sw)}$ (Wennekens, 1959; Kroopnick, 1985; Bender, 1990; Silva et al., 2009; Bostock et al. 2010). The $\delta^{13}C_{(sw)}$ tends to follow the same trends as nutrient levels. Waters with low $\delta^{13}C_{(sw)}$ levels are found in conjunction with nutrient rich waters, and high $\delta^{13}C_{(sw)}$ levels are found in conjunction with low nutrient waters (Kroopnick, 1985; Lynch-Stieglitz and Fairbanks, 1994). The uptake of carbon into the calcite tests of those organisms that produces a calcite test is a good record of seawater $\delta^{13}C_{(sw)}$, with an accuracy of ±0.2‰ (Duplessy, J-C, et al., 1984; Lynch-Stieglitz and Fairbanks, 1994).

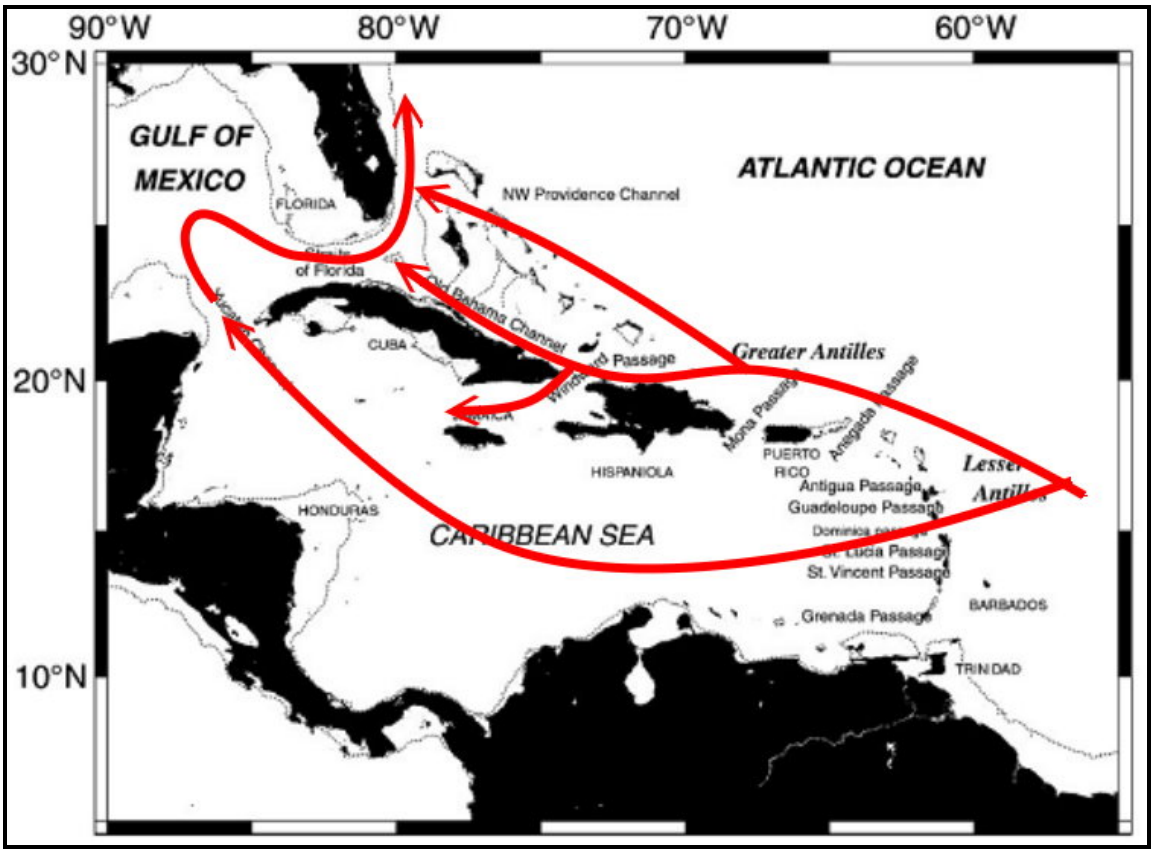

Figure 1. Map of the Caribbean Sea. The red arrows indicate the major transport pathways, contributing to the total transport of the Florida Current. The Leeward Passage in the Lesser Antilles includes the Anegada, Antigua, Guadeloupe, and Dominica passages, while the Windward Island Passage includes the St. Lucia, St. Vincent and Grenada passages. Figure is adapted from Johns et al. (2002).

North Atlantic Central Water is considered one of the most important water masses of the Gulf Stream as it occupies most of the upper 1000m. Its temperature ranges from 8°C to 19°C and its salinity ranges from 35.0‰ to 36.7‰. Another water mass which is considered important to the Gulf Stream system is the North Atlantic Deep Water, which has a temperature range of 2.2°C to 3.5°C and a salinity range of 34.90‰ to 34.97‰ (Stommel, 1966). The lowest calculated potential vorticity appear on the anticyclonic edge of the stream, and is most prevalent off Cape Hatteras, North Carolina, near where the "18°C water" is formed. A thick layer of 18°C water flows though the Northwest Providence Channel and a thinner layer flows through the Santaren Channel, and empties into the northern section of the Florida Current (Leaman et al. 1989).

1.2. The Caribbean Sea and the Gulf of Mexico

1.2.1. Current Transport

From the Caribbean Sea, the waters flow through the Yucatan Channel to the Gulf of Mexico, known as the Loop Current, then through the Florida Straits, to become what is known as the Florida Current. The transport model by Johns et al. (2002) estimates that contributions to the total Florida Current transport from the Caribbean Sea through the Yucatan Channel is about 28 Sv (Sverdrup: $1Sv = 10^6$ m^3/sec). Sheinbaum et al. (2002) recorded transport through the Yucatan Channel to be significantly less at 23.8 ± 1 Sv, suggesting that more systematic and long-term observations must be conducted in the area to determine the magnitude of variability. Variability in transport values over long time scales, for example climate-relevant, is small, while variation in the transport values on a monthly and seasonal basis is larger. Over the course of a 2-3 year period, variation in transport values in the southern Florida Straits and in the Caribbean Sea showed

fluctuations of only about 1 Sv, which seems to be linked to the changing sea level throughout the Caribbean (Schott and Zantopp 1985).

1.2.2. Eddies

In the Florida Current, cyclonic frontal eddies will occasionally form over the continental shelf along the northern boundary in the southern Florida Straits and western boundary in the northern Florida. Although the formation is not completely understood, it is associated with the offshore meandering cyclonic front and southward flowing warm Gulf Stream waters on the western edge of the current (Lee at al. 1981; Zantopp et al. 1987; Lee et al. 1995). When the Loop Current extends far into the Gulf the flow overshoots the Straits of Florida and enters on the southern side (Figure 2). In combination with cyclonic vorticity in this area, a cold cyclonic gyre forms. This gyre decreases in size as it travels to the east, mostly due to narrowing of the Straits When the Loop Current does not extend far into the Gulf of Mexico, the flow enters the Straits of Florida close to the Florida Keys leading to a strong downstream flow inshore with no gyre formation (Figure 3). (Lee et al. 1995).

1.3. The Florida Current

1.3.1. Current Properties

The Florida Current is a fast moving current that begins at the westernmost Florida Keys (83^{o}W) and then travels north between the east coast of Florida and the Bahama Bank to Jupiter, FL (27^{o}N). From the 28 Sv of transport from the Yucatan Channel, the Florida Current transport increases by about 3 Sv due to the flow from the Old Bahama Channel, most likely via the Santaren Channel, and from the Northwest Providence Channel (Atkinson et al. 1995; Johns et al. 2002). Most studies are in

agreement with an average transport value of the Florida Current off the southeast coast of Florida to be close to 32 Sv (Molinari et al. 1985; Leaman et al. 1987; Leaman et al. 1989).

A study done by Schmitz and Richardson (1968) examined the average transport along four transects across the Straits of Florida at Sombrero Key, Cat Cay (Bahamas), Miami/Bimini, and Ft. Pierce. Transport increased from 29.6 Sv at Sombrero Key to 32.2 Sv at Miami/Bimini, then 33.1 Sv at Ft. Pierce. Lee et al. (1985) and Leaman et al. (1987) recorded transport values at 27^{o}N to be 30.1 Sv and 31.7 Sv respectively. Based on the previous studies, Leaman et al. (1987) assumed that the increase in transport from south to north was due to inputs from the Northwest Providence Channel and was later confirmed by Leaman et al. (1995) while studying the transport into the Florida Current from the Santaren Channel and the Northwest Providence Channel. Through velocity and temperature measurements, it was estimated that each channel contributed 1.8 Sv and 1.2 Sv, respectively. This input contributes roughly 10% of the total transport downstream in the Florida Current.

A look at the annual variance in transport values at Jupiter, FL from 1982-1984 indicated a range of 8 Sv and a standard deviation of ± 1.5 Sv. An analysis of variance on a monthly scale showed a greater range in transport values (10 Sv) and higher standard deviation (± 2.5 Sv). During the summer months, transport values had the highest variance for the 10-30 day, 30-100 day and 100-180 day ranges, while the highest variances in the winter occurred during the 5-10 day, 10-30 day and 30-100 day ranges.

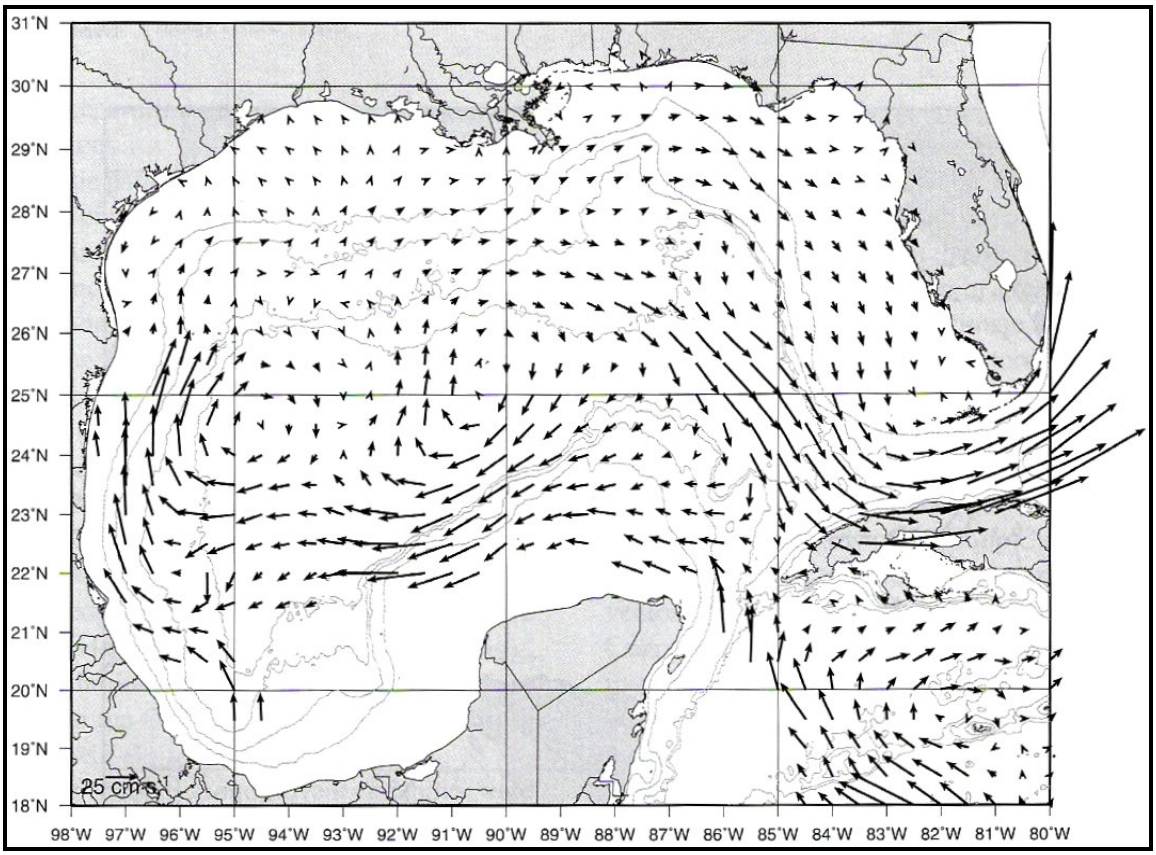

Figure 2. Near-surface velocity averages from 1989-1999 during the summer months (June-August). Velocity measurements indicate a large Loop Current, extending far north and west into the Gulf of Mexico during the summer. From DiMarco et al. (2005).

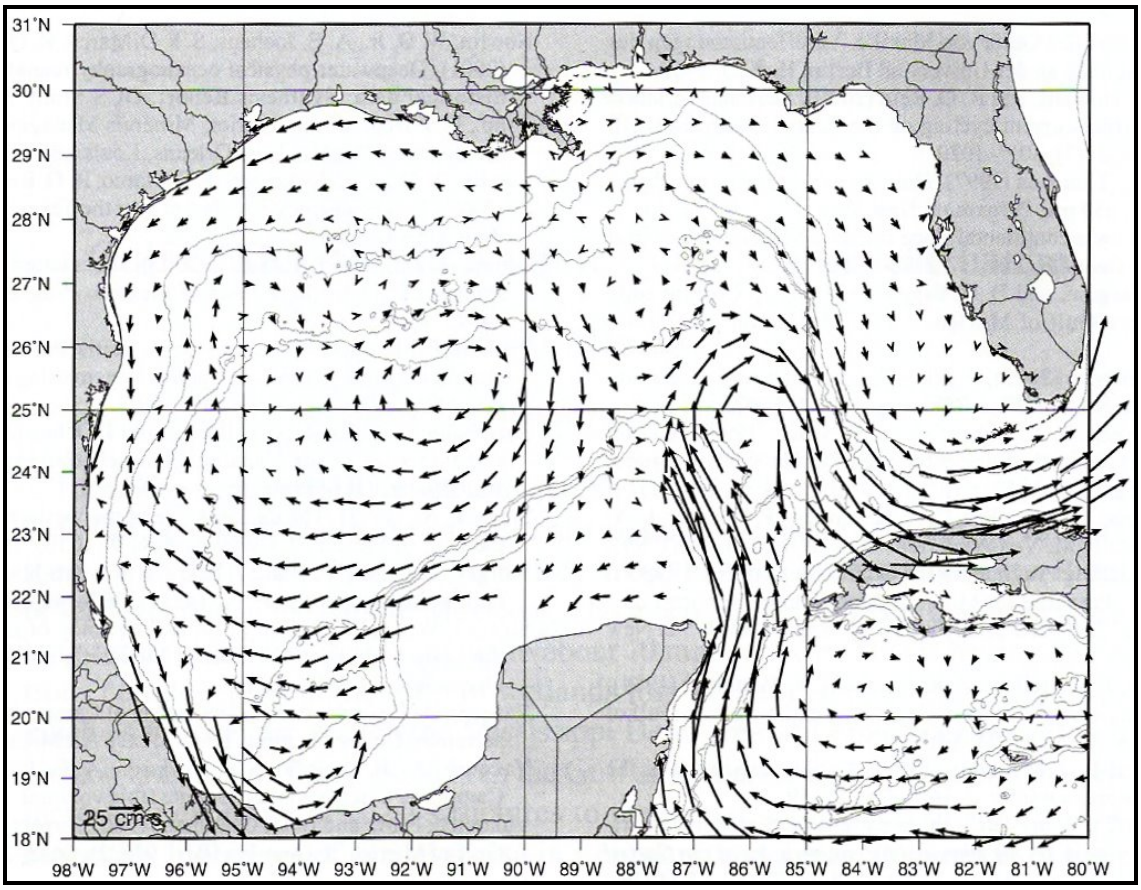

Figure 3. Near-surface velocity averages from 1989-1999 during the winter months (December-February). Velocity measurements indicate a small Loop Current that does not extend far into the Gulf during the winter. From DiMarco et al. (2005).

Overall, the winter months (November – April) showed the highest variance compared to summer (May – October). In regards to location, the highest variance occurred on the Florida Shelf, while the lowest variance occurred at the central axis of the Florida Current (Schott et al. 1988). Brooks (1979) observed axis meandering over a distance of 24 km (27 to 51 km off the Miami coast), which is approximately 30% of the entire passage width. The east-west meandering had a large effect on the transport at each stations, but less so on the total transport of the entire stream. Diurnal tides are responsible for up to 20% of the total transport variance on the Miami Terrace, while they account for almost 40% of the variance near the Bahama Bank. Semidiurnal tides are responsible for the total transport variance in the interior of the stream (Brooks, 1979).

An anomalous feature of the Florida Current is the spatial and temporal variability of its meandering from its central axis. Along the transects at Cat Cay, Miami and Ft. Pierce, Schmitz and Richardson (1968) observed meanders of the western boundary of the Florida Current with maximum amplitudes up to 5 km, whereas the meanders at Sombrero Key measured up to 15 km. However, Brooks (1979) observed that the axis of the Florida Current meandered over a range of 25 km off the coast of Miami on a timescale of a few days to two weeks. The variability in current velocity as well as the variations in individual station transport (not total current transport), mostly towards the western edge, was generally attributed to the east-west meandering of the central axis of the current (Brooks 1979; Johns and Schott 1987; Leaman et al. 1987).

Similar to the increase in average transport downstream, the velocity of the Florida Current also increases. The velocity of the current intensifies as it moves down stream mostly due to the narrowing of the channel in the Florida Straits and the shoaling

bottom topography, with a maximum depth greater than 2000 m at 83°W, decreasing to a depth of about 800 m at Jupiter, FL. Inflows from the Old Bahama Channel and the Northwest Providence Channel also add to the current's intensification (Leaman et al. 1987; Wang and Mooers, 1997). Records of velocities indicate the Florida Current moving at 1.8 m/s at 83°W and increasing to 2.0 m/s at Jupiter, FL (Wang and Mooers, 1997). An analysis of velocity data collected at this location indicates that velocity variability on the small time scale (one week) is just as large as the variability on an annual time scale, particularly on the western side of the current. The annual cycle indicates a maximum velocity during May and a minimum velocity during November, with amplitude of about 1 m/s. This amplitude decreases to only 0.5 m/s on the eastern side of the current (Leaman et al. 1987).

1.3.2. Meander and Eddy Formation

Zantopp et al. (1987) observed meanders as well as the formation of cold-core eddies along a transect of the Florida Current at Daytona, FL. Meanders are not isolated events but periodic events on a weekly timescale. Observations of the formation of cold-core eddies show a warm surface filament that extends across the shelf then curls cyclonically around a cold core. When the eddy is large enough, a southward flow can be produced, with some measurements reaching 50 cm/s. This southward flow is preceded by a strong onshore flow, and developed in conjunction with a large offshore meander of the Florida Current (Lee et al. 1981; Zantopp et al. 1987). Generally, the coastal shelf waters are cooler than the waters of the northward moving Florida Current. Water in these eddies is not trapped coastal water as in the cold core rings in the North Atlantic, but rather upwelled cold, nutrient rich North Atlantic Central Water (NACW).These

waters can be easily determined by T-S plots, as coastal water is lower in salinity (36.0 ‰) and tends to exhibit salinity stratification, while waters of the Gulf Stream are fairly uniform and have a higher salinity (36.5 ‰). The diameters of these eddies increase past Jupiter, Florida as the width of the continental shelf increases (Lee et al. 1981; Yoder et al. 1981).

1.3.3. Deep Water Flow Reversal

Another anomaly associated with the Florida Current is the presence of an aperiodic, deep-water flow reversal, flowing south, rather than north with the Florida Current. During the months of September and October 1972, May and October 1973 and January 1974, deep water flow reversals were detected in the Florida Straits off the coast of Miami (Stepien 1980). These flow reversals lasted anywhere between two and five days. Generally, when the flow is to the north, the cross-flow is to the east (offshore). When there are deep reversals to the south, the cross flow is to the west (onshore). Duing and Johnson (1971) also confirmed the presence of southward flowing deep water counter currents in the Florida Straits at a station 26 km east of Fowey Rock, off Miami in November 1970. In a vertical profile extending 500 m, southward flow was detected in the lower 100m of the water column and sustained a maximum velocity of 30 cm/s, while strong westward flow recorded a maximum 70 cm/s. No change in velocity or direction was detected in the water mass above the counter current. It was estimated that the southward flow constituted up to 11% of the transport in this area. Observations of southward flow were also made off the coast of Key Biscayne in January 1971, constituting approximately 25% of the transport in that area. Profiles of the water column on the east side of the Florida Current, near Bimini, indicated no southward flow.

Zantopp et al. (1987) observed southward flow as well, but they attributed this to the formation of an eddy. These southward flowing counter currents seemed to be only associated with western boundary (cyclonic front) of the Florida Current, and occupied the bottom of the water column following the bottom topography. Uncertainty exists as to the relation of these counter currents to eddies, but they are most likely caused by the meandering Florida Current.

1.3.4. Water Masses of the Florida Current

The water masses that affect the southern section of the Florida Current originate in the Caribbean Sea and the Gulf of Mexico, and only to a small extent, the waters of the Western North Atlantic. In the section of the Straits of Florida between the Florida Keys and Cuba, Yucatan Water is suggested to have North Atlantic origin water mixing with South Atlantic water. There is also evidence to suggest Antarctic Intermediate water infiltrates between 200m and 1000m, based on the salinity minimum. Yucatan water undergoes seasonal variation in the upper 200m, with summer salinity ranges between 35.9 to 36.6 ‰, and summer temperature ranges between 21 to 30^{o}C. Winter salinity ranges are between 35.9 to 36.6 ‰ and temperature ranges between 20 to 28^{o}C (Wennekens, 1959; Schmitz and Richardson, 1991; Schmitz and McCartney, 1993). Evaporation and seasonal cooling modify the upper 300m of the original Yucatan water, which create new water masses in the NW Gulf of Mexico. Not found in the Straits of Florida, but contributing to the water masses found there, is the Western Gulf Water. This water mass is formed in the Gulf of Mexico, west of a line drawn from the Yucatan Peninsula and the Mississippi delta. Seasonal temperature variations were observed but salinities remained constant (36.1-36.8 ‰, 22-29^{o}C, in the upper 100m) (Sverdrup et al.

1946; Wennekens, 1959). Continental Edge water is defined by the waters of the Eastern Gulf of Mexico between the northern and eastern edge of the Yucatan Peninsula and the coastal regions between the Mississippi delta and western tip of Florida. This water mass is hypothesized to be an intermediate water mass between the Yucatan and Western Gulf waters. Patterns of the T-S plots are not as homogeneous as the Yucatan water and Western Gulf water. Below 200m, the T-S plots are very similar to those of the Western Gulf water. The greater spread in salinity ranges are found in the upper 150m of the water column. Differentiation between Yucatan water and Edge water is found in the upper 300m. There is a seasonal difference in the Edge water mass, where summer salinity ranges from 36.1 to 36.7 ‰, and temperature ranges from 15 to 30^{o}C. Winter salinity ranges from 36.1 to 36.7‰, and temperature ranges from 11 to 26^{o}C (Fuglister, 1946; Pheleger, 1951; Wennekens, 1959).

The northern Straits of Florida, from Miami to north of Bimini, are characterized by well differentiated Continental Edge water and Yucatan water. Edge water has a very narrow T-S range in the upper 150m, also accompanied by large temperature and salinity fluctuations at the surface. Yucatan water has the same characteristics as previously described. There is very little temperature fluctuation in the upper 100m, but there is a disappearance of a salinity minimum. This is due to the constraints of the bathymetry which prevents intrusion of waters greater than 800m into this part of the Straits (Wennekens, 1959, Schmitz et al., 1993).

The boundary between the Edge water and the Yucatan water in the northern Straits is found approximately 16 km – 24 km from the east coast of Florida, about one-third the distance from Miami to Bimini. A cross channel transect showed that on the

Bimini side of the straits, a salinity maximum exists of 36.8 ‰ between 100-200m, characteristic of Yucatan water. Eight kilometers off Florida's east coast, T-S plots are characteristic of Edge water, with no salinity maximum, and the water is nearly isohaline at about 36 ‰ to over 100m. At stations approximately 16 and 32 km offshore, there are noticeable salinity variations between 50 and 200m. These stations are located near the meandering axis of the Florida Current; therefore, salinity variations may be explained by the meandering of the boundary edge between the Edge water and Yucatan water. Salinity fluctuations must be considered carefully as they are dependent on a spatial distribution that varies on a temporal scale. The continental margin of the Florida Current is characterized by Continental Edge water, and the insular margin is characterized by Yucatan water (Parr, 1938; Wennekens, 1959; Schmitz et al., 1993).

The meandering front of the Florida Current determines where the boundary exists for these two water masses. Seasonal temperature fluctuations occur from the surface to about 150m and vary between 25^{o}C and 28^{o}C (Bsharah, 1957; Wennekens, 1959). Temperature is highly variable between 50 and 100m, ranging from 13^{o}C to 23^{o}C, possibly indicating the location of the thermocline. The coldest water found in the Straits of Florida has been record at 7^{o}C, and has an origin in the South Atlantic and flows through the Caribbean Sea and out through the Straits (Schmitz and Richardson, 1991; Schmitz and McCartney, 1993). A water mass found in the Santaren Channel at the 24.5-27.0^{o}C layer is Subtropical Underwater (STUW). There is no indication that the 18^{o}C water, described previously, exists in the Florida Current before the flow reached the Santaren Channel. Maximum rate of transport increase is found in the 18^{o}C water layer

from Jupiter, FL downstream to Cape Hatteras, increasing from 4.5 Sv to 19.1 Sv (Leaman et al. 1989).

1.4. Marine Production

1.4.1. General Information

The majority of phytoplankton and zooplankton occupy the water column from the surface down to 75 to 200 m, dependent on light availability. There are estimates that these waters support 95% of marine primary production, and possibly 30% of the total global primary production (Daly and Smith, 1993). Low latitude ocean waters are characterized by high species richness, but lower biomass. From a basin-wide perspective, higher levels of chlorophyll exist along the coastal areas and areas of upwelling, and remain low in the subtropical gyres. High levels of chlorophyll indicate high levels of phytoplankton which generally translates to increased zooplankton biomass. Within these regions, phytoplankton and zooplankton exhibit a patchy distribution, both vertically and horizontally, as well as seasonal variations (Omori and Hammer, 1982; Legendre and Demers, 1984; Daley and Smith, 1993). Aggregations of zooplankton, which vary by species, age and size classes, can be caused by physical properties such as temperature and salinity gradients and water movement, as well as by biological properties such as the presence of food sources and predator avoidance, or seasonal-based spawning periods (Omori and Hammer, 1982, Steele; 1989).

1.4.2. Primary Production

Primary production tends to follow similar patterns of phytoplankton distribution. Primary production of a community is defined as the change in biomass over a period of time. Production is a function of the formation of new organic matter, and the additions

and losses due to respiration, sinking, grazing, diffusion and advection (Niebauer and Smith, 1989; Daly and Smith, 1993; Cowles et al. 1998). Primary production can be divided into two different types. New production is primary production from freshly upwelled nitrate as well as atmospheric nitrogen, and regenerated production is from ammonia that has been excreted by other organisms and converted into a useable form for primary producers (Eppley and Peterson, 1979; Mann and Lazier, 2006).

In the tropical waters and subtropical summer water, phytoplankton is generally nutrient-limited but can move within the water to overcome this limitation by regulating diffusion, regulating sinking rates, and turbulent motion of the water (Pasciak and Gavis, 1974, 1975). Savidge (1981) found that in some diatoms and flagellates, increased turbulence caused an increase in nitrogenous nutrient uptake and an increase in growth rate by 25-40% and 60%, respectively. In this in situ experiment, light levels may have been influenced by the turbulence, contributing to the results. Other studies (Pasciak and Gavis, 1975; Thomas and Gibson, 1990, 1992) have shown that diatoms tend to be positively affected by turbulence while dinoflagellates are negatively affected. It is difficult to determine the actual effect of turbulence when comparing different species, as the turbulence levels simulated in these multiple studies were sometimes outside of the range experienced in the natural ocean. Li (2002) examined different phytoplankton sizes and stratification as a proxy for different degrees of turbulence, finding that the greatest diversity was found in the intermediate degrees of stratification. When relating this to an ecological perspective, it is in accordance with the intermediate disturbance theory, which states that community diversity levels are the highest when environment is subjected to intermediate levels of disturbance (Mann and Lazier 2006).

1.4.2.1. Primary Production Estimates

Ryther (1969) synthesized the data collected by Schaefer (1965) and described different regions of the ocean as having different productivity. The open ocean, accounting for 90% of the total area, contributes up to 81.5% (16.3 PgC/yr) (1 Pg = 1 Petagram = $1x10^{15}$g) of the world's ocean primary production. The coastal waters over the continental shelf and areas of divergent fronts account for almost 10% of the total area and contribute to 18% (3.6 PgC/yr) of the world's ocean primary productivity. Finally, upwelling regions account for a very small fraction (0.1%) of the total area but contribute to 0.5% (0.1 PgC/yr) of the total primary production. Based on satellite near-surface chlorophyll measurements and local data on the chlorophyll maximum, Longhurst et al. (1995) were able to estimate the net global production to be 44.70 Pg C/year, more than double the estimates of Schaefer (1965). The total amount of global primary production is uncertain, but with better technology and methods of primary production estimation, total global production estimates are bound to change. What can be agreed upon is that when comparing primary production by total area in the world ocean, upwelling regions are the most productive regions. Waters over the continental shelf are the next most productive, and then the open ocean (Schaefer, 1965; Ryther, 1969; Pomeroy, 1974; Chavez and Barber, 1987; Laws et al. 1987; Platt et al. 1989; Longhurst et al., 1995).

1.4.3. Primary Consumers and Secondary Consumers

Even more uncertain than the primary production estimates are the global patterns of primary and secondary consumers, as zooplankton community structure is dependent on growth, reproduction, mortality and advection of each individual species. Zooplankton

densities are a good proxy for phytoplankton production as they are quick to use new food resources associated with phytoplankton blooms, and therefore, their seasonal patterns mirror the phytoplankton seasonal patterns, both peaking in late summer, for the shallow shelf waters as well in the deeper waters (Turner et al., 1979a). It was previously thought that primary consumers were large zooplankton such as copepods, mysids and euphausiids, but it has now been suggested that micro-plankton are the larger group of primary consumers. They are almost equal in biomass to the larger zooplankton, but have higher metabolic rates, meaning they transfer greater amounts of energy into the system. This complicates the ever expanding food web and makes it difficult to establish the role of lower trophic level organisms within it (Pomeroy, 1974).

Many different taxa of zooplankton are well described, but their spatial and temporal variations, as well as trophic position and mortality, are rather difficult to study. To complicate this situation further, advection by ocean currents and tidal flow transport in and species' transport out from certain regions (Iles and Sinclair, 1982; Daly and Smith, 1993). Boundaries between water masses, characterized by different temperature, nutrient levels, and/or current speed, tend to be areas of increased biological production. The types of fronts that tend to be associated with the highest levels of production are continental shelf-breaks, estuarine fronts, tidal fronts, and current boundaries (Steel, 1989; Daly and Smith, 1993).

1.4.4. Production on the Southeast Continental Shelf

The southeast continental shelf of the United States, and even more specific, the East Florida Shelf, is characterized by having generally low production, but blooms of phytoplankton, and consequently zooplankton, are known to occur. They are associated

with pulses of nutrients from coastal rivers and estuaries, as well as isolated upwelling events associated with frontal eddies (Haines and Dunston, 1975; Yoder et al., 1981). The continental shelf break at the 200m contour along the east coast of Florida, the East Florida Shelf (EFS), extends roughly 160 km along Miami-Dade, Broward, and Palm Beach counties, and extends an average of 6 km offshore, encompassing an area of 600 km^2 at a depth of 55m (Finkl et al., 2005). Beyond the EFS, the slope bathymetry drops to 800 m (Wang and Mooers, 1997). Processes occurring within estuaries can have affects on the plankton communities of the continental shelf. Seasonal patterns of estuarine primary production are mirrored by production on the continental shelf. As estuarine plankton are transported out to the shelf where there is an increase in light attenuation, primary production increases but then rates of primary production drop significantly just 10 km off shore. (Turner et al., 1979b).

It was once assumed that waters seaward of the shelf and bordered by the western edge of the Gulf Stream, were low in nutrients and relatively unproductive, but further studies of the cyclonic eddies formed along this region provide a different perspective. The western front of the Gulf Stream can be detected by a sharp temperature gradient (23^oC to 26^oC) with the Gulf Stream waters being warmer than the coastal waters. Water that is $>21^oC$, as well as slightly lower in salinity (36.0 ‰), along this front indicates the presence of upwelled, nutrient rich North Atlantic Central Water (NACW), in the core of the eddy. Highest chlorophyll levels (>4 µg/L) are detected in the cold, upwelled waters, and chlorophyll levels drop to 0.1 µg/L when upwelling is not present (Bishop et al. 1980, Yoder et al. 1981). Primary production levels ranged from 1.2-2.4 g C/m^2/day and assimilation ranged from 15 to 19 mg C/ mg Chl-a/ hour. At the highest level of recorded

primary production (6 g C/m^2/day), the depth of the euphotic zone was only 25-40m. The maximum concentration of diatoms observed was 1.8x10^6 cells/ L (Yoder et al. 1981). Assuming that an eddy passed by an area once every two weeks and the eddies were of similar size, Lee et al. (1981) calculated the estimated annual nitrogen input as well an annual production levels for the area that the eddy covered. In this case, Lee et al (1981) observed an eddy that was 225 km in diameter and waters with nitrate levels of 10µmol/L in an area that normally does not exceed 1µmol/L. Assuming a constant rate of nitrate influx, annual direct nitrogen input into the area was roughly 6.4 g N/m^2/yr. Since C:N ratios range from 5:1 to 10:1, theoretically, eddy passages could annually contribute 32-64 g C/m^2/yr to the area. Due to the eddy-forced upwelling of NACW on a time scale of weeks and resulting phytoplankton blooms, the southeast coast of the United States is an important area for secondary producers and larval species of consumers to develop (Yoder et al. 1981).

1.4.5. Study Species

1.4.5.1. Calanoid Copepod (phylum: Crustacea; subclass: Copepoda; order: Calanoida;)

Roughly 11,500 species of calanoid copepods are known, divided into 200 families and 1650 genera Within the order Calanoida, there are roughly 1800 species of marine copepods, encompassing 195 genera, most being pelagic species. They are one of the most numerous multi-cellular organisms on the planet. Copepods inhabit freshwater, brackish, and hypersaline environments. They are distributed vertically throughout the water column, and are found over the continental shelves as well as in the pelagic waters. Some species, generally the pelagic species, can withstand wide ranges of salinity and

temperature and can, therefore, be distributed throughout many geographical regions. Other species are somewhat limited in their tolerances and are confined to specific regions (Humes, 1994; Mauchline, 1998).

Copepods tend to aggregate at the vertical or horizontal front between different water masses. In coastal regions bordered by fast moving western boundary currents, such as the Gulf Stream, communities of copepods often become entrained in the cyclonic eddies, preventing them from being transported downstream (Ashjian, 1993; Piontkovski et al. 1995). Cross shelf flow and undercurrent velocity, coupled with diel vertical movement, determines if an organism stays over the shelf or moves offshore to continue transport downstream. Temperature and salinity gradients also play a role in dictating cross-shelf movement (Hopkins et al. 1981; Mauchline, 1998).

Copepod species at middle and higher latitudes tend to show more seasonality in their breeding than do those species in the lower latitudes. In high latitudes, several generations of copepods can exist within one breeding season, as generation times usually span a time frame of two weeks to two months, although some species have generation times upwards of a year or two (Diel and Tande, 1992; Mauchline, 1998). Periodicity of breeding can vary between species as well. Some breed continuously; some are discontinuous but breed over long periods of time; and some are sporadic breeders. Specifically in the lower latitudes, breeding appears to be continuous as abundance tends to be consistent, although there are peaks in abundance following phytoplankton blooms (Heinrikh, 1962).

Copepods are important to marine ecosystems because they provide a trophic link between phytoplankton and small fish, baleen whales, and many invertebrate species

(Frost, 1987). Availability of food resources, whether it be phytoplankton production for herbivorous species, or eggs and nauplii of other species of carnivorous copepods, can create a cascading effect in the larval production of other organisms, whether planktonic or benthic (Lonsdale et al. 1996; Mauchline, 1998). In a feeding study, *Acartia tonsa* selectively fed on organisms that were higher in protein content, even though smaller, less protein enriched organisms were present. This suggests that copepods selectively feed in order to maximize their nitrogenous ingestion (Cowles, 1988). When small scale turbulent events are introduced to the environment, copepod metabolism increases, most likely due to increased stimulation to the sensory organs, resulting in increased feeding and excretion rates (Alcaraz et al., 1994).

During a comprehensive zooplankton sampling regime from Cape Hatteras to southern Florida along the continental shelf, Bowman (1979) identified about 100 species of calanoid copepods. Bowman noted a clear zonation between inshore and offshore species. Also, the species richness tended to increase with increased distance from shore. To give an example of the extremes, at an inshore station, only *Acartia tonsa* was found, whereas at an offshore station, 42 species of copepod were found. *Acartia tonsa*, an estuarine species, and *Labidocera aestiva,* a coastal species, were the most predominant species found in the coastal assemblage. Particular to the cruise along the Florida coast, *Paracalanus parvus, Centropages furcatus, Eucalanus pileatus,* and *Labidocera aestiva* were the most dominant species in the shelf assemblages. Based on distribution patterns of all the other species found, they are classified in the oceanic assemblage. In the continental shelf waters, rarely were only shelf species found. Most often a combination of the coastal, shelf and oceanic species of copepods were collected (Bowman, 1979).

1.4.5.2. Chaetognath (phylum: Chaetognatha)

Roughly 100 species of chaetognaths exist. They are a fairly ubiquitous species in the world's oceans, occupying coastal and pelagic environments in both tropical and polar regions They are flat, transparent organisms, reaching lengths between 1 and 2cm, with their chitinous grasping hooks being one of its most identifiable structures (Casanova, 1999; Johnson and Allen, 2005). Chaetognaths play an important role in marine ecosystems, both as a predator and prey. They are voracious predators, with body size being the limiting factor in prey selection. Adults tend to feed primarily on copepods but have been known to feed on tintinnids, barnacle larvae, fish larvae and other chaetognaths. Newly hatched chaetognaths tend to prey on smaller organisms, especially copepod nauplii. High abundance of chaetognaths in coastal waters can have serious impacts on the copepods populations (Baier and Purcell, 1997; Johnson and Allen, 2005). Some species are also known to be cannibalistic (Casanova, 1999). In an in situ study done by Baier and Purcell (1997), they concluded that chaetognaths are more active feeders at night as the number of prey per chaetognath, determined from gut content analysis, was almost twice as great at night than during the day. Also, when Baier and Purcell (1997) compared these data with previous feeding rate information as well as with temperature data, they determined that the cooler temperatures caused a longer digestion rate and, therefore, lower feeding rate in the chaetognaths.

Breeding and spawning in tropical and subtropical waters is mostly uninterrupted, although rates of production can be influenced by biotic and abiotic changes within the environment. It is suggested that spawning is also determined by chemical stimuli from algae and diatom growth, an indication that there is a plentiful food supply for the larvae,

and chemical stimuli given off by the males and females to synchronize spawning behaviors (Alvarino, 1994).

Stepien (1980) examined the occurrence of chaetognaths in the Florida Current off the coast of Miami in the deep water flow reversals at roughly 600m. In addition to the twenty species described for that area, this study described five additional species. Vertical distribution of species was clearly defined in the epipelagic (0-200m), mesopelagic (200-600m), and meso-bathypelagic (>500-600m). Species were also zonally specific, with certain species occupying the neritic waters and others occupying the oceanic environment. When sampling different locations, the presence or absence of certain species can be used as an indicator of different water masses. The unusual co-occurrence of many epipelagic, mesopelagic and meso-bathypelagic species of chaetognath within the deep southward flow indicated that a down welling of coastal water may have occurred in association with the flow reversal. In addition to vertical distribution by species, there is also distribution by size. Chaetognaths in the larval and juvenile stages tend to occupy the surface water while adults will occupy the deeper waters below 225m (Alvarino, 1994).

1.5. Stable Isotopes in Ecology

1.5.1. General Information

The analysis of stable isotope ratios have been utilized to determine differences in terrestrial and aquatic systems; differences in freshwater, brackish water, and marine environments; and differences between coastal and open ocean environments. They have been used in a variety of ecosystem types to understand historical and present food web interactions, including the recreation of historical and present-day food webs for the polar

oceans (McConnaughey and McRoy, 1979; Hobson and Welch, 1992), for native species of freshwater lakes for potential restoration (Vander Zanden and Rasmussen, 2001; Vander Zanden et al., 2003), and effects of exotic species on local ecosystems (Vander Zanden et al., 1999). Tracking the changing stable isotope ratios of only a few organisms within an ecosystem can be used as a proxy for environmental changes whether it is on a small, seasonal scale or on a large, climatic scale. Stable isotopes can also be used to determine environmental changes along a spatial scale, including small scale from shelf water to oceanic environments, or ecosystems with large spatial scales, such as latitudinal differences (Rau et al. 1982; Rau et al., 1983; Schell et al., 1998; Perry et al., 1999). In the marine environment, this method has been used to determine ecosystem importance for organisms as small as zooplankton and benthic organisms, to larger species such as fish, mammals, and some apex predators.

The stable isotope ratios of carbon and nitrogen, $^{13}C/^{12}C$ ($\delta^{13}C$) and $^{15}N/^{14}N$ ($\delta^{15}N$), are commonly used to determine food web structure within an ecosystem. The ratios of these non-decaying, heavier to lighter isotopes give an indication of how energy is passed through the food web (DeNiro and Epstein, 1978, 1981; Minagawa and Wada, 1984; Hirons 2001). The heavier isotopes (^{13}C and ^{15}N) are preferentially conserved by the organism while the lighter isotopes (^{12}C and ^{14}N) are lost to the environment, leading to an enrichment of the heavier isotopes within the organisms with increasing trophic levels. The predator assimilates the heavier isotope of its prey into its tissues while respiring and egesting/excreting the lighter isotope. This is called the trophic enrichment factor (TEF) and is defined as $\Delta\ \delta$ (study isotope) = $\delta_{\text{animal}} - \delta_{\text{food}}$. Stable isotope ratios are always expressed in terms of the heavier to lighter isotope (Peterson and Fry, 1987;

Michener and Kaufman, 2007). Stable isotope analysis proves to be a more useful tool in estimating an organism's diet compared to gut content analysis, fecal content analysis and field/laboratory observations, as these methods represents a snap-shot in time while stable isotopes represent the diet over a period of time, particularly in the case of an opportunistic predator (Sholto-Douglas et al., 1991). The period of time in which the stable isotope ratios represent is dependent on the tissue turnover time. Age, tissue type and physiological state of an organism influence the metabolic rate and, in turn, affect the turnover rate. Zooplankton stable isotope ratios tend to represent the current environmental conditions, as they have a short life span and fast tissue turnover time. Stable isotope ratios of larger, longer-lived organisms will represent environmental conditions more in the past (Fry and Arnold, 1982; Tieszen et al., 1983; Sholto-Douglas et al., 1991). In situations where analyzing the entire body of an organism is not practical, multiple tissue types should be analyzed to determine the overall stable isotope composition of the organism and its diet, as it has be shown that different tissue types have different stable isotope values (DeNiro and Epstien, 1978, 1981).

1.5.2. Carbon ($\delta^{13}C$)

Differences in $\delta^{13}C$ values among organisms indicate a different source of carbon at the base of the food web from their respective environments, and can be identified by their origin (i.e.: marine, freshwater, terrestrial), or by the different photosynthetic pathways utilized by the primary producers (i.e.: C_3, C_4, CAM). In the marine environment, $\delta^{13}C$ values can be used to track movement of migratory species, and species entrained in a certain water mass (Schell et al., 1998). Carbon isotopic ratios are generally preserved between prey and predator, but can vary by 1-3‰. In some cases the

enrichment can be even higher and also vary by season. Since these values are highly variable and small between trophic level, the stable isotope values of carbon are not recommended for use in determining trophic changes in a particular food web, but rather aiding in determining the source of energy input into the system (Fry and Quinones, 1994).

When analyzing the isotopic carbon content of organisms with carbonate shells and bones, it is important to remember that the soft tissue will provide information on the diet while the bones and shells will provide information on the CO_2 which was dissolved in the water. It is also important to consider the biochemical components of the tissue being analyzed. Tissues and/or organisms high in lipid will have more negative $\delta^{13}C$ values than those low in lipids. This relationship tends to be transferred to the next trophic level as well (DeNiro and Epstein, 1978).

When comparing the $\delta^{13}C$ values across latitudes in the northern and southern hemisphere oceans, it was determined that change in temperature is not the only factor affecting carbon isotope composition, as each hemisphere showed different variations, although there was a very general trend of decreasing $\delta^{13}C$ values poleward. Different rates of lipid production as well as different rates of metabolism must be considered (Rau et al., 1982)

The utilization of $\delta^{13}C$ analyses is most useful in determining the diets of near shore organisms as the $\delta^{13}C$ values of terrestrial plants do not overlap with aquatic plants, as well as determining the contribution of C_3 and C_4 plants to a diet, since those values do not overlap either. The $\delta^{13}C$ values for C_3 plants range from -24‰ to -34‰, while the values for C_4 plants range from -6‰ to -19‰ (DeNiro and Epstein, 1978; Peterson and

Fry, 1987). In the marine environment, atmospheric CO_2 is at equilibrium with the bicarbonate CO_2 in the surface waters. The fractionation of this dissolved carbon gives marine phytoplankton $\delta^{13}C$ values between -19‰ and -24‰ (Sackett et al., 1965; DeNiro and Epstein, 1978; Rau et al., 1982; Fry 2006).

1.5.3. Nitrogen ($\delta^{15}N$)

The variations in $\delta^{15}N$ values within an ecosystem can be used to determine the trophic position of an organism. The $\delta^{15}N$ values are more enriched from prey to predator because $\delta^{15}N$ accumulates stepwise in the food chain, but values can vary between individuals of the same species fed the same diet, as well as vary between different species fed the same diet. All the tissue types of an organism are enriched relative to their diet, but vary significantly between each other.

In regards to the plant types, those that fix atmospheric nitrogen, for example blue-green algae in oligotrophic waters, will have lower $^{15}N/^{14}N$ ratios than those that assimilate inorganic nitrogen in the forms of ammonia and nitrate, like diatoms, in more nutrient rich waters. The $\delta^{15}N$ values from the oligotrophic East China Sea were low (-2.1‰) compared to the nutrient rich Bering Sea (5.6‰) (DeNiro and Epstein, 1981; Minagawa and Wada, 1984). Ultimately, $\delta^{15}N$ values of producers are dependent on the inorganic source of nitrogen and these values are enriched stepwise at every trophic level. The general stepwise enrichment is 3-3.4‰ per trophic level regardless of the nitrogen source or habitat, but the many deviations from this value indicate that there is no simple food chain in an ecosystem, but rather an expansive food web with different producers and varying feeding preferences/habits by consumers contributing to its complexity

(DeNiro and Epstein, 1981; Minagawa and Wada, 1984; Mullin et al., 1984; Schell et al., 1998).

1.5.4. Stable Isotope Ratios and Zooplankton

When examining carbon and nitrogen isotope ratios of zooplankton with regional differences, Fry and Quinones (1994) deduced that variations in the combinations of isotope ratios between the different regions was most likely due to the variations in phytoplankton types in the lower trophic levels. The $\delta^{13}C$ values were more variable in the coastal and shelf area, ranging between -18‰ and -24‰, compared to stations in the oligotrophic Sargasso Sea, having values ranging between -18‰ and -21‰.

Buskey et al. (1999) evaluated the variations of $\delta^{13}C$ in the copepod *Acartia tonsa* within an estuary over spatial and temporal scales. The $\delta^{13}C$ values were enriched by 4-8‰ in the summer months, compared to winter months. In keeping with the concept that differing $\delta^{13}C$ values indicate different carbon sources, Buskey et al. found that $\delta^{13}C$ values were enriched by 2-5‰ in *A. tonsa* collected over seagrass compared to those collected over muddy bottoms. Spatial differences, whether they be small on a scale of a couple kilometers or large on a scale of hundreds of kilometers, or temporal differences (i.e. seasonal), can be reflected in $\delta^{13}C$ values in zooplankton, allowing these stable isotope values to be used to determine different source carbon.

A comparison of the $\delta^{15}N$ values between these regions was less variable but there was a clear distinction between regions. Coastal and shelf values ranged between 5‰ and 8‰, where the open ocean values ranged between 2‰ and 4‰. Although regional values are evident, organism size is an important variable for all regions. Increasing size

generally led to increased trophic level based on the $\delta^{15}N$ values (Sholto-Douglas et al., 1991; Fry and Quinones, 1994).

Schell et al. (1998) observed 3‰ enrichment in $\delta^{15}N$ values from less carnivorous copepods and euphausiids to the more carnivorous chaetognaths, implicating different trophic positions between those organisms. When specifically looking at zooplankton (calanoid copepods and chaetognaths), Mullin et al. (1984) observed the reverse of what is expected when different organic nitrogenous nutrients are present for photosynthesis. It was previously expected that when NO_3^- is most readily available (compared to NH_4^+), the $\delta^{15}N$ values of the zooplankton will be low, yet Mullin et al. observed higher $\delta^{15}N$ values. Enrichment in $\delta^{15}N$ of the copepods and chaetognaths has been attributed to the increased levels NO_3^-, decreased levels of NH_4^+, and rapid turnover of nitrogen in the euphotic waters. The $\delta^{15}N$ values for zooplankton clearly define different trophic levels within the ecosystem, as well as identify different sources of nitrogen acquisition by the primary producers in the ecosystem, allowing these isotope values to be used for trophic determination as well as source determination.

1.6. Preservative Effects on Stable Isotope Ratios

The effect of chemical preservation methods on stable isotope results, especially $\delta^{13}C$, is still varied. A number of studies have focused on the effects of formalin and ethanol preservation methods on plant and animal tissues. In general, preservation in formalin generally led to a depletion in the $\delta^{13}C$ values of the organic material, specifically in marine and freshwater zooplankton (Mullin et al., 1984; Syvaranta et al., 2008), avian muscle (Hobson et al., 1997), fish muscle and other fish tissues (Bosley and Wainright, 1999; Kaehler and Pakhomov, 2001; Sarakinos et al., 2002; Sweeting et al.,

2004; Kelly, et al., 2006), a certain fruit fly species (Ponsard and Amlou, 1999; Sarakinos et al., 2002) and a species of kelp (Kaehler and Pakhomov, 2001). Some studies have found contradictory results with formalin preservation causing enrichment in $\delta^{13}C$ values, specifically in the Asian clam (Sarakinos et al., 2002) and freshwater zooplankton (Feuchtmayr and Grey, 2003).

Contradictory effects have occurred in both in the magnitude and direction of $\delta^{15}N$ values as a result of chemical preservation, but in most cases, regardless of direction, the change in the isotope ratio was less than 1‰. The few exceptions include the study by Bosley and Wainright (1999) which showed enriched juvenile winter flounder muscle tissue (1.21‰ for formalin, and 1.41‰ for formalin/ethanol combination) and enriched mud shrimp (2.49‰ for formalin, and 1.10‰ for formalin/ethanol combination).The study by Sweeting et al. (2004) showed an enrichment of 1.05‰ in the muscle tissue of the Atlantic cod for ethanol treatment only. The liver and roe were also analyzed, but did not show enrichment greater than 1‰.

Uncertainties exist as to how chemical preservative specifically affect the stable isotope ratios of the organic material. Bosley and Wainright (1999) suggested that chemical preservatives may promote the leaching of compounds rich in the lighter ^{14}N isotope and compounds rich in the heavier ^{13}C isotope to explain the enriched $\delta^{15}N$ and depleted $\delta^{13}C$ values in their study. The binding of lighter carbon from the preservatives with tissues (specifically formalin) and the hydrolysis of proteins could also cause depletion in the $\delta^{13}C$ values (Arrington and Winemiller, 2002; Edwards et al., 2002; Sarakinos et al., 2002; Kelly et al., 2006). The magnitude of the depletion may be due to

varying isotopic content of the preservatives from the manufacturer (Arrington and Winemiller, 2002).

Based on the discussion by Kelly et al. (2006), variations in the magnitude of the stable isotope ratio shift between chemically preserved organic materials, specifically fish tissue in this case study, and dried samples may be due to the different lipid types and the ratios of the lipid types within the tissue. Fish tissue contains phospholipids and free fatty acids, which are polar molecules, and triglycerides, which are non-polar molecules. These lipids of differing polarity react differently with different preservation media, specifically ethanol (a polar compound) and formalin (a non-polar compound).

Ethanol is responsible for removing the greatest proportion of lipids compared to formalin (75% versus 45%). Using calanoid copepods and cyclopoid copepods and Cladocera as the study organisms, Syvaranta et al. (2008) deduced that ethanol definitely acts as a lipid extracting agent, due to the enriched $\delta^{13}C$ values and the lower C:N ratio in preserved samples, as lipids are depleted in $\delta^{13}C$. The high variability in the effect of ethanol treatment on the copepods is due to the high variability in the lipid content of copepods.

It will be expected that if the study organisms are high in lipids, the ethanol treatments will show an increase in $\delta^{13}C$ values and relatively no change in $\delta^{15}N$ values as ethanol is a lipid extraction agent. If the study organisms are high in protein, the formalin treatments will show a decrease in $\delta^{13}C$ values, and will show relatively no change in $\delta^{15}N$ values since formalin does not remove protein, but rather binds to it.

2. Statement of Purpose and Hypothesis

2.1. Purpose

Ocean currents provide the primary means of transportation for holoplanktonic and meroplanktonic zooplankton, including the larvae of both pelagic and benthic species. These planktonic organisms are confined to the water mass they inhabit as they are not large or strong enough to cross the physical barriers that separate different water masses. Physical characteristics of water masses are defined by temperature, salinity, and current velocity and direction. Temporal and spatial variability exists for biotic and abiotic measures, such as spawning periodicity and environmental inter-annual variability.

The stable isotope ratios of zooplankton are used as a proxy for primary production, and production often varies between current boundaries and water masses (Bishop et al., 1980; Lee et al., 1981; Yoder et al., 1981). The purpose of this research is to examine (1) the characteristics of the zooplankton composition and densities, (2) stable isotope analyses of the zooplankton, and (3) changing physical parameters of the Florida Current, the inshore subsurface counter current, and the waters surrounding these water masses, along an east-west (E-W) transect off the coast of Fort Lauderdale, Florida. Sampling occurred during April, May, July, September and November in 2007, and sample data were analyzed from three stations designated inshore, middle and offshore. These results will contribute to the growing current scientific knowledge on the spatial and temporal variation of the water masses at this location.

2.2. Hypotheses

Zooplankton densities, stable isotope ratios and physical oceanographic measurements were utilized to test for distinct currents and water masses. Differences in these biotic and abiotic parameters were expected to exist between the different currents, previously defined by acoustic Doppler current profiler (ADCP) data, and different water masses, identified by temperature-salinity data collected by a conductivity-temperature-depth sensor (CTD), along an east-west transect of the East Florida Shelf.

Hypothesis 1 (H1): The subsurface counter current is biologically and isotopically different from the Florida Current and intermediate water

Hypothesis 2 (H2): The intermediate water is biologically and isotopically different from the Florida Current and the subsurface counter current.

Hypothesis 3 (H3): The Florida Current is biologically and isotopically different from the subsurface counter current and the intermediate water.

Hypothesis 4 (H4): Continental Edge Water is biologically and isotopically different from Yucatan Water.

Hypothesis 5 (H5): The western edge of the Florida Current delineates the vertical boundary between the Continental Edge Water and the Yucatan Water.

3. Materials and Methods

3.1. Biological and Physical Analysis of Currents and Water Masses

3.1.1. Study Site

A series of research cruises took place during April, May, July, September, and November of 2007 aboard the R/V *F.G. Walton Smith*. Zooplankton samples and physical measurements of the water masses surrounding the E-W transect were collected

on every cruise. The 10 km long transect was located 6.5 km off the coast of southeast Florida at 26.2^{o}N, and ranged from 80.03^{o}W to 79.93^{o}W. The inshore station was located 6.5 km offshore (~80.035^{o}W), over a water depth of ~200m, the middle station was 12.5 km offshore (~79.975^{o}W), over a water depth of ~250m, and the offshore station was located 16.5 km offshore (~79.933^{o}W), over a water depth of ~300, all located over the East Florida Shelf (Figure 4).

3.1.2. Physical Data Collection

Acoustic Doppler current profiler (ADCP) data were collected during each cruise and was used to define direction and velocity of the currents present along the E-W transect. Conductivity-Temperature-Depth (CTD) data were collected in conjunction with each tow and verified the tow depth. These data provided information to determine the depth of the thermocline and possible halocline; and were also used to construct temperature-salinity (T-S) plots used to determine water masses along the transect. A continuous water flow-through system aboard the *R/V F.G. Walton Smith* collected sea surface temperature (^{o}C), surface density (kg/m3), and a relative fluorescence measurement along the entire cruise track. Water was sampled from a depth of 1m.

3.1.3. Zooplankton Collection

Daytime zooplankton tows were conducted at the inshore, middle and offshore stations along the E-W transect at intended depths of 25 m (Shallow) and 200 m (Deep). Three different net types were used at each station. A bongo net with 202µm and 335µm mesh was deployed at each intended depth. A Tucker multiple net mid-water trawl, with 760µm mesh, was deployed to the intended depth of 200 meters. Due to the large mesh size of the Tucker trawl, many smaller organisms passed through the nets, and the

densities reported indicated counts of the larger and adult organisms. Net A collected samples from 0-25 meters, net B collected samples from 25-200 meters, and net C collected samples from 200-0 meters. A 0.6 m ring net was deployed to a depth of 10 meters. Samples from the bongo net and Tucker trawl nets were immediately preserved in 5% seawater buffered formalin, and then transferred to 70% ethanol for long-term storage once at the laboratory. Samples collected in the ring net were immediately frozen for long-term storage. Flow meters were attached to each of the bongo and Tucker net openings to record the volume of water flowing through the nets which was used to calculated zooplankton density. A separate study specifically intended to determine the effect of preservation media, on both δ13C and δ15N values, was also performed. In November 2008, zooplankton samples were collected along the continental slope off the coast of Miami. Samples were collected using a Multiple Opening/Closing Net and Environmental Sampling System (MOCNESS) with 335µm mesh nets. Samples from 3 nets were immediately frozen in a standard -20oC freezer in 500ml high-density polyethylene bottles prior to analysis in the laboratory.

3.1.4. Laboratory Analysis

Zooplankton samples were sorted and counted to determine composition and density, as well as frozen samples analyzed for $\delta^{13}C$ and $\delta^{15}N$, to assess the biological and biochemical differences of the water masses. Analysis of samples collected at depth from the inshore station, offshore station and middle station provided information on the properties of the inshore Subsurface Counter Current, the Florida Current, and the Intermediate water between the two water masses. Biological, biochemical, and physical information, was used to describe the similarities and differences of these water masses.

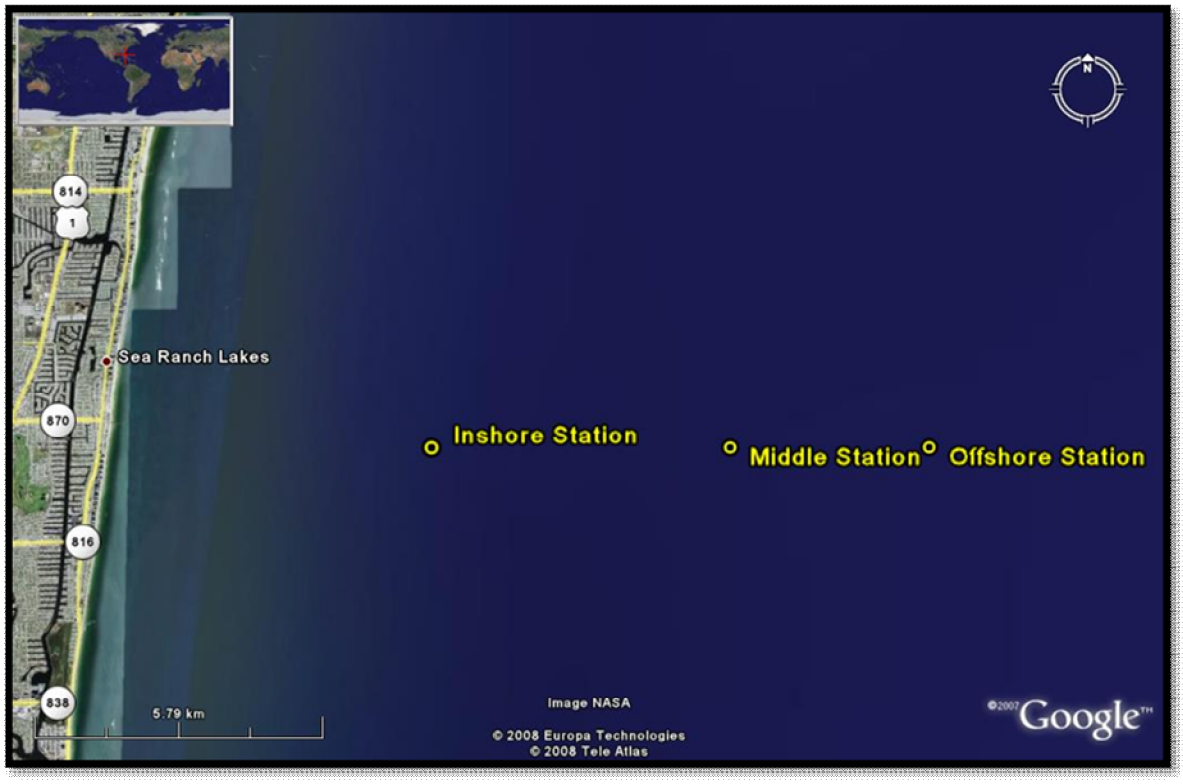

Figure 4. Map of stations sampled along the East-West transect in April, May, July, September, and November 2007.

3.1.5. Stable Isotope Analysis

Zooplankton samples collected from the Tucker trawl net A (0-25m) and net B (25-200m) were sorted for stable isotope analysis. Tucker trawl samples ensured that no mixing of plankton from the upper water mass and the water mass at depth occurred. Based on a preliminary analysis of four samples from four different months, it was determined that zooplankton from the order Calanoida and the phylum Chaetognatha were most abundant zooplankton in the four samples analyzed, with calanoid copepods composing greater than 39% of the total abundance and chaetognaths composing greater than 18% of the total abundance for most samples.

Samples collected for the preservation study were slowly thawed in tepid water in the laboratory immediately prior to analysis. Zooplankton samples from each net were sorted for calanoid copepods and chaetognaths. Only completely intact and whole organisms, as well as non-gravid females, were selected for preservation. A bulk zooplankton sample, which includes the previously defined study species, and all other taxa collected in the nets, was collected for analysis. The samples were treated using four preservation methods: 1) Frozen (Control), 2) 70% Ethanol, 3) Formalin, 4) Formalin fixed then transferred to 70% Ethanol. The frozen sample was used as the control for this experiment. The entire preservation treatment lasted 6 weeks. The Formalin/Ethanol treated samples were treated in formalin for 1 week and then transferred to 70% Ethanol for 5 more weeks (Figure 5).

All preserved organisms for stable isotope analysis were rinsed in distilled water to remove the excess preservative. The samples were dried at 60^{o}C in a drying oven for a minimum 96 hours to evaporate any water. The samples will then be fumed with

concentrated HCl for 24 hours in order to eliminate the inorganic carbon structures in the zooplankton. For the samples collected along the E-W transect, approximately 0.2-0.4 mg of dried sample was placed in a tin capsule for stable isotope analysis at the Alaska Stable Isotope Facility at the University of Alaska Fairbanks. For the samples collected for the preservation study, between 0.6 and 0.8 mg of sample were weighed and packed into aluminum tins in preparation for analysis at the Smithsonian Institution OUSS/MCI Stable Isotope Mass Spectrometry Facility. The samples were run on a Thermo Delta V Advantage mass spectrometer in continuous flow mode, coupled to a Costech 4010 Elemental Analyzer (EA) via a Thermo Conflo IV. Sample standards include USGS40 (L-glutamic acid), USGS (L-glutamic acid), and Costech acetanilide. The $\delta^{13}C$ and $\delta^{15}N$ notation is derived from the equation:

$$\delta X\ (‰) = (R_{sample} / R_{standard} - 1) \times 1000$$

where X is the isotope being evaluated and R_{sample} is the ratio of the heavy isotope to the lighter isotope. Reproducibility for the standards is <0.2‰ (1σ) for both $\delta^{13}C$ and $\delta^{15}N$. These results were used to determine if a correction factor could be created and applied to previously preserved samples in order to establish the natural stable isotope values.

3.1.6. Statistical Analysis

Statistical tests were performed to determine the differences in zooplankton density, and the differences in the stable isotope values on a spatial and temporal scale (Month, Location, Depth, Month*Location, Month*Depth, and Location*Depth). Statistical tests were then performed on the data sets defined by the physical properties of the water from the physical data collected by the ADCP and CTD sensor. The Shapiro-Wilk's test of normality was used to determine if the variables were normally distributed

and to determine if parametric or non-parametric analyses should be employed. The Kruskal-Wallis ANOVA by Ranks was used for the analyses involving the non-parametric data.

The Kruskal-Wallis ANOVA by Ranks is not as powerful as the ANOVA because it does not assume normally distributed data and, therefore, if no significant differences exist, it cannot be assumed that the populations are identical. The one-way ANOVA was used to compare the differences between parametric sets of data. Multiple comparison analysis was used to determine specific differences as a post-hoc analysis for the Kruskal-Wallis ANOVA by Ranks. The Tukey post-hoc analysis was used to determine specific differences for the one-way ANOVA. At times, the Kruskal-Wallis ANOVA by Ranks showed a significant difference, but the multiple comparisons showed no difference between groups. According to Daniel (1990) the multiple comparisons approach uses the experiment-wise error rate, which is a conservative approach. Tukey HSD is a less conservative post-hoc analysis, and it was used to evaluate where the statistical differences may lie. When the one-way ANOVA results showed a significant difference, but the Tukey did not show between which groups the differences were, the less conservative Fisher LSD was used as the post-hoc analysis.

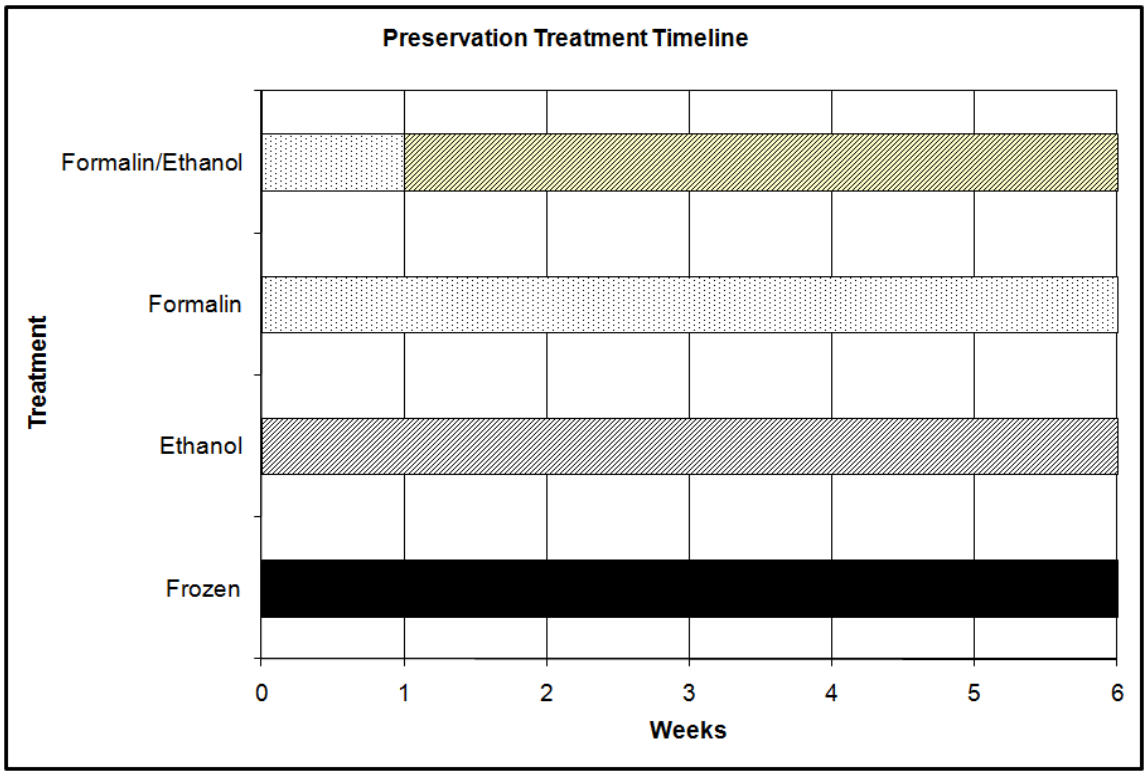

Figure 5. Illustration of the preservation timeline. 1) Frozen treatment (solid), 2) 70% Ethanol treatment (hash marks), 3) Formalin treatment (dotted).

4. Results

4.1. Preservation Effect Results

4.1.1. Carbon Isotope Ratios - δ13C

Each preservation media led to an increase in mean δ13C values in calanoid copepods, chaetognaths, and the bulk samples, when compared to the control, except for the formalin treatment in the bulk sample. Calanoid copepod sample δ13C values increased from formalin, to ethanol, to formalin/ethanol only. Chaetognath sample δ13C values increased from formalin, to formalin/ethanol, to ethanol only. For bulk sample values, formalin decreased and sample values increased from formalin/ethanol to ethanol only. When compared to the control value, calanoid copepod enrichment ranged from 0.23‰ to 0.73‰; chaetognath enrichment ranged from 0.06‰ to 1.77‰, and the bulk sample change ranged from -0.72‰ to 0.62‰ (Table 1, Figure 6). Shapiro-Wilk's test of normality indicates that $\delta^{13}C$ values are normally distributed for all taxa and parametric methods should be used for further statistical analyses (Table 2). One-Way ANOVA results indicate that there was a significant difference in mean $\delta^{13}C$ values between treatment types for calanoid copepods and chaetognaths but not for the bulk zooplankton sample ($p=0.014$, $p=0.001$, $p = 0.131$, $\alpha = 0.05$, respectively). Tukey HSD Post-hoc test showed significant differences in calanoid copepod tests, specifically between frozen*ethanol, and frozen*formalin/ethanol treatments ($p = 0.032$, $p=0.024$, $\alpha = 0.05$, respectively). Tukey HSD Post-hoc test for chaetognaths show the specific treatment differences were specifically between frozen*ethanol, frozen*formalin/ethanol, ethanol*formalin, and formalin*formalin/ethanol treatments ($p=0.002$, $p=0.014$, $p=0.002$, $p=0.018$, $\alpha = 0.05$, respectively) (Table 3).

4.1.2. Nitrogen Isotope Ratios - $\delta^{15}N$

Each preservation media led to an increase in mean $\delta^{15}N$ values in calanoid copepods, chaetognaths, and the bulk zooplankton samples, when compared to the control. The bulk sample values increased from formalin/ethanol, to ethanol, to formalin. Calanoid copepod sample values increased from formalin to formalin/ethanol, to ethanol. Chaetognath sample values increased from formalin/ethanol, to ethanol, to formalin. Compared to the frozen control, calanoid copepod change ranged from 0.72‰ to 0.81‰, chaetognath change ranged from 1.34‰ to 2.20‰, and the bulk sample change ranged from 0.41‰ to 0.95‰ (Table 4, Figure 7). Shapiro-Wilk's test of normality indicates that $\delta^{15}N$ values are normally distributed for all taxa and parametric methods should be used for further statistical analyses (Table 5). One-Way ANOVA results indicate that there was a significant difference in mean $\delta^{15}N$ values between treatment types for chaetognaths but not for calanoid copepods or the bulk zooplankton sample ($p=0.001$, $p=0.205$, $p=0.387$, $\alpha = 0.05$, respectively). Tukey HSD Post-hoc test showed that for chaetognaths, the specific treatment differences were specifically between frozen*ethanol, frozen*formalin, and frozen*formalin/ethanol treatments ($p=0.003$, $p=0.029$, $p=0.002$, $\alpha = 0.05$, respectively) (Table 6).

Table 1. Mean δ13C values for each treatment and their deviation from the Control Frozen.

Mean $\delta^{13}C$ Values by Treatment						
		N	**Mean (‰)**	**SD**	**Δ Control (‰)**	**Effect**
Calanoid Copepod	Ethanol	3	-20.23	0.31	0.69	Increase
	Formalin/EtOH	3	-20.19	0.10	0.73	Increase
	Formalin	3	-20.69	0.27	0.22	Increase
	Frozen (C)	3	-20.91	0.22	-	-
Chaetognath	Ethanol	3	-18.18	0.19	1.77	Increase
	Formalin/EtOH	3	-18.74	0.62	1.22	Increase
	Formalin	3	-19.89	0.18	0.06	Increase
	Frozen (C)	3	-19.95	0.25	-	-
Bulk	Ethanol	3	-19.95	0.64	0.62	Increase
	Formalin/EtOH	3	-20.12	0.27	0.45	Increase
	Formalin	3	-21.29	1.02	-0.72	Decrease
	Frozen (C)	3	-20.57	0.44	-	-

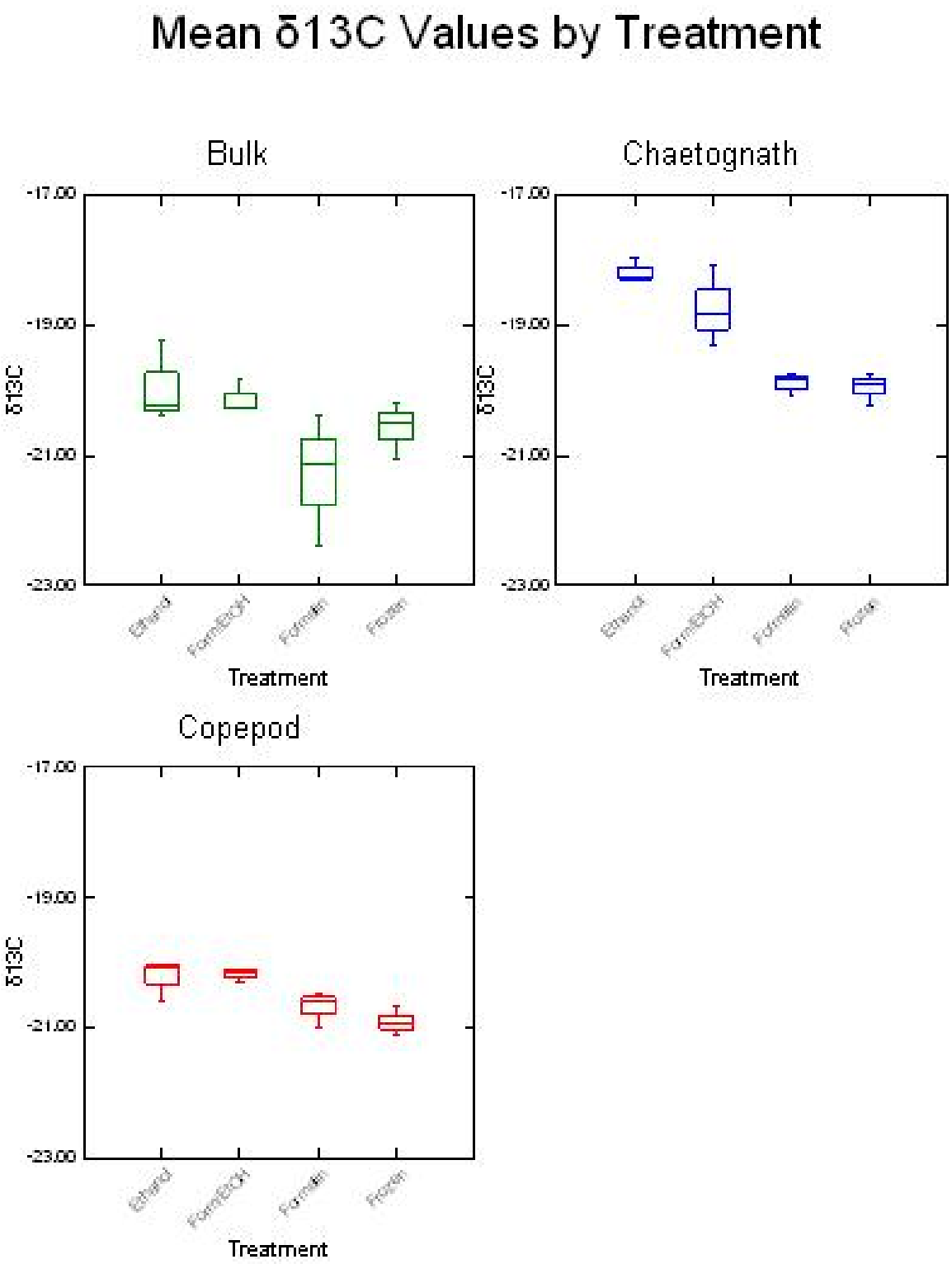

Figure 6. The $\delta^{13}C$ values (‰) and one standard deviation for all taxa and all treatments. The box indicates the values of the first quartile, median, and third quartile. The whiskers indicate the next values below the first quartile and above the third quartile.

Table 2. Shapiro-Wilk's test of normality of $\delta^{13}C$ for each taxa. P values < 0.05 are considered not normally distributed.

Shapiro-Wilk's Test of Normality for $\delta^{13}C$

$\alpha = 0.05$, p value

	p value
Bulk	0.101
Calanoid Copepod	0.338
Chaetognath	0.070

Table 3. One-way ANOVA and Tukey HDS Post-hoc results comparing $\delta^{13}C$ values between each preservation type for each taxa. P values < 0.05 indicate a significant difference.

One-Way ANOVA $\delta^{13}C$ By Treatment

$\alpha = 0.05$

	H/F Value	**p value**
Calanoid Copepod	(3, 3) = 6.658	0.014
Chaetognath	(3, 3) = 17.933	0.001
Bulk	(3, 3) = 2.528	0.131

Tukey HDS Post Hoc Analysis

$\alpha = 0.05$

Dependent Variable	**Treatments**	**p value**
Calanoid Copepod	Frozen (Ethanol)	0.032
	Frozen (Formalin/EtOH)	0.024
Chaetognath	Frozen (Ethanol)	0.002
	Frozen (Formalin/EtOH)	0.014
	Ethanol (Formalin)	0.002
	Formalin (Formalin/EtOH)	0.018

Table 4. Mean $\delta^{15}N$ values for each treatment and their deviation from the Control.

Mean $\delta^{15}N$ Values by Treatment						
		N	**Mean (‰)**	**SD**	**Δ Control (‰)**	**Effect**
Calanoid Copepod	Ethanol	3	3.56	0.23	0.82	Increase
	Formalin/EtOH	3	3.53	0.72	0.79	Increase
	Formalin	3	3.45	0.84	0.71	Increase
	Frozen (Control)	3	2.74	0.56	-	-
Chaetognath	Ethanol	3	5.14	0.40	2.07	Increase
	Formalin/EtOH	3	5.27	0.37	2.20	Increase
	Formalin	3	4.41	0.20	1.34	Increase
	Frozen (Control)	3	3.07	0.71	-	-
Bulk	Ethanol	3	3.62	0.55	0.49	Increase
	Formalin/EtOH	3	3.55	0.37	0.41	Increase
	Formalin	3	4.08	0.70	0.95	Increase
	Frozen (Control)	3	3.13	0.15	-	-

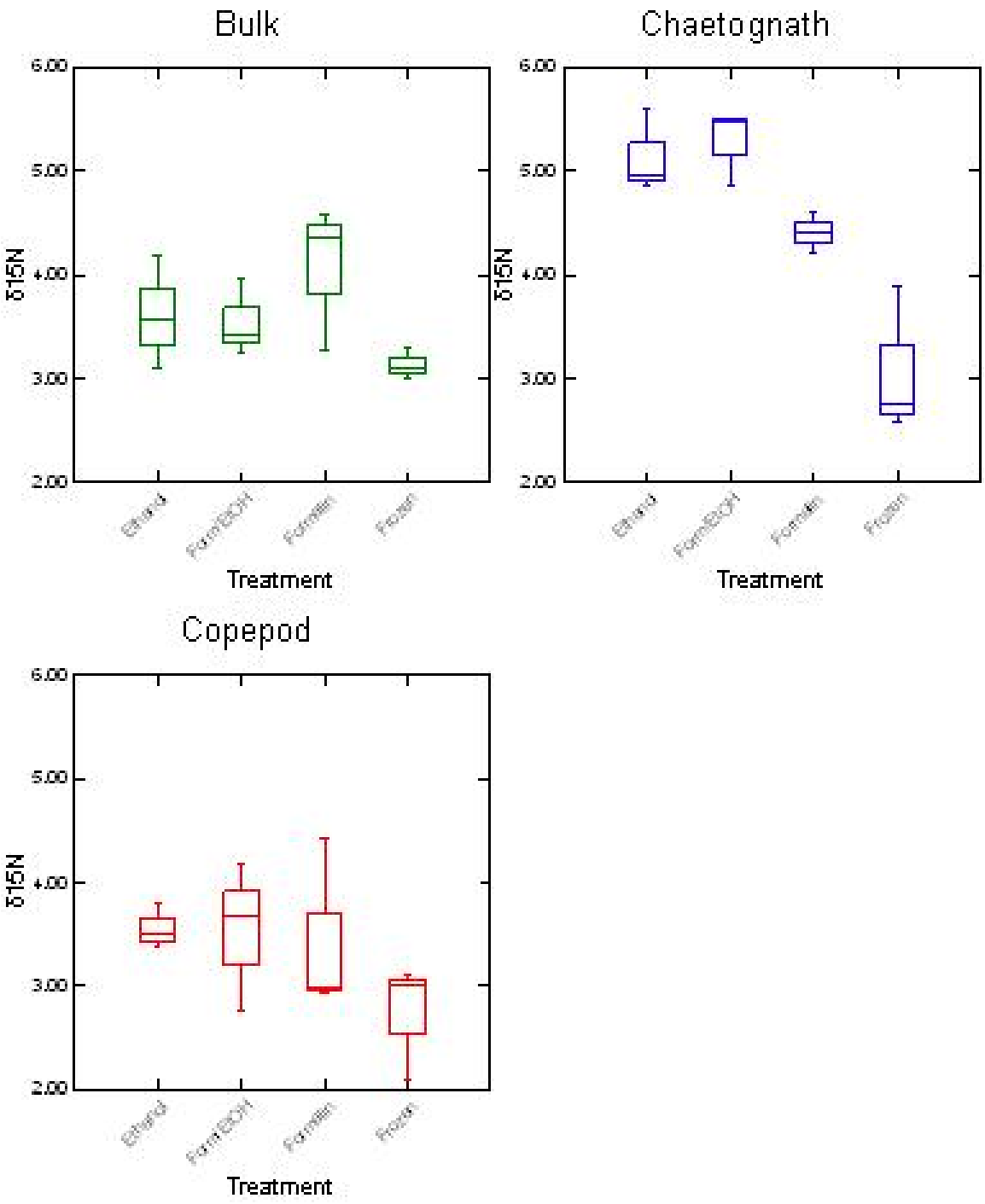

Figure 7. The $\delta^{15}N$ (‰) values and one standard deviation for all taxa and all treatments. The box indicates the values of the first quartile, median, and third quartile. The whiskers indicate the next values below the first quartile and above the third quartile.

Table 5. Shapiro-Wilk's test of normality of $\delta^{15}N$ for each taxa. P values < 0.05 are considered not normally distributed.

Shapiro-Wilk's Test of Normality for $\delta^{15}N$ $\alpha = 0.05$, p value	
	p value
Bulk	0.780
Calanoid Copepod	0.979
Chaetognath	0.119

Table 6. One-way ANOVA and Tukey HDS Post-hoc results comparing $\delta^{15}N$ values between each preservation type for each taxa. P values < 0.05 indicate a significant difference.

One-Way ANOVA $\delta^{15}N$ By Treatment $\alpha = 0.05$		
	H/F Value	**p value**
Calanoid Copepod	(3, 3) = 1.148	0.387
Chaetognath	(3, 3) = 14.542	0.001
Bulk	(3, 3) = 1.920	0.205

Tukey HDS Post Hoc Analysis
$\alpha = 0.05$

Dependent Variable	**Treatments**	**p value**
Chaetognath	Frozen (Ethanol)	0.003
	Frozen (Formalin)	0.029
	Frozen (Formalin/EtOH)	0.002

4.2. Biological and Physical Properties of Currents and Water Masses

4.2.1. Physical Properties of the E-W Transect

4.2.1.1. Acoustic Doppler Current Profiler (ADCP) Data

The ADCP data indicated that there were three currents present throughout the sampling period. The fast (500-2200 mm/s), northward flowing current was the Florida Current (FC). An aperiodic, sub-surface counter-current (SSCC) was characterized by predominately southward flowing water with a speed between 500 and 1100 mm/s. The third current describes the water not encompassed by either the FC or SSCC, and was referred to as intermediate water (Interm). The intermediate current flows to the north and is slower than the other currents (< 500 mm/s).

In April current velocity direction data from the ADCP showed a strong SSCC covering the cross-sectional area from the Inshore station to just west of the Middle station, extending from about 40m to the bottom (100-200m) (Figure 8). Current velocity magnitude data showed the strongest flow was in the center of the SSCC, flowing at 1100 mm/s (Figure 9). The ADCP data also showed the western boundary of the FC was located at the Offshore station, having a strong north-northeast flow of 1100mm/s. A bottom flow of water extended eastwardly offshore nearly 75 m up into the water column.

In May, current velocity direction data showed the SSCC located at the Inshore station, but was diminished in cross-sectional area when compared to April. The SSCC extended from the bottom to about 70 m into the water column (Figure 10). Current velocity magnitude information showed the SSCC was flowing at roughly 550mm/s. The western boundary of the northerly flowing FC extended just westward of the Inshore

Station (in the surface waters) and obtained a maximum velocity of 2200mm/s between the Inshore and Middle stations. From this area of maximum velocity, FC current velocity diminished vertically through the water column as well as horizontally east and west (Figure 11).

In July, current velocity direction data showed the SSCC was shoreward of the Inshore station and its eastern boundary just reached the Inshore station, extending along the bottom roughly 70 m into the water column (Figure 12). Current velocity magnitude data showed the western boundary of the FC extended shoreward of the Inshore station, encompassing the Inshore, Middle, and Offshore stations. Maximum flow existed between the Middle and Offshore stations, reaching a velocity of roughly 1650mm/s and flowing north (Figure 13).

In September, the current velocity direction data showed the SSCC encompassed the entire horizontal section west of the Inshore station to just about the Middle station, extending along the bottom to roughly 100 m into the water column (Figure 14). Current velocity magnitude data showed the western boundary of the FC extended between the Middle and Offshore stations, with maximum flow reaching 1100mm/s in this area (Figure 15). A multi-directional flow along the ocean bottom extended 50m up into the water column, suggesting a highly turbid area.

In November, the current velocity direction data showed no evidence of the SSCC (Figure 16). The current velocity magnitude data showed the western boundary of the FC extends to the Inshore station, encompassing the Inshore, Middle, and Offshore stations. Maximum flow existed between the Middle and Offshore stations, reaching a velocity of roughly 2200mm/s at the Middle station and flowing northerly (Figure 17).

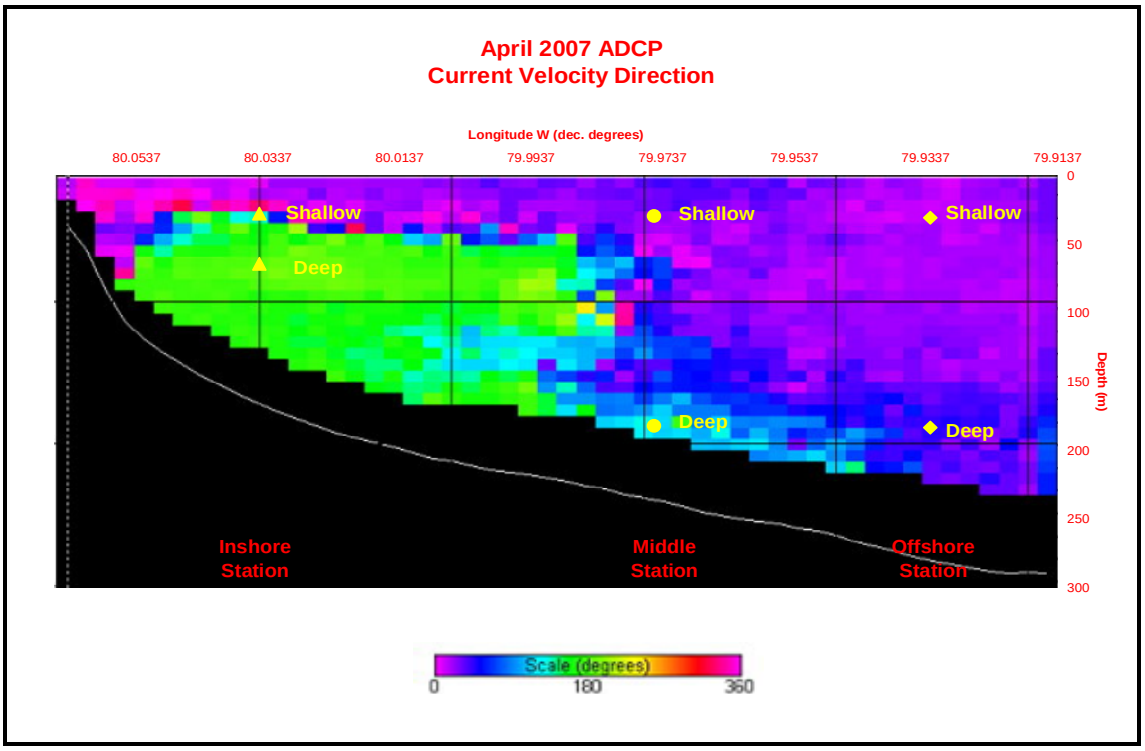

Figure 8. April 2007 ADCP current velocity direction.

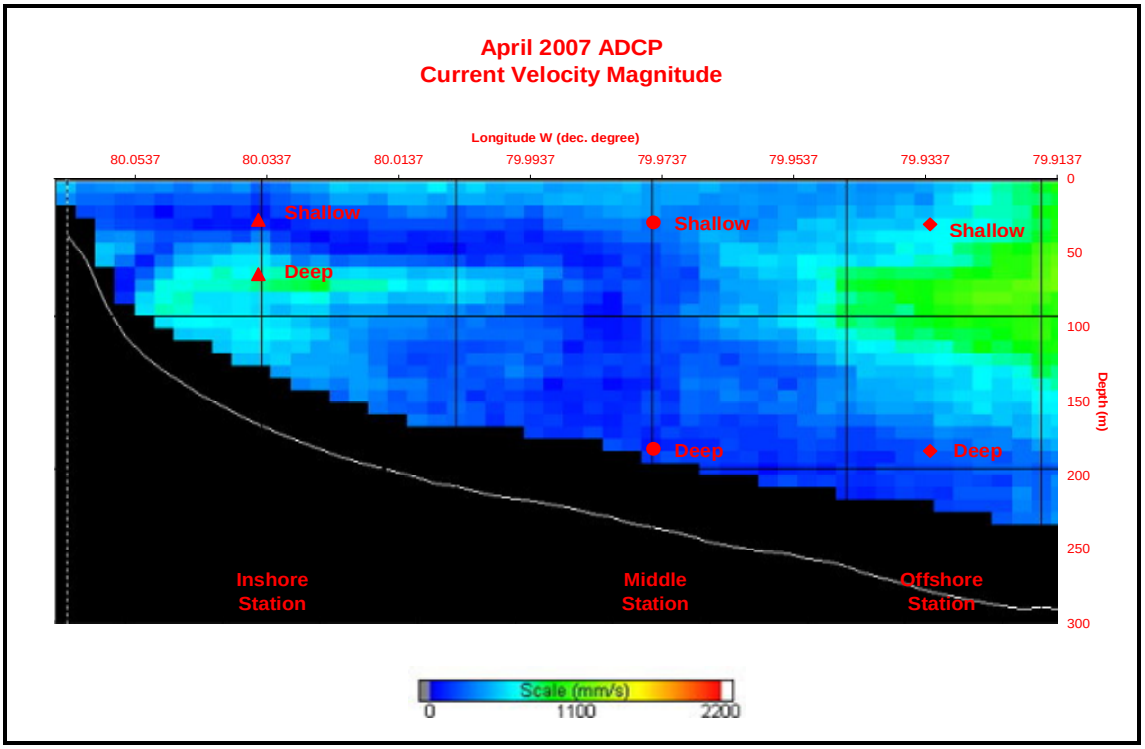

Figure 9. April 2007 ADCP current velocity magnitude.

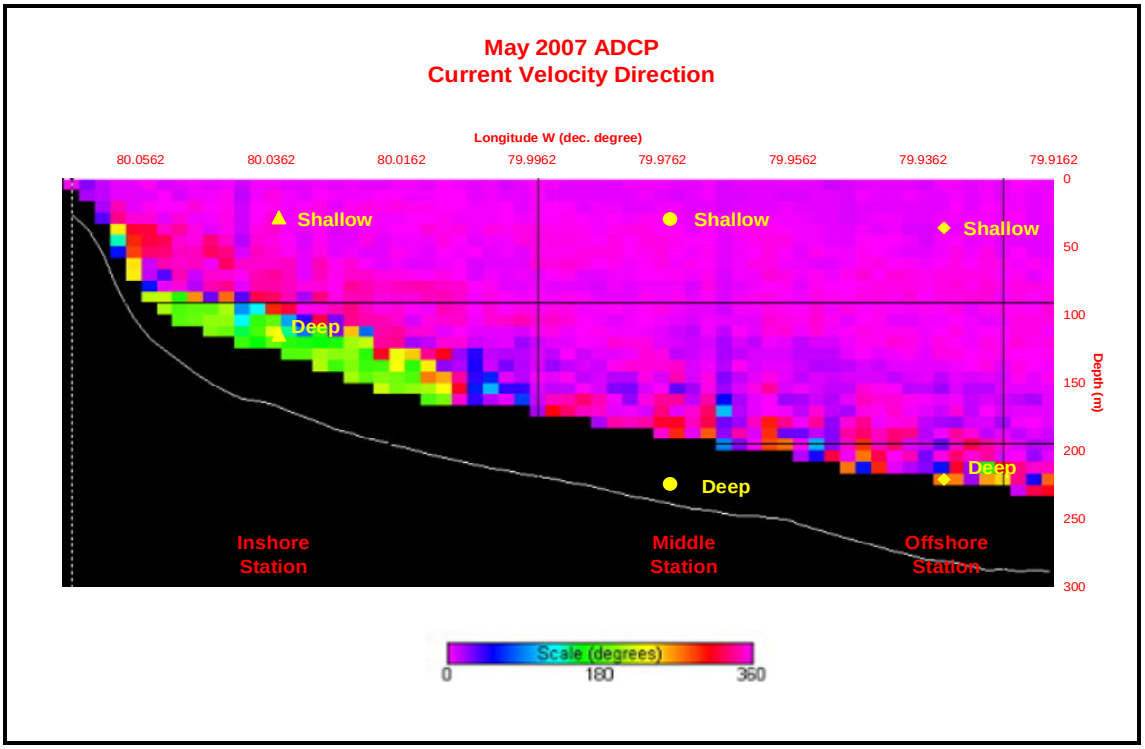

Figure 10. May 2007 ADCP current velocity direction.

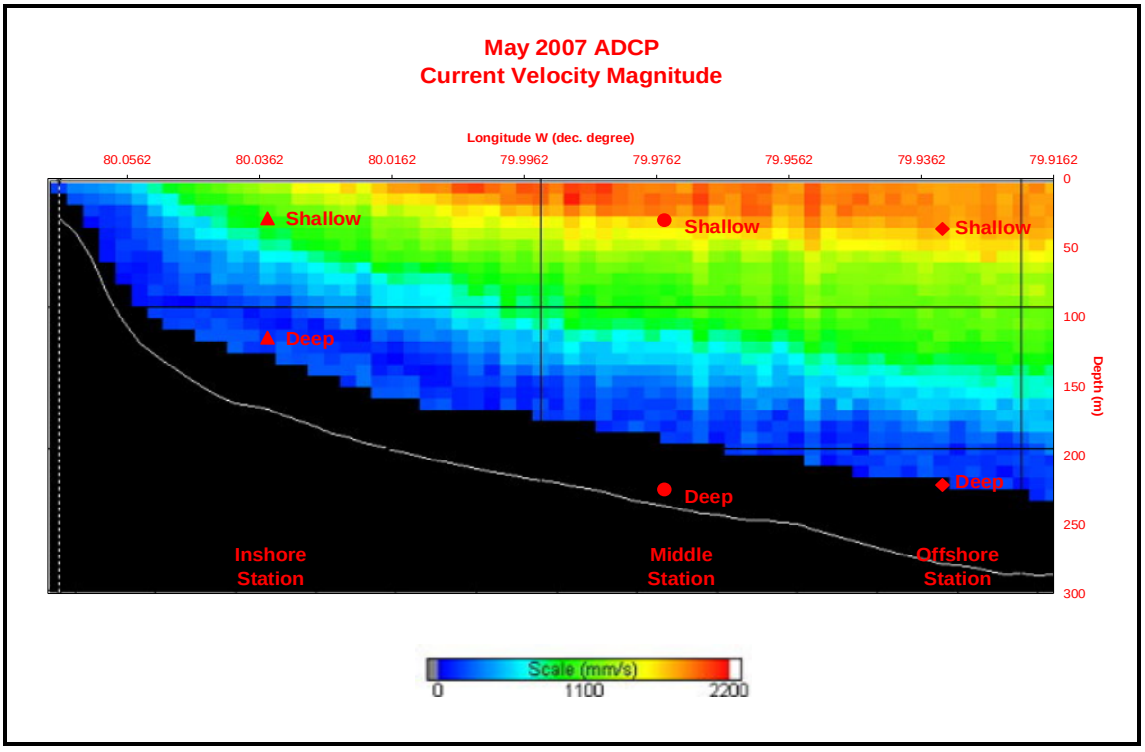

Figure 11. May 2007 ADCP current velocity magnitude.

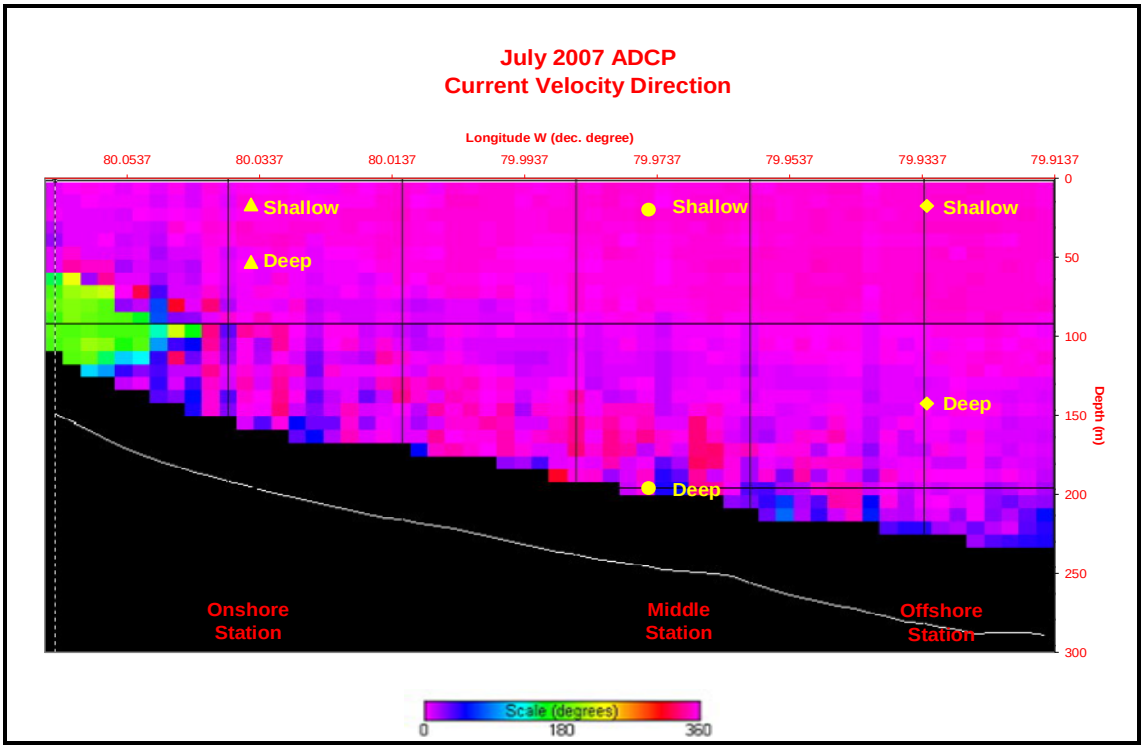

Figure 12. July 2007 ADCP current velocity direction.

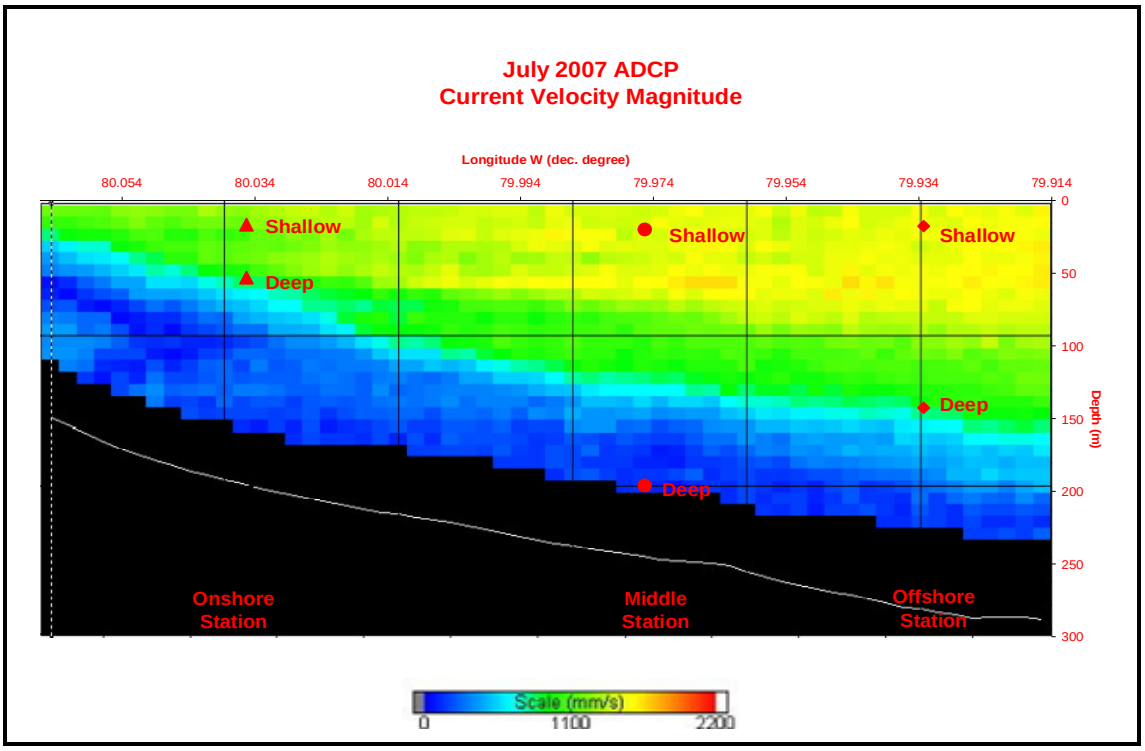

Figure 13. July 2007 ADCP current velocity magnitude.

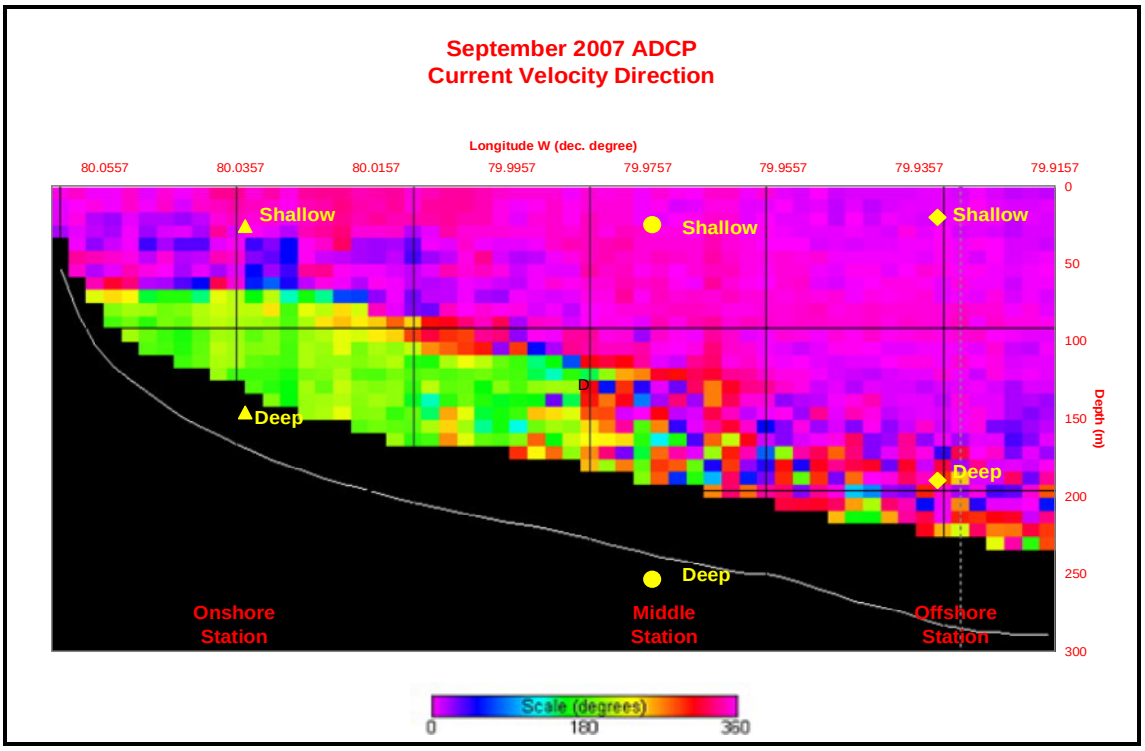

Figure 14. September 2007 ADCP current velocity direction.

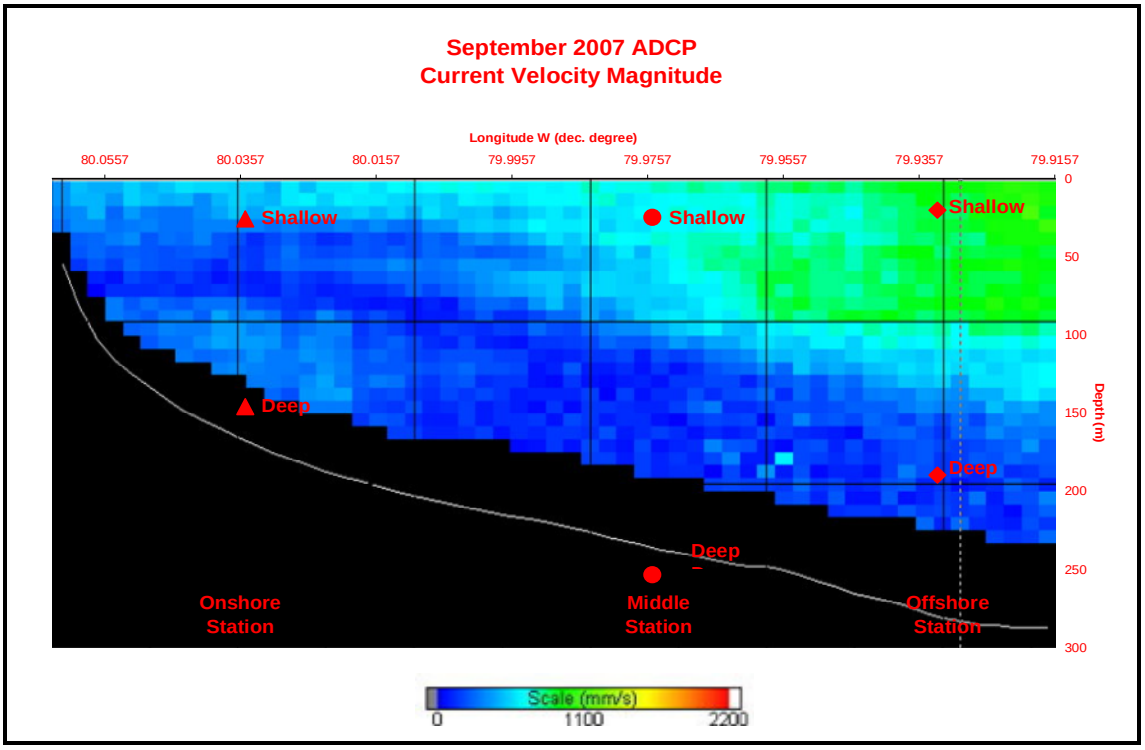

Figure 15. September 2007 ADCP current velocity magnitude.

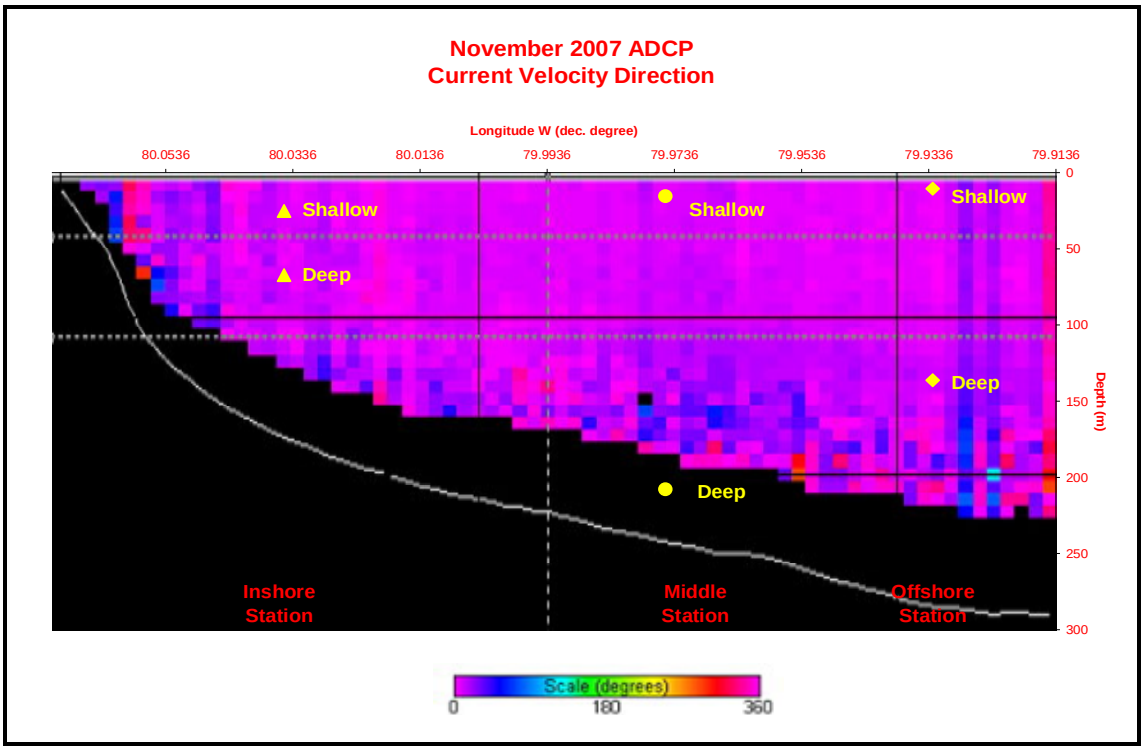

Figure 16. November 2007 ADCP current velocity direction.

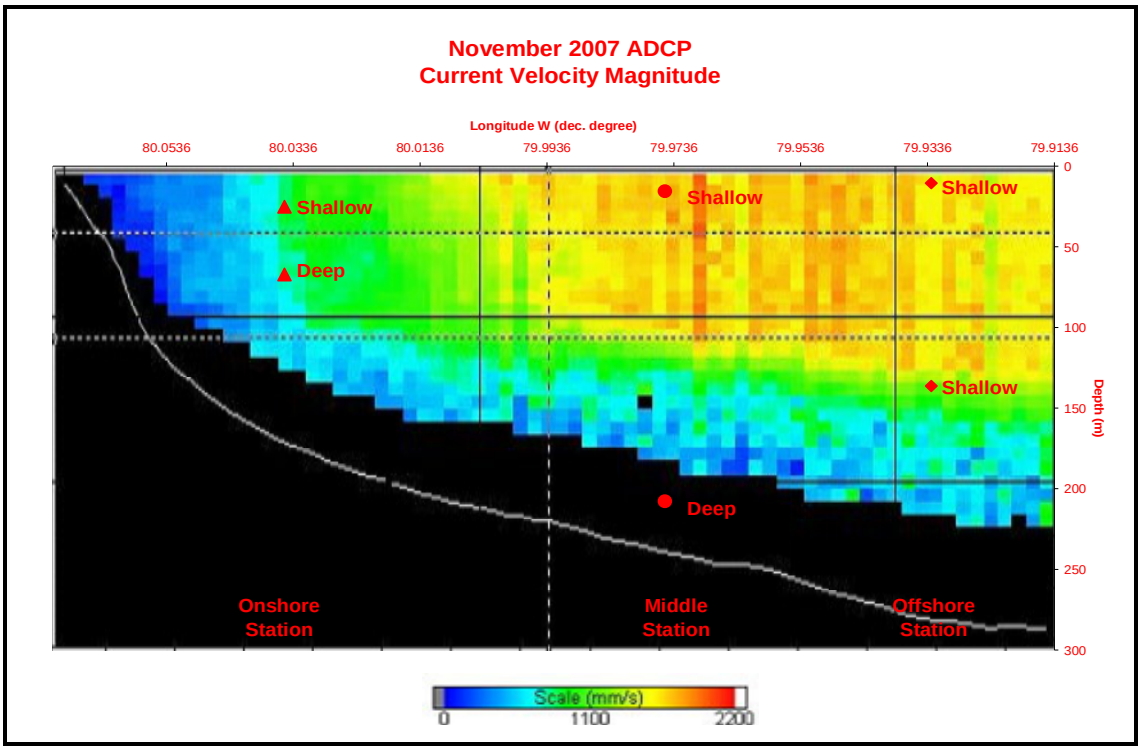

Figure 17. November 2007 ADCP current velocity magnitude.

Table 4.9 illustrates the diversity of current magnitude and direction observed at each station during the 2007sampling period. Based on the current direction and magnitude, conclusions about the present water masses were made for each station.

4.2.2. Conductivity-Temperature-Depth Sensor (CTD) Data

Due to instrument failure, CTD information was not collected at any station during April or May. Available CTD data showed that all Shallow tows were conducted between 10.5m and 26m, while all the Deep tows were conducted between 53m and 253.7m. All shallow tows occurred above the thermocline during all months. All deep tows occurred below the thermocline, excluding the November Inshore station tow. This was due to a particularly shallow tow coinciding with a particularly deep thermocline, indicated by the thermocline information collected at the Middle and Offshore stations (Table 8).

In July, the Middle and Offshore stations had similar temperature profiles. The temperature above the thermocline was ~29^{o}C and the thermocline began at a depth of 27m for both stations. The inshore station thermocline began at a shallower depth of 19m. Water below the thermocline at the inshore station was 0.5-1.0^{o}C cooler than the water below the thermocline at the Middle and Offshore stations (Figure 18). The depth of the thermocline was shallowest at the Inshore station (16.60m) compared to the Middle and Offshore stations (24.6m and 23.4m, respectively).

Table 7. Direction and magnitude of the current at each tow station.

Current Summary For Each Tow					
			Direction	**Velocity mm/s**	**Current**
April	**Inshore**	Shallow	NNE (30^o)	350	Interm
		Deep	S (180^o)	600	SSCC
	Middle	Shallow	ENE (60^o)	350	Interm
		Deep	SE (130^o)	350	Interm
	Offshore	Shallow	NNE (30^o)	600	FC
		Deep	E (90^o)	350	Interm
May	**Inshore**	Shallow	N (0^o)	1100	FC
		Deep	SSE (150^o)	300	SSCC
	Middle	Shallow	N (0^o)	1700	FC
		Deep	Unkn	Unkn	~Interm
	Offshore	Shallow	N (0^o)	1650	FC
		Deep	W (270^o)	350	Interm
July	**Inshore**	Shallow	N (0^o)	1100	FC
		Deep	NNE (30^o)	600	FC
	Middle	Shallow	N (0^o)	1375	FC
		Deep	NNE (30^o)	350	Interm
	Offshore	Middle	N (0^o)	1375	FC
		Deep	NNE (30^o)	1100	FC
September	**Inshore**	Shallow	N (0^o)	600	Interm
		Deep	S (180^o)	600	SSCC
	Middle	Shallow	N (0^o)	800	FC
		Deep	Unkn	Unkn	~Interm
	Offshore	Shallow	NNE (30^o)	1100	FC
		Deep	W (270^o)	350	Interm
November	**Inshore**	Shallow	NNE (30^o)	1100	FC
		Deep	ENE (60^o)	600	Interm
	Middle	Shallow	NNE (30^o)	1650	FC
		Deep	Unkn	Unkn	~Interm
	Offshore	Shallow	N (0^o)	1550	FC
		Deep	N (0^o)	1550	FC

Table 8. Water mass and thermocline information interpolated from CTD data.

Water Mass Summary at Each Tow							
			Tow Depth (m)	**Temp (^{o}C)**	**Salinity (‰)**	**Water Mass**	**Thermo-Cline**
July	**Inshore**	Shallow	16.6	28.98	36.27	YW	Above
		Deep	53.0	25.33	36.42	YW	Mixed
	Middle	Shallow	19.9	29.09	36.22	YW	Above
		Deep	196.1	11.63	35.51	OTHER	Mixed
	Offshore	Shallow	17.6	29.1	36.22	YW	Above
		Deep	142.6	16.19	36.13	OTHER	Mixed
September	**Inshore**	Shallow	26	30.11	36.01	CEW	Above
		Deep	146.1	15.23	36.01	CEW	Below
	Middle	Shallow	25.0	30.08	35.89	CEW	Above
		Deep	253.7	10.45	35.28	OTHER	Below
	Offshore	Shallow	20.3	30.61	35.9	CEW	Above
		Deep	189.9	14.43	35.88	CEW	Below
November	**Inshore**	Shallow	25.1	26.29	36.24	YW	Above
		Deep	67.2	26.24	36.24	YW	Above
	Middle	Shallow	15.5	26.69	36.17	YW	Above
		Deep	207.8	8.93	35.13	OTHER	Below
	Offshore	Shallow	10.5	27.24	36.21	YW	Above
		Deep	136.3	20.85	36.61	YW	Mixed

Like the water temperature profiles, the Middle and Offshore stations showed similar salinity profiles. Salinity was consistent from the surface (~36.2‰) to the halocline at ~29m, again similar to the depth of the thermocline. The Middle station salinity profile deviated slightly from the Offshore station profile by attaining a salinity maximum of 36.8‰ at ~100m, while the Offshore station had a salinity of 36.5‰ at this depth. The Inshore station showed a different profile from the other stations. Salinity consistently increased from 35.7‰ to 36.3‰ from the surface to ~17m (Figure 19).

In September all stations had similar temperature profiles, with the temperature above the thermocline consistently hovering around 30^{o}C. The thermocline at all stations began at ~26m. Below the thermocline, the Inshore station exhibited slightly cooler water (0.5-1.0^{o}C) than the Middle and Offshore stations (Figure 20). Salinity profiles of all stations were also similar. The halocline started at ~29m at the Inshore and Middle stations, but was shallower at the Offshore station (~18m) (Figure 21).

In November, all stations showed similar temperature profiles, varying only by ~1^{o}C between the Inshore and Offshore stations, with the water above the thermocline hovering around 26^{o}C. The thermocline begins at ~90m and the mixed layer of the thermocline ended at ~190m at a temperature of 9^{o}C (Figure 22). All stations showed similar salinity profiles as well. The salinity ranged between 35.7‰ and 36.2‰ between the Offshore station and the Inshore station, but then only varied by ~0.1‰ for the remainder of the profile. The first halocline began at ~67m and ended at 108m, increasing by ~0.5‰. The salinity rapidly decreased by ~1.5‰ from 108m to 190m (Figure 23).

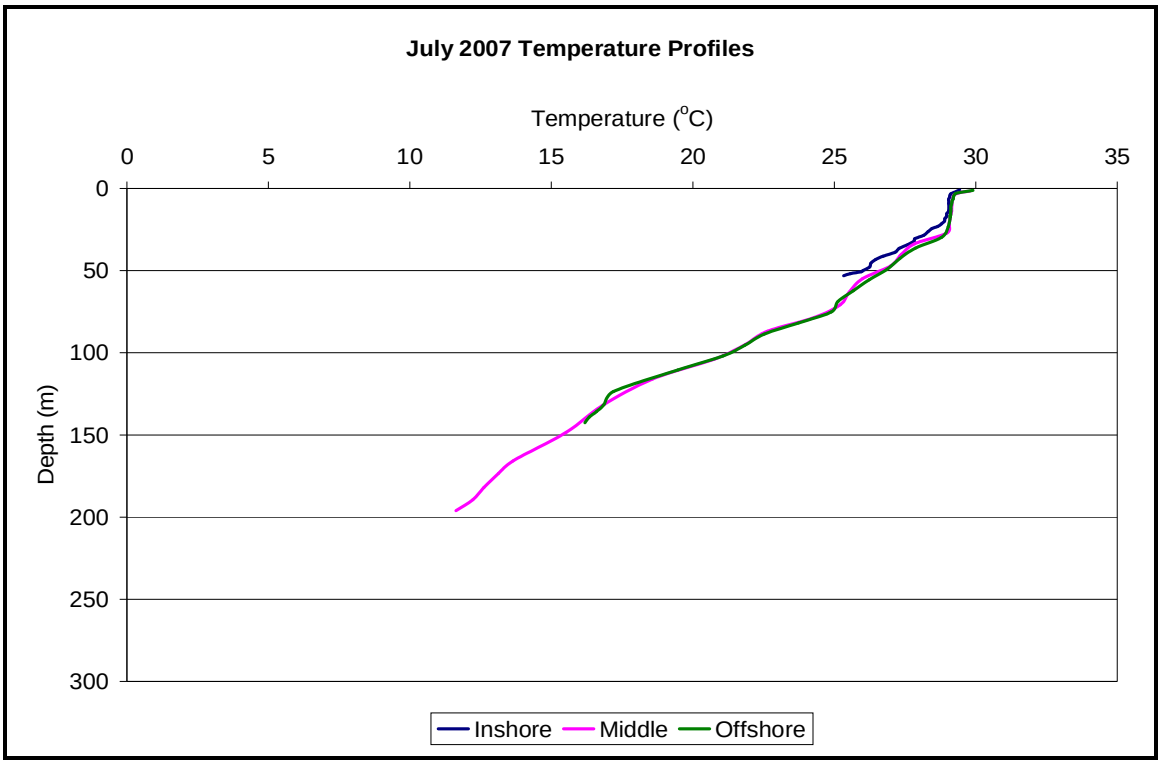

Figure 18. July 2007 temperature profiles collected from CTD information.

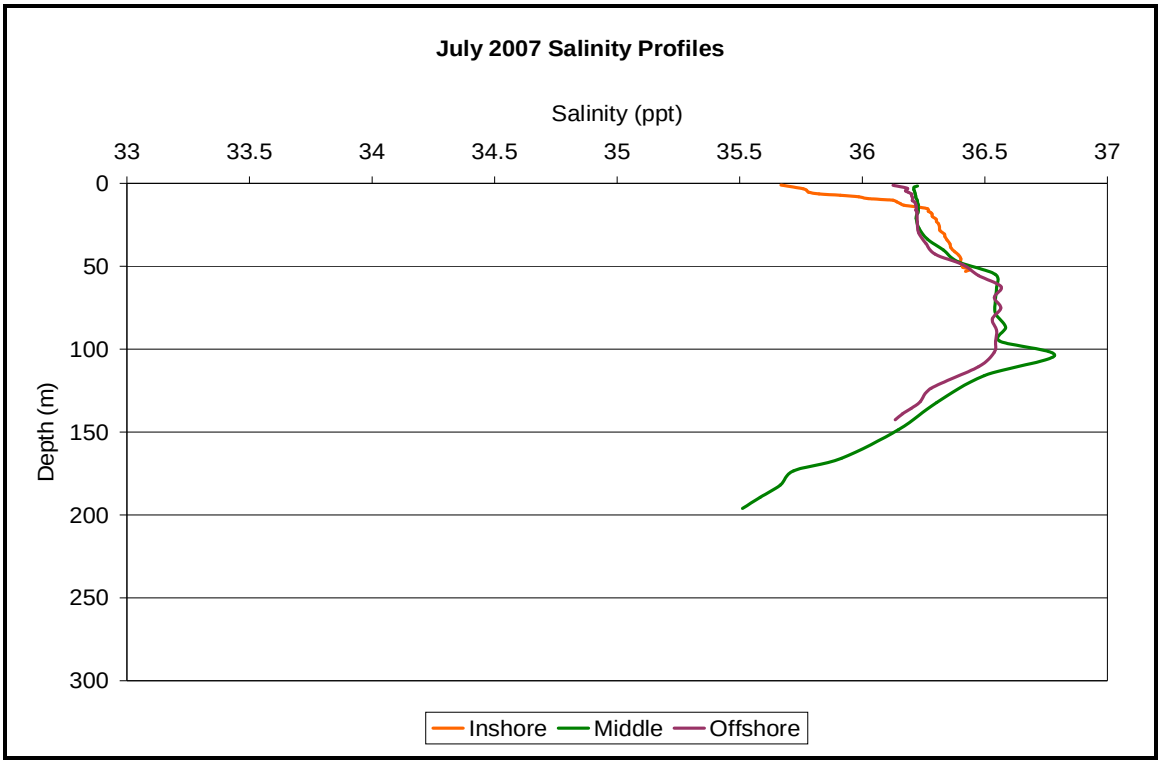

Figure 19. July 2007 salinity profiles collected from CTD information.

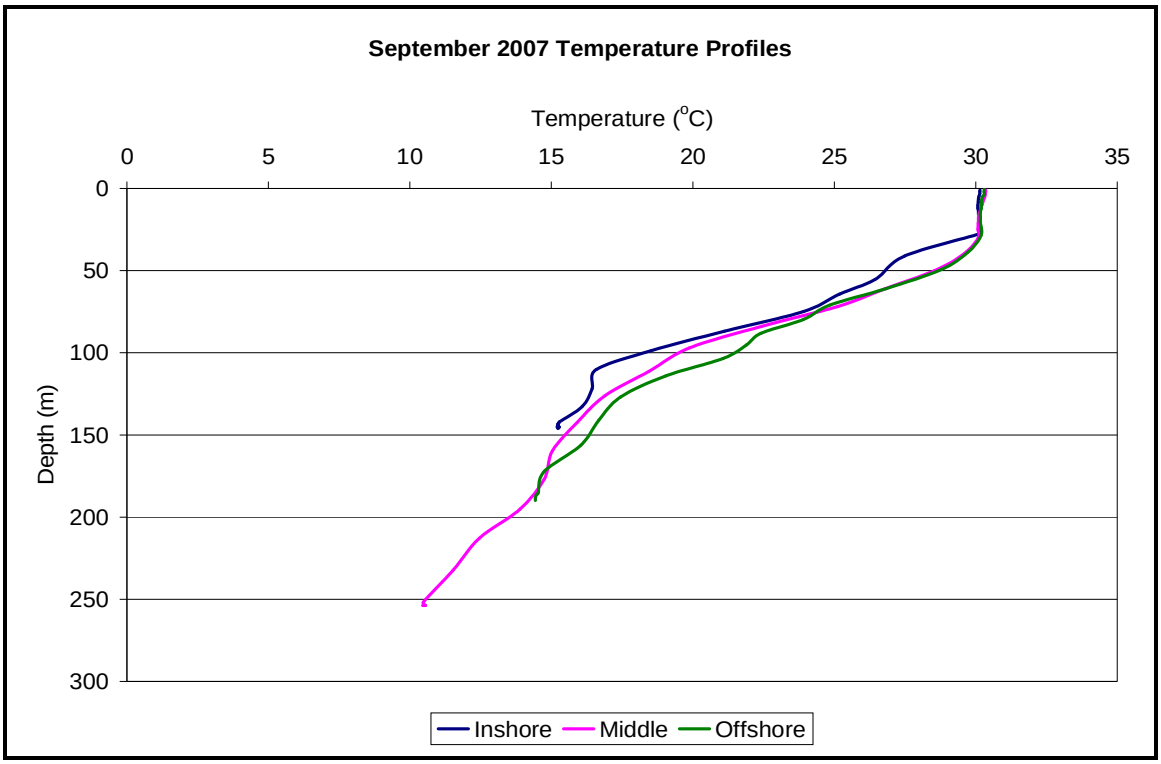

Figure 20. September 2007 temperature profiles collected from CTD information.

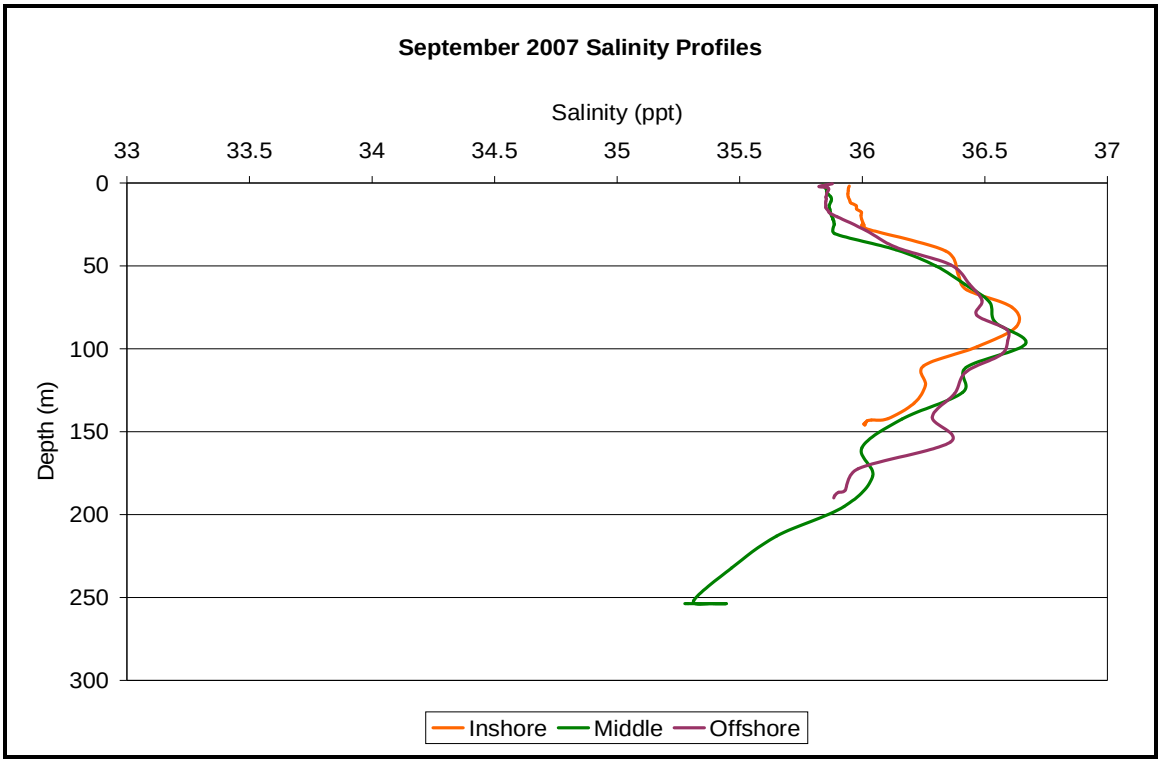

Figure 21. September 2007 salinity profiles collected from CTD information.

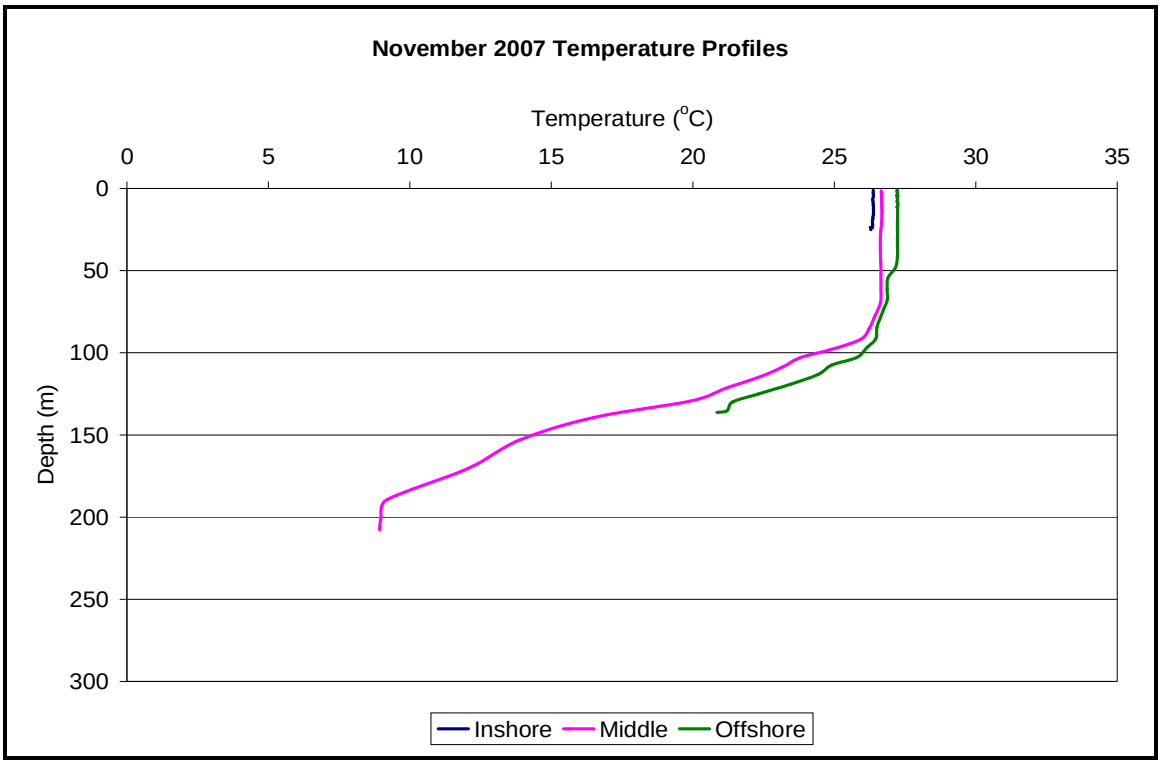

Figure 22. November 2007 temperature profiles collected from CTD information.

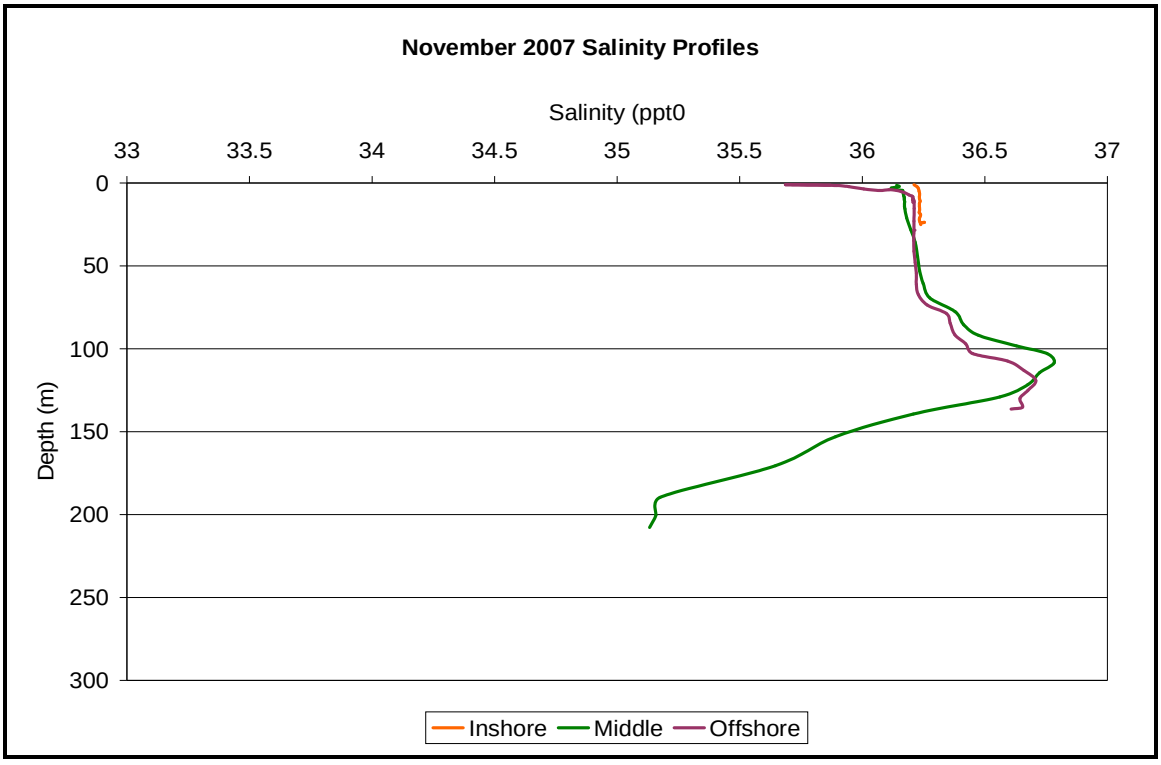

Figure 23. November 2007 salinity profiles collected from CTD information.

The average thermocline depths at all stations for July and September were relatively shallow (21.5m ± 4.3, n=3; 29.0 m ± 1.5, n=3) compared to November (91.7 m ± 0.2, n=2). When examining the depth of the mixed layer, the greatest tow depth for all stations in July and the Offshore station in November did not reach below the mixed layer. For these stations, the bottom of the mixed layer was assumed to be below the greatest tow depth. Even with this consideration, the average mixed layer depth was shallowest in September (82.5 m ± 15.9, n=3), while July and November had similar minimum mixed layer depths (121.1 m ± 60.3m, n=3; 117.0 m ± 27.3, n=2).

Temperature and salinity information from the CTD casts were also compiled to create temperature-salinity plots (T-S) and these plots were utilized to identify water masses, based on defined conservative temperature and salinity properties unique to individual water masses, as defined in the introduction. During July and November, most of the tows occurred in the Yucatan Water (YW), although during July the deep tows were possibly in STUW or another water source, indicated by the low temperature. These water masses were listed as OTHER. During September, all tows except the Middle Deep tow were located in the Continental Edge Water (CEW) (Table 8, Figures 24-26).

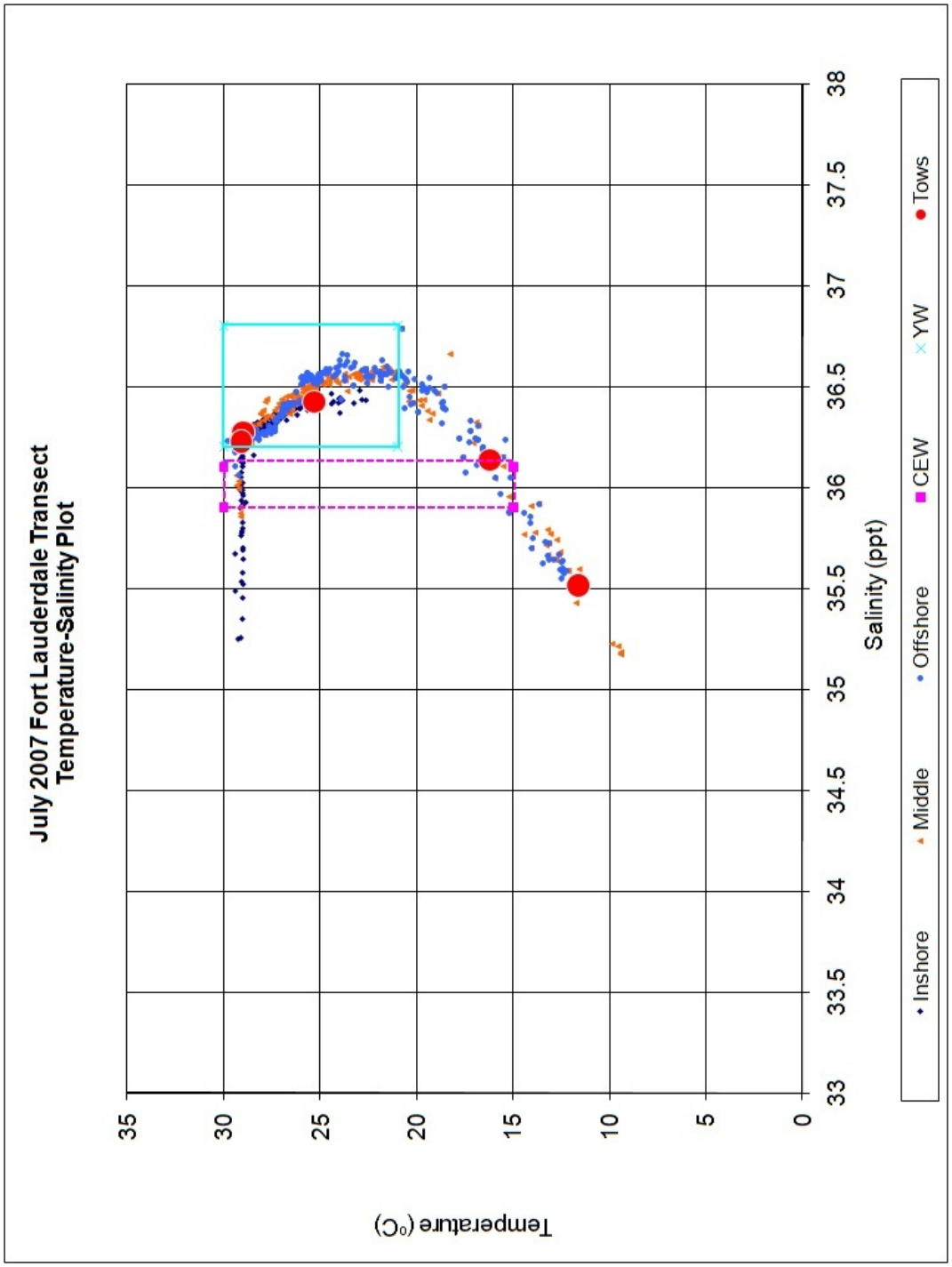

Figure 24. July 2007 T-S plot of all stations, compiled from CTD data. In the legend, (---) indicates temperature and salinity ranges of Coastal Edge Water (CEW), (—) indicates temperature and salinity ranges of Yucatan Water (YW), (♦) indicates Inshore CTD data, (▲) indicates Middle CTD data, (●) indicates Offshore CTD data, (◙) indicates tow temperature and salinity.

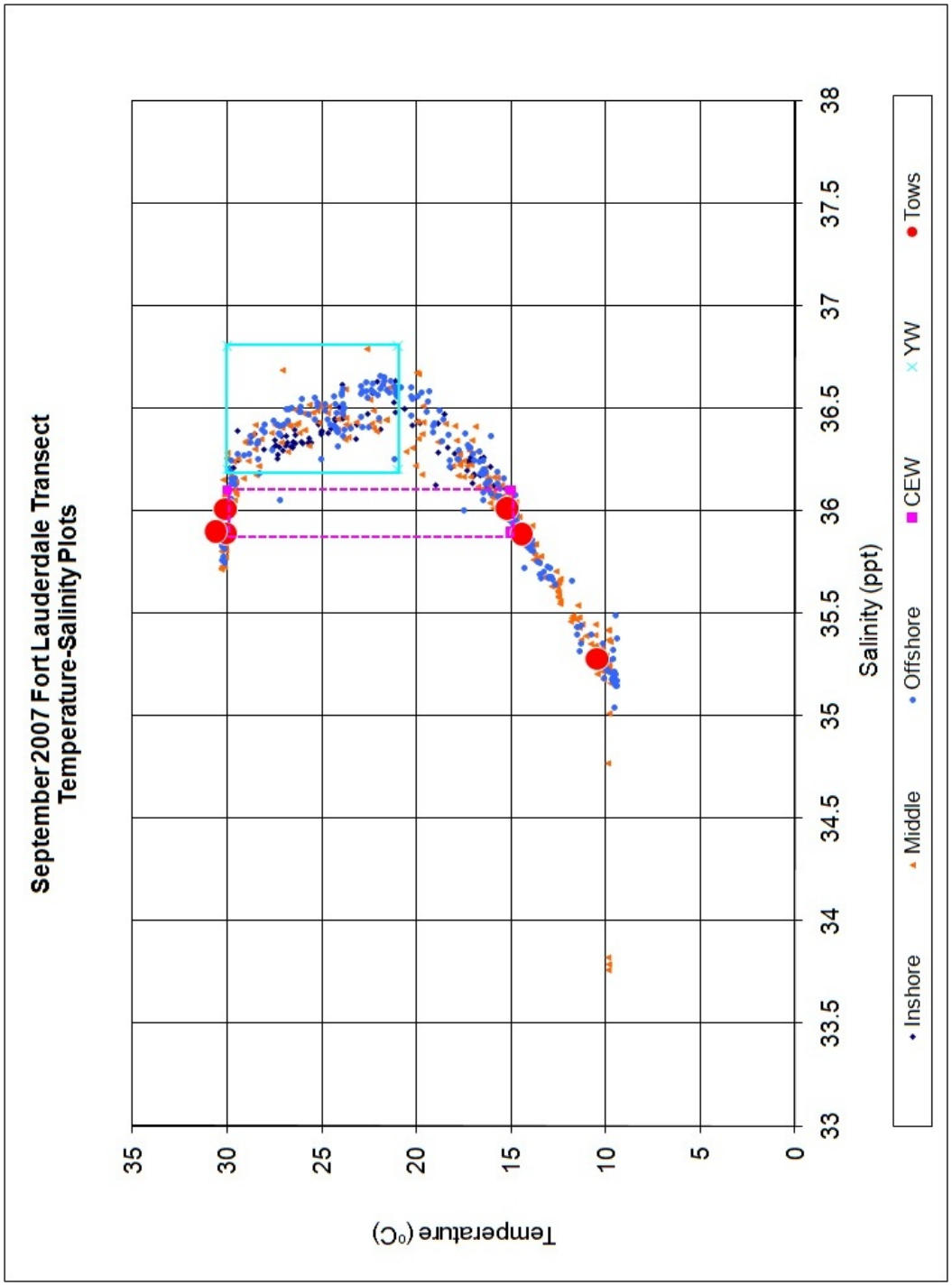

Figure 25. September 2007 T-S plot of all stations, compiled from CTD data. In the legend, (---) indicates temperature and salinity ranges of Coastal Edge Water (CEW), (—) indicates temperature and salinity ranges of Yucatan Water (YW), (♦) indicates Inshore CTD data, (▲) indicates Middle CTD data, (●) indicates Offshore CTD data, (◙) indicates tow temperature and salinity..

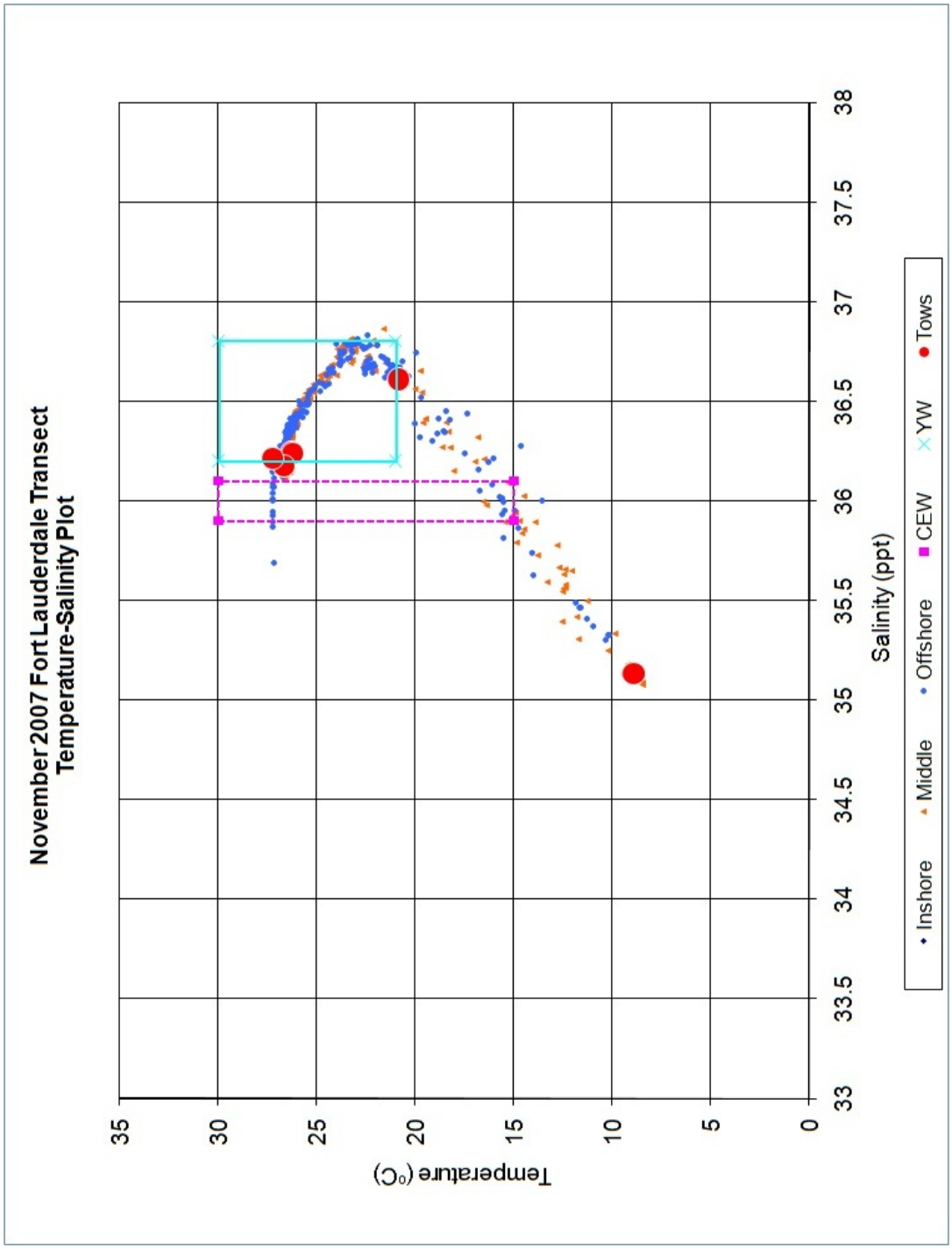

Figure 26. November 2007 T-S plot of all stations, compiled from CTD data. In the legend, (---) indicates temperature and salinity ranges of Coastal Edge Water (CEW), (—) indicates temperature and salinity ranges of Yucatan Water (YW), (♦) indicates Inshore CTD data, (▲) indicates Middle CTD data, (●) indicates Offshore CTD data, (◙) indicates tow temperature and salinity.

4.2.3. Zooplankton Properties of the E-W Transect

4.2.3.1. Density and Stable Isotope Results by Species

During the sampling regime, for all months, at all locations and at all depths, mean calanoid copepod density (#/m^3) was 5.9 (SD=6.1, n=30), and mean chaetognath density (#/m^3) was 2.3 (SD=2.5, n=30). Mean $\delta^{13}C$ (‰) values were -20.1 (SD=0.8, n=29 and -18.9 (SD=0.8, n=29) for calanoid copepods and chaetognaths, respectively. Mean $\delta^{15}N$ (‰) values were 5.2 (SD=0.9, n=29), and 6.1 (SD=0.7, n=29), for calanoid copepods and chaetognaths, respectively (Table 9, Figures 27 – 29). Shapiro-Wilk's test of normality indicated that calanoid copepod density, chaetognath density and chaetognath $\delta^{13}C$ were not normally distributed and non-parametric methods should be used for further statistical analyses (Table 10).

4.2.3.2. Density and Stable Isotope Results by Month

Analysis values by month only showed mean density for both calanoid copepods and chaetognaths was highest in April and lowest in September. Mean calanoid copepod density (#/m^3) ranged from 12.4 (SD=8.0, n=6), to 3.0 (SD=2.5, n=6). Mean chaetognath density (#/m^3) ranged from 3.8 (SD=2.8, n=6), to 1.5 (SD=2.8, n=6).

Mean $\delta^{13}C$ was lowest in April for both taxa, and highest in November for calanoid copepods and September for chaetognaths. Mean calanoid copepod $\delta^{13}C$ (‰) ranged from -21.0 (SD=0.3, n=6), to -19.2 (SD=0.3, n=6). Mean chaetognath $\delta^{13}C$ (‰) ranged from -19.8 (SD=0.1, n=6) to -18.1 (SD=0.4, n = 6). Mean calanoid copepod $\delta^{15}N$ (‰) was lowest in September and highest in July. Mean calanoid copepod $\delta^{15}N$ (‰) ranged from 4.8 (SD=0.9, n=6) to 5.6 (SD=1.1, n=5). Mean chaetognath $\delta^{15}N$ (‰) was

lowest in November and highest in April. Mean chaetognath $\delta^{15}N$ (‰) ranged from 5.4 (SD=0.5, n = 6) to 6.7 (SD=0.4, n=6) (Table 11, Figures 30 - 32).

Shapiro-Wilk's test of normality indicated that calanoid copepod density, chaetognath density, and chaetognath $\delta^{13}C$ were not normally distributed for at least one of the months, and nonparametric methods should be used for further statistical analyses (Table 12). The ANOVA results indicated that calanoid copepod $\delta^{13}C$ was significantly different between months ($F(1,4) = 26.911$, $p<0.001$, $\alpha = 0.05$) and Kruskal-Wallis ANOVA by Ranks results indicated that chaetognath $\delta^{13}C$ was significantly different between months ($H(4, 29) = 22.437$, $p<0.001$, $\alpha = 0.05$). Tukey HSD showed calanoid copepod $\delta^{13}C$ in April was significantly different from July, September, and November ($p=0.001$, $p<0.001$, $p< 0.0001$, $\alpha = 0.05$, respectively). Values in May were significantly different from those in July, September, and November ($p=0.008$, $p<0.001$, $p<0.001$, $\alpha = 0.05$, respectively), and values in July were significantly different from those in November ($p=0.023$, $\alpha = 0.05$). Multiple comparisons post-hoc analysis showed that chaetognath $\delta^{13}C$ in April was significantly different from September and November ($p=0.003$, 0.049, $\alpha = 0.05$, respectively), and values in May were significantly different from those in September and November ($p=0.002$, 0.032, $\alpha = 0.05$, respectively). No other variables were significantly different (Tables 13 - 14).

Table 9. Descriptive statistics by Taxa.

Descriptive Statistics by Taxa							
	N	**Mean**	**Med**	**Min**	**Max**	**Rng**	**SD**
Copepod Density (#/m^3)	30	5.60	3.22	0.08	22.57	22.49	6.08
Chaetognath Density (#/m^3)	30	2.32	1.41	0.11	8.35	8.25	2.46
Copepod δ^{13}C (‰)	29	-20.08	-19.99	-21.34	-18.57	2.77	0.75
Chaetognath δ^{13}C (‰)	29	-18.91	-18.67	-20.13	-17.84	2.29	0.79
Copepod δ^{15}N (‰)	29	5.22	5.10	3.94	7.18	3.24	0.85
Chaetognath δ^{15}N (‰)	29	6.10	6.22	4.70	7.43	2.73	0.68

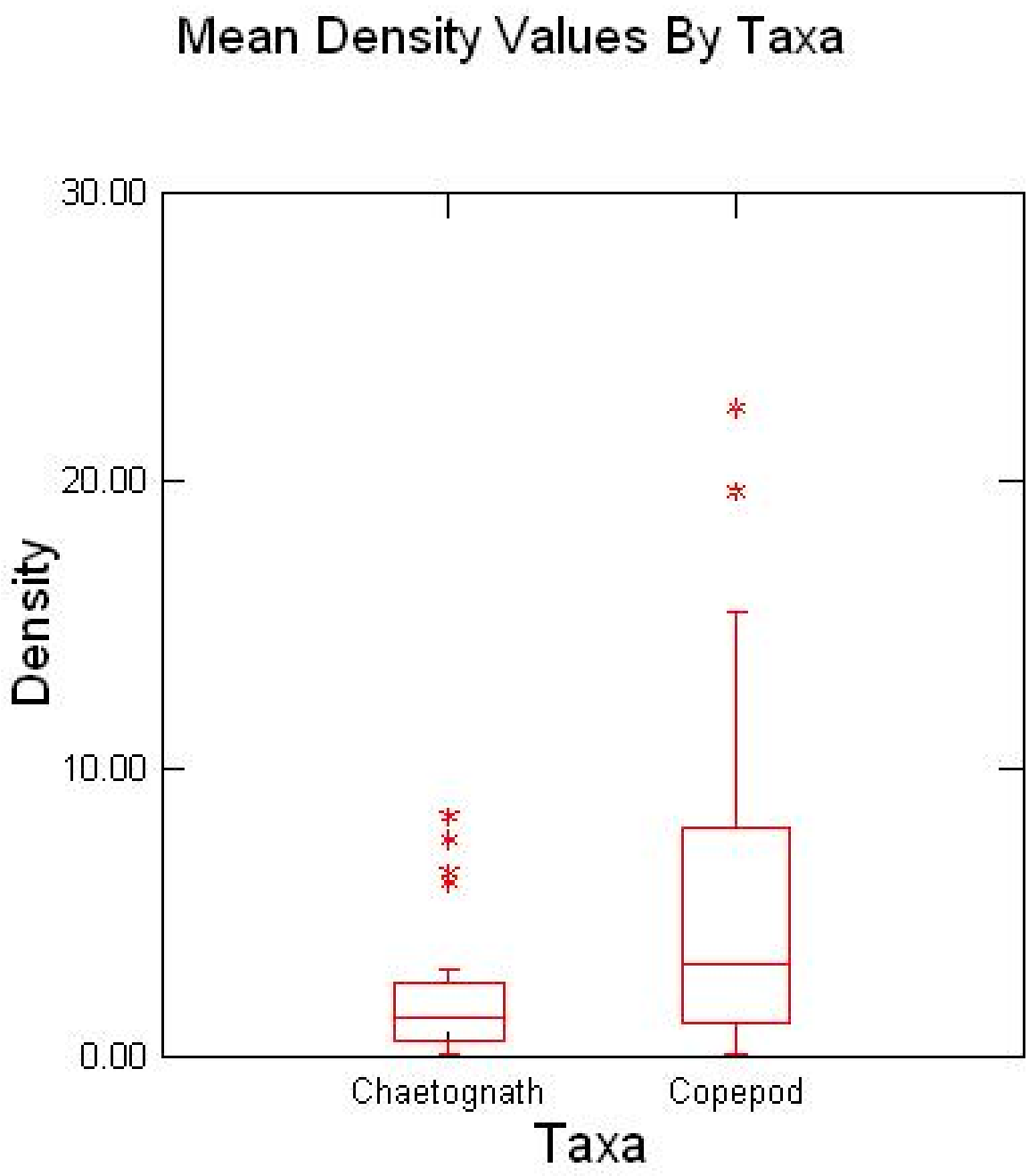

Figure 27. Density values (#/m^3) by taxa. The box indicates the values of the first quartile, median, and third quartile. The whiskers indicate the next values below the first quartile and above the third quartile. The stars represent the far outside values.

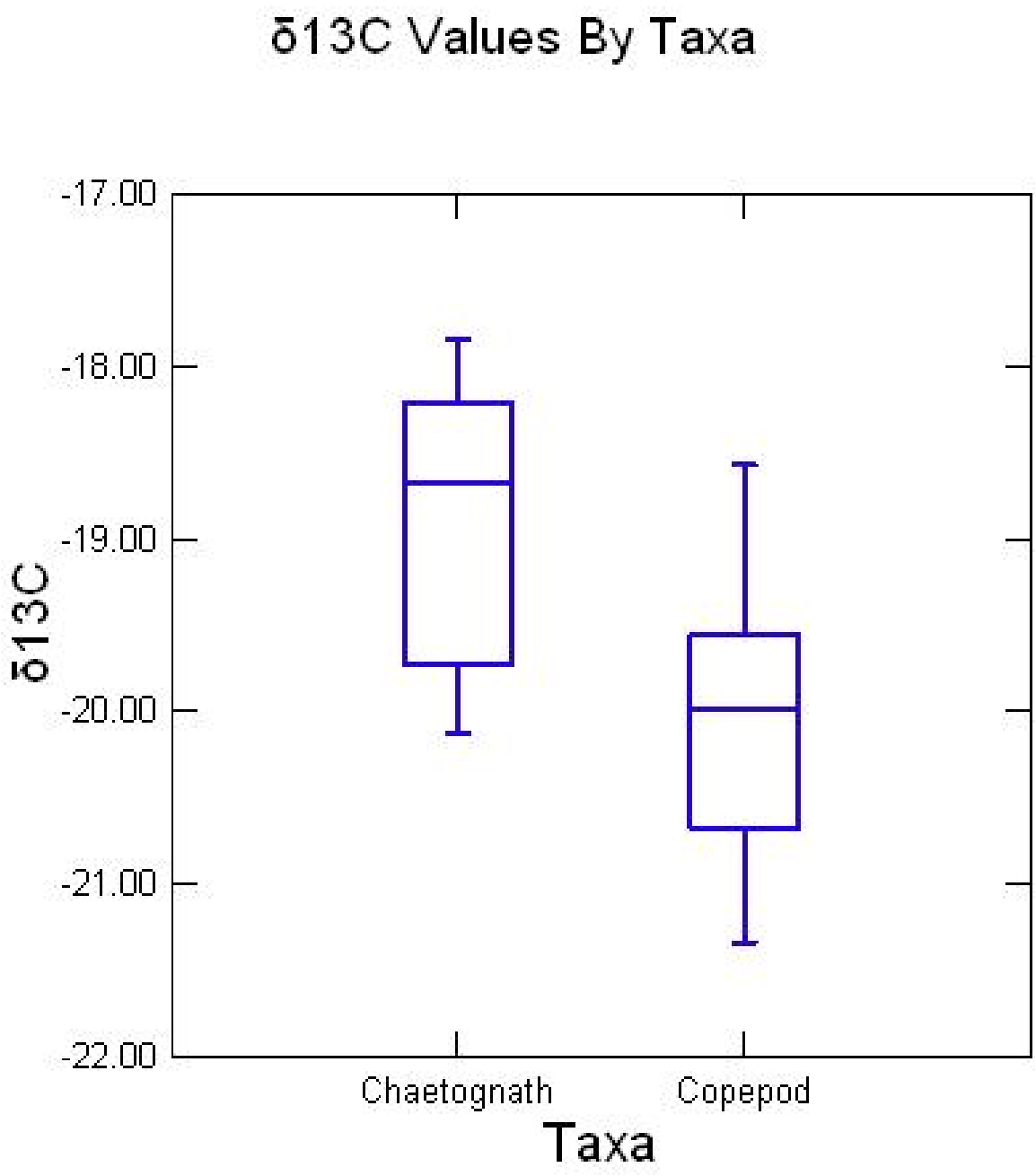

Figure 28. The $\delta^{13}C$ values (‰) by taxa. The box indicates the values of the first quartile, median, and third quartile. The whiskers indicate the next values below the first quartile and above the third quartile. The stars represent the extreme values. Open circles (when present) represent the outliers.

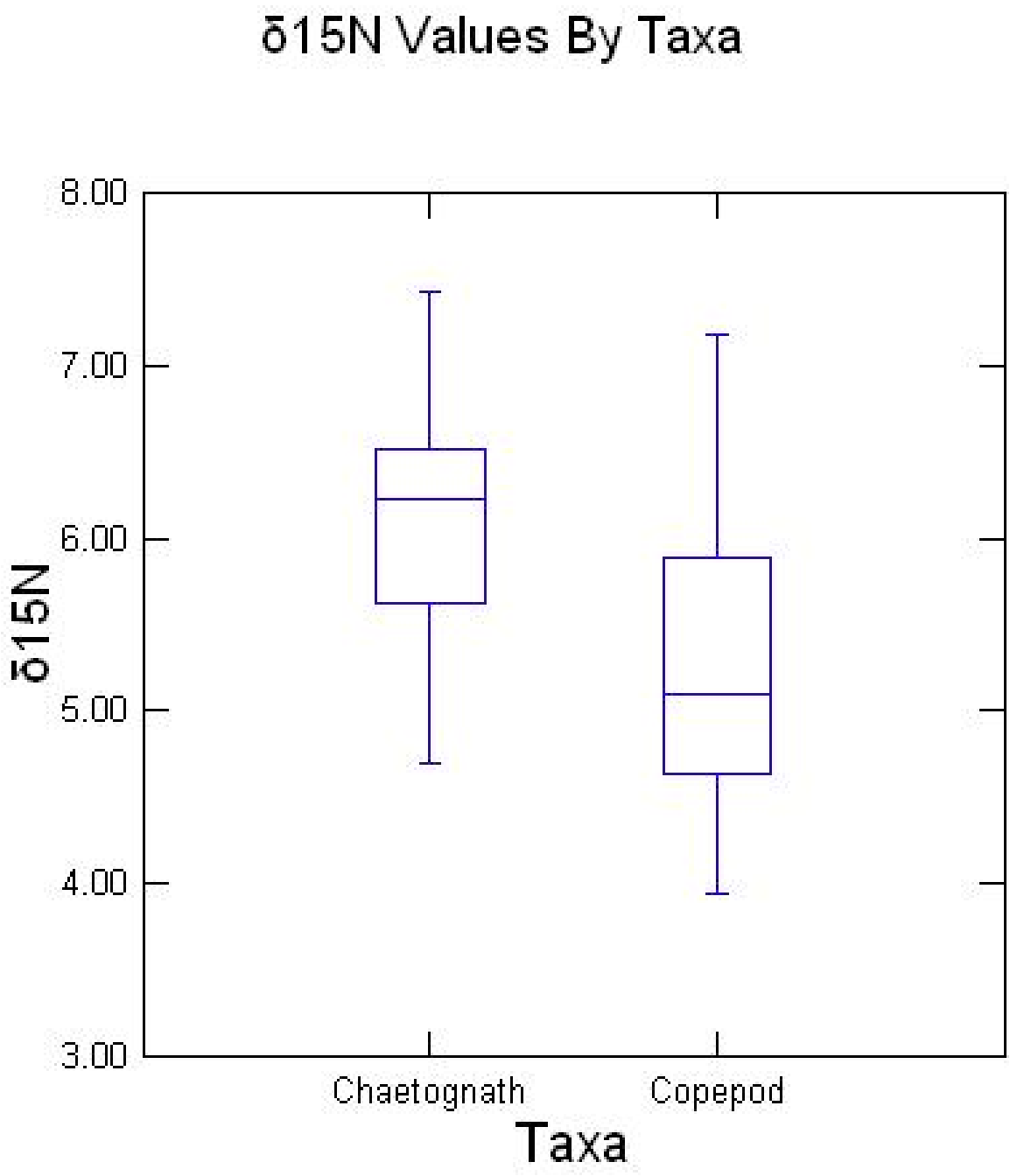

Figure 29. The $\delta^{15}N$ values (‰) by taxa. The box indicates the values of the first quartile, median, and third quartile. The whiskers indicate the next values below the first quartile and above the third quartile. The stars represent the extreme values. Open circles (when present) represent the outliers.

Table 10. Shapiro-Wilk's test of normality for each taxa. P values < 0.05 are considered not normally distributed.

Shapiro-Wilk's Test of Normality $\alpha = 0.05$		
	N	**p value**
Copepod Density (#/m^3)	30	0.002
Chaetognath Density (#/m^3)	30	0.000
Copepod δ^{13}C (‰)	29	0.201
Chaetognath δ^{13}C (‰)	29	0.004
Copepod δ^{15}N (‰)	29	0.290
Chaetognath δ^{15}N (‰)	29	0.674

Table 11. Descriptive statistics by Month for each taxa.

Descriptive Statistics by Month			N	Mean	Med	Min	Max	Rng	SD
Density	**Calanoid**	**April**	6	12.36	11.57	2.91	22.57	19.66	7.95
(#/m3)	**Copepod**	**May**	6	4.52	2.69	0.21	11.29	11.08	4.91
		July	6	3.50	2.24	0.08	11.17	11.09	4.37
		Sept	6	2.89	2.15	1.18	7.70	6.51	2.46
		Nov	6	4.71	3.23	0.51	15.50	14.98	5.56
	Chaet	**April**	6	3.85	2.41	1.23	8.35	7.13	2.84
		May	6	1.57	0.77	0.13	6.39	6.26	2.40
		July	6	1.62	0.67	0.11	6.06	5.96	2.28
		Sept	6	1.48	1.41	0.53	3.10	2.57	0.87
		Nov	6	3.11	2.05	0.24	7.54	7.30	3.13
$\delta^{13}C$	**Calanoid**	**April**	6	-20.95	-20.90	-21.34	-20.59	0.76	0.34
(‰)	**Copepod**	**May**	6	-20.70	-20.71	-20.83	-20.49	0.34	0.12
		July	5	-19.91	-19.88	-20.46	-19.40	1.07	0.38
		Sept	6	-19.58	-19.59	-20.04	-19.25	0.79	0.26
		Nov	6	-19.22	-19.39	-19.78	-18.57	1.21	0.51
	Chaet	**April**	6	-19.76	-19.79	-19.90	-19.58	0.32	0.13
		May	6	-19.76	-19.78	-20.13	-19.21	0.91	0.32
		July	5	-18.60	-18.62	-19.17	-18.12	1.06	0.39
		Sept	6	-18.12	-17.98	-18.95	-17.84	1.12	0.42
		Nov	6	-18.28	-18.24	-18.56	-17.94	0.62	0.22
$\delta^{15}N$	**Calanoid**	**April**	6	5.56	5.49	4.54	7.03	2.49	0.98
(‰)	**Copepod**	**May**	6	5.41	5.36	4.80	5.99	1.20	0.46
		July	5	5.58	5.67	4.07	7.18	3.11	1.14
		Sept	6	4.78	4.45	3.94	6.17	2.23	0.85
		Nov	6	4.82	4.66	3.96	5.56	1.60	0.62
	Chaet	**April**	6	6.67	6.54	6.30	7.43	1.13	0.43
		May	6	6.35	6.31	5.61	7.22	1.61	0.59
		July	5	5.85	6.26	4.70	6.65	1.96	0.88
		Sept	6	6.16	6.11	5.62	6.63	1.01	0.36
		Nov	6	5.43	5.42	4.78	6.00	1.23	0.47

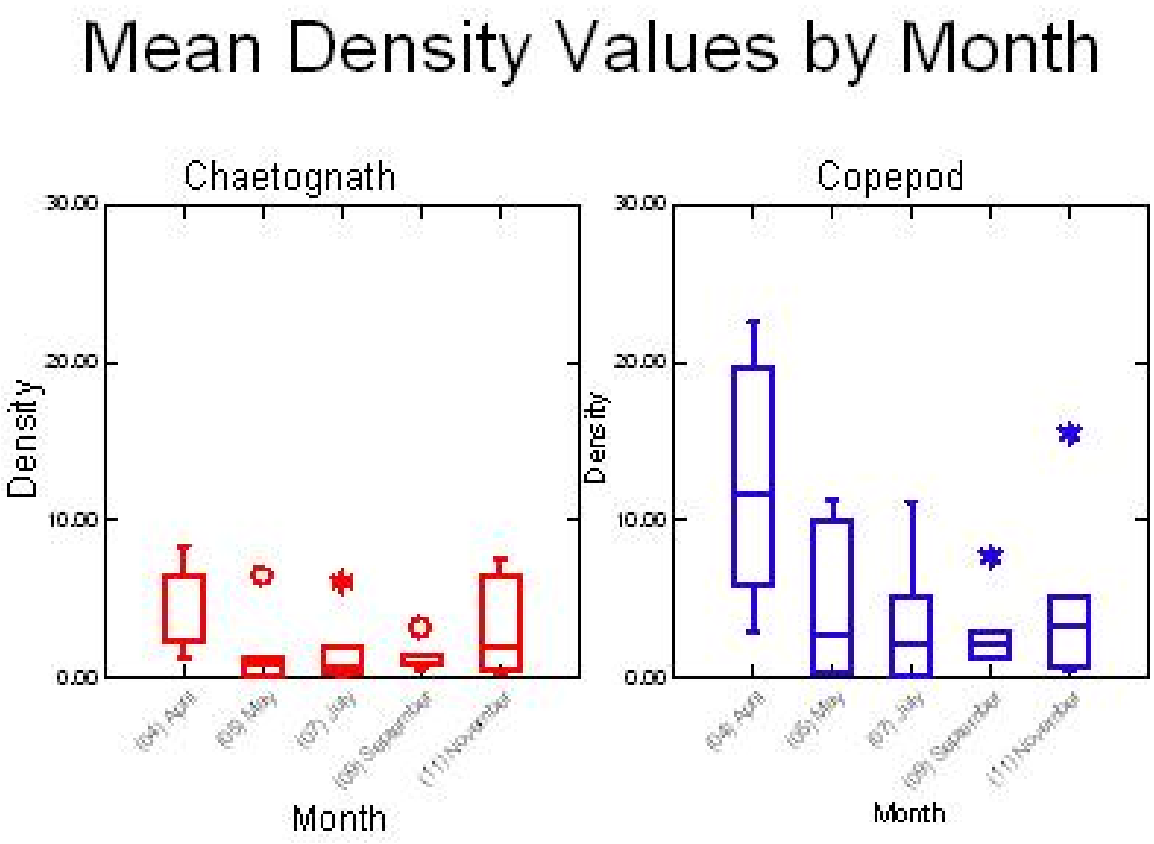

Figure 30. Density values (#/m^3) by month for each taxa. The box indicates the values of the first quartile, median, and third quartile. The whiskers indicate the next values below the first quartile and above the third quartile. The stars represent the far outside values. Open circles represent the outliers.

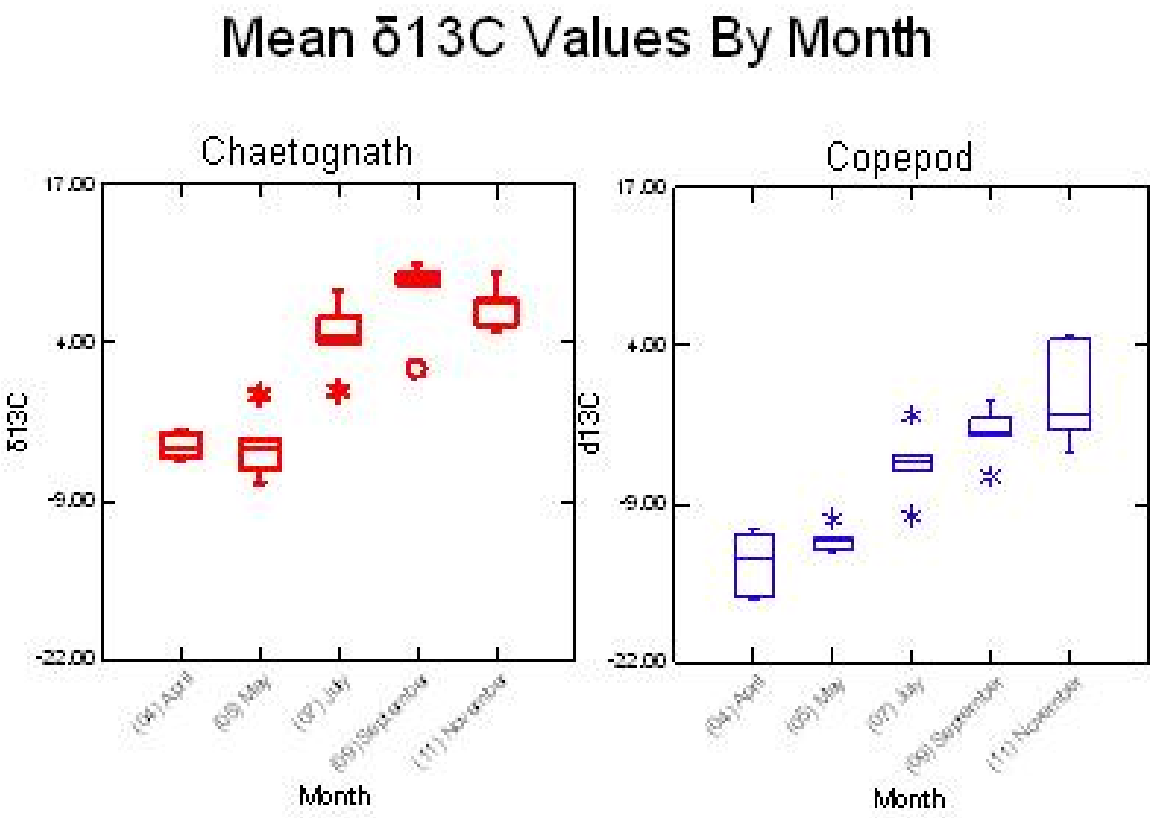

Figure 31. The $\delta^{13}C$ values (‰) by month for each taxa. The box indicates the values of the first quartile, median, and third quartile. The whiskers indicate the next values below the first quartile and above the third quartile. The stars represent the far outside values. Open circles represent the outliers.

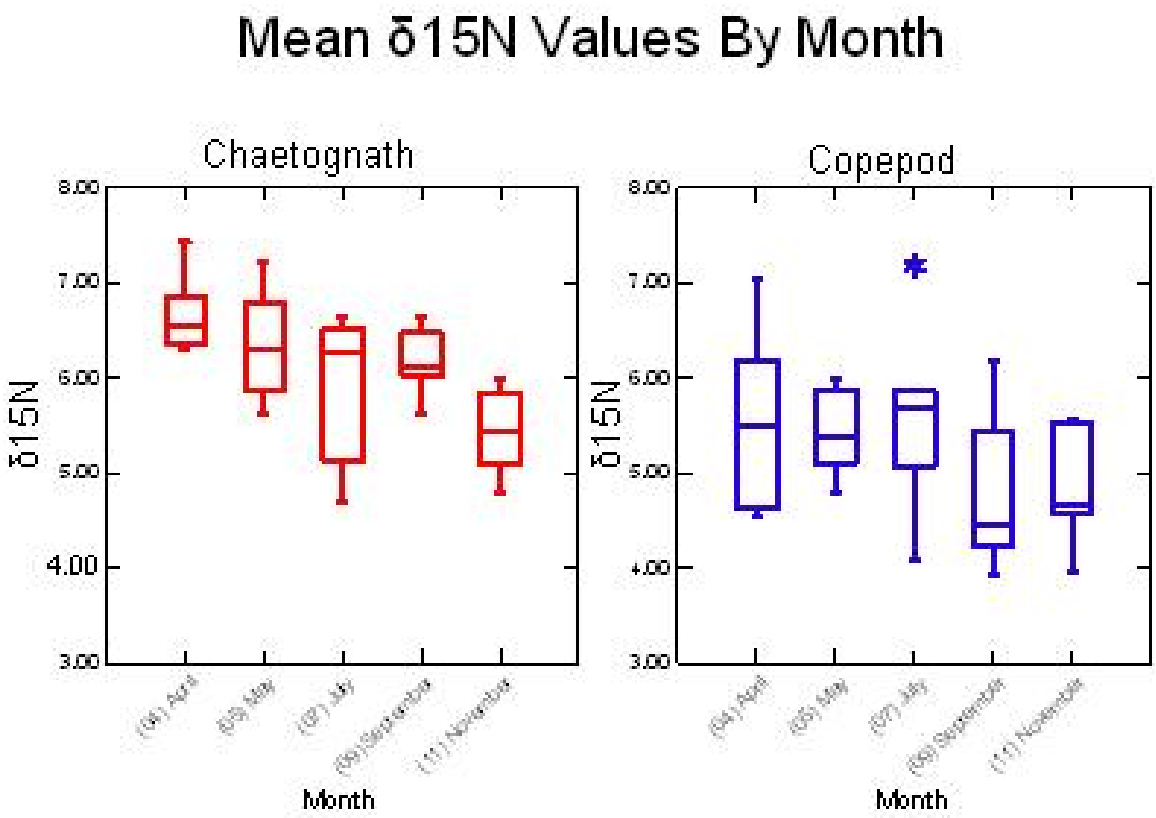

Figure 32. The $\delta^{15}N$ values (‰) by month for each taxa. The box indicates the values of the first quartile, median, and third quartile. The whiskers indicate the next values below the first quartile and above the third quartile. The stars represent the far outside values.

Table 12. Shapiro-Wilk's test of normality for each taxa by month. N = 6 for all variables, except for July copepod and chaetognath carbon and nitrogen isotope values, where N = 5. P values < 0.05 are considered not normally distributed.

Shapiro-Wilk's Test of Normality α = 0.05, p value					
	April	**May**	**July**	**Sept**	**Nov**
Copepod Density (#/m^3)	0.575	0.104	0.098	0.017	0.031
Chaetognath Density (#/m^3)	0.089	0.002	0.012	0.179	0.183
Copepod δ13C (‰)	0.136	0.350	0.816	0.477	0.195
Chaetognath δ13C (‰)	0.524	0.636	0.859	0.003	0.567
Copepod δ15N (‰)	0.534	0.771	0.958	0.322	0.307
Chaetognath δ15N (‰)	0.213	0.966	0.222	0.860	0.893

Table 13. Parametric and non-parametric ANOVA results. P values < 0.05 indicate a significant difference.

Parametric and Nonparametric ANOVA Results by Month α = 0.05			
	Test	**H/F values**	**p value**
Copepod Density (#/m^3)	Kruskal-Wallis ANOVA	(4, 30) = 7.385	0.110
Chaetognath Density (#/m^3)	Kruskal-Wallis ANOVA	(4, 30) = 7.411	0.116
Copepod δ13C (‰)	One-way ANOVA	(1, 4) = 26.911	< 0.001
Chaetognath δ13C (‰)	Kruskal-Wallis ANOVA	(4, 29) = 22.437	< 0.001
Copepod δ15N (‰)	One-way ANOVA	(1, 4) = 1.332	0.287
Chaetognath δ15N (‰)	One-way ANOVA	(1, 4) = 4.287	0.009

Table 14. Parametric and non-parametric post-hoc analysis results. P values < 0.05 indicate a significant difference.

Post Hoc Analysis Test	**Dependent Variable**	**Months**	**p value**
Tukey HSD	**Calanoid Copepod $\delta^{13}C$**	April (July)	0.001
		April (September)	0.000
		April (November)	0.000
		May (July)	0.008
		May (September)	0.000
		May (November)	0.000
		July (November)	0.023
Tukey HSD	**Chaetognath $\delta^{15}N$**	April (November)	0.006
Multiple Comparisons	**Chaetognath $\delta^{13}C$**	April (September)	0.003
		April (November)	0.049
		May (September)	0.002
		May (November)	0.032

4.2.3.3. Density and Stable Isotope Results by Location

Analysis of values by location only showed the highest mean density was found at the Inshore station for both taxa, and the lowest mean density was found at the Middle station for calanoid copepods and at the Offshore station for chaetognaths. Mean calanoid copepod density (#/m^3) ranged from 2.2 (SD=3.6, n=10) to 7.3 (SD=7.8, n=10). Mean chaetognath density (#/m^3) ranged from 1.1 (SD=1.0, n=10) to 4.3 (SD=3.0, n=10).

Mean calanoid copepod $\delta^{13}C$ was lowest at the Middle station and highest at the Inshore station. Mean calanoid copepod $\delta^{13}C$ (‰) ranged from -20.1 (SD=0.5, n=10) to -20.0 (SD=1.0, n=9). Mean chaetognath $\delta^{13}C$ was lowest at the Inshore station and highest at the Offshore station. Mean chaetognath $\delta^{13}C$ (‰) ranged from -19.1(SD=0.9, n=9) to -18.8 (SD=0.7, n=10). Both mean calanoid copepod and chaetognath $\delta^{15}N$ was lowest at the Offshore station and highest at the Middle station. Mean calanoid copepod $\delta^{15}N$ (‰) ranged from 4.9 (SD=0.9, n=10) to 5.6 (SD=0.9, n=10). Mean chaetognath $\delta^{15}N$ (‰) ranged from 6.0 (SD=0.8, n=10) to 6.2 (SD=0.7, n=10) (Table 15, Figures 33 - 35).

Shapiro-Wilk's test of normality indicated that all variables were normally distributed at all Locations and parametric methods should be used for further statistical analyses. Despite the result of the Shapiro-Wilk's test, non-parametric methods were used for calanoid copepod and chaetognath density analyses due to inherent, patchy nature of zooplankton distribution (Table 16). Kruskal-Wallis ANOVA by Ranks results indicated that chaetognath density was significantly different between locations ($H(2, 30) = 6.970$, $p=0.031$, $\alpha = 0.05$). Multiple comparisons post-hoc analysis showed that chaetognath density was significantly different between the Inshore and Offshore stations ($p=0.038$, $\alpha = 0.05$). No other variables were different (Table 17 and Table 18).

Table 15. Descriptive statistics by location for each taxon.

Descriptive Statistics By Location									
			N	**Mean**	**Med**	**Min**	**Max**	**Rng**	**SD**
Density	**Calanoid**	Inshore	10	7.26	3.85	0.25	22.57	22.32	7.77
(#/m3)	**Copepod**	Middle	10	3.17	2.06	0.17	11.17	11.01	3.64
		Offshore	10	6.36	5.50	0.08	15.50	15.42	5.95
	Chaet	Inshore	10	4.27	4.74	0.24	8.35	8.12	3.04
		Middle	10	1.56	1.29	0.16	6.06	5.90	1.71
		Offshore	10	1.14	0.91	0.11	2.63	2.53	0.98
$\delta^{13}C$	**Calanoid**	Inshore	9	-20.03	-19.82	-21.31	-18.57	2.75	0.97
(‰)	**Copepod**	Middle	10	-20.11	-20.23	-21.34	-18.60	2.74	0.81
		Offshore	10	-20.09	-19.96	-20.74	-19.40	1.34	0.52
	Chaet	Inshore	9	-19.08	-18.95	-20.13	-17.84	2.29	0.88
		Middle	10	-18.87	-18.83	-19.90	-17.93	1.98	0.85
		Offshore	10	-18.80	-18.59	-19.74	-17.92	1.82	0.71
$\delta^{15}N$	**Calanoid**	Inshore	9	5.18	5.23	3.94	6.19	2.25	0.63
(‰)	**Copepod**	Middle	10	5.58	5.78	4.24	7.18	2.94	0.88
		Offshore	10	4.89	4.65	3.96	7.03	3.08	0.93
	Chaet	Inshore	9	6.12	6.26	5.28	6.78	1.50	0.45
		Middle	10	6.16	6.11	4.70	7.22	2.52	0.73
		Offshore	10	6.02	6.26	4.78	7.43	2.65	0.84

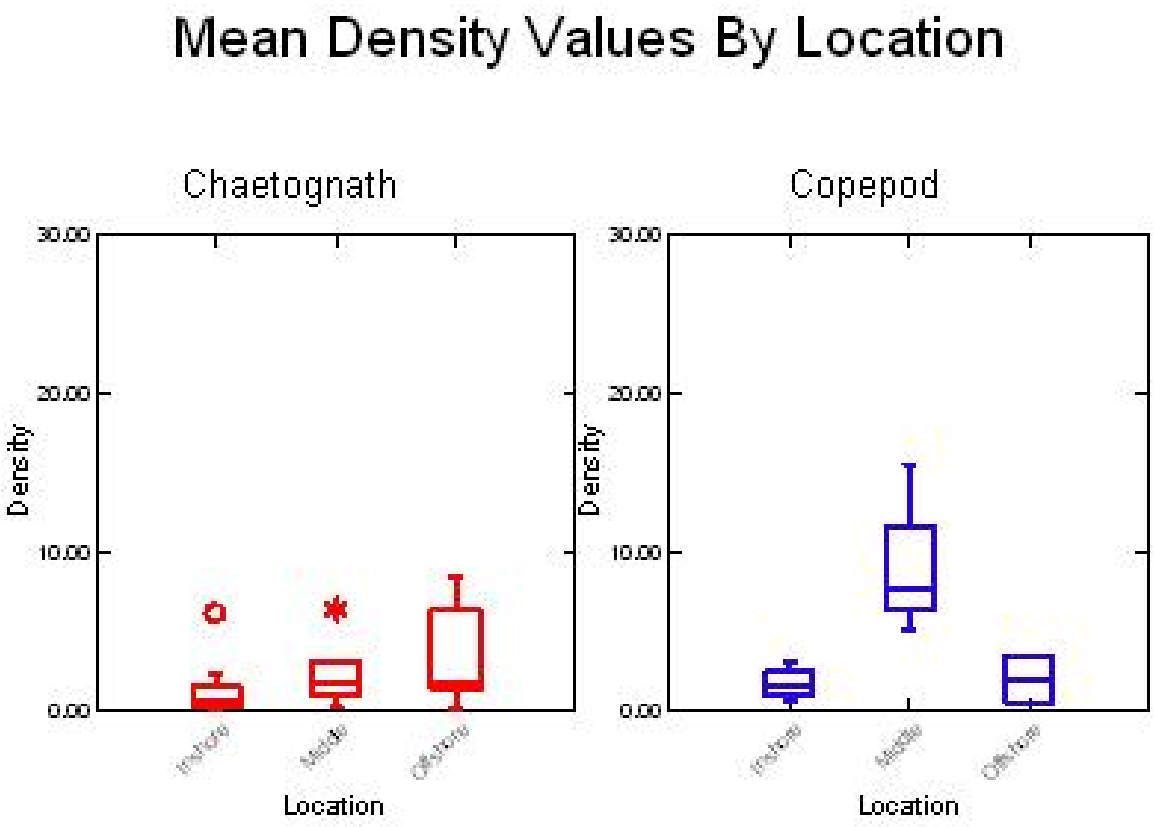

Figure 33. Density values (#/m^3) by location for each taxon. The box indicates the values of the first quartile, median, and third quartile. The whiskers indicate the next values below the first quartile and above the third quartile. The stars represent the far outside values. Open circles represent the outliers.

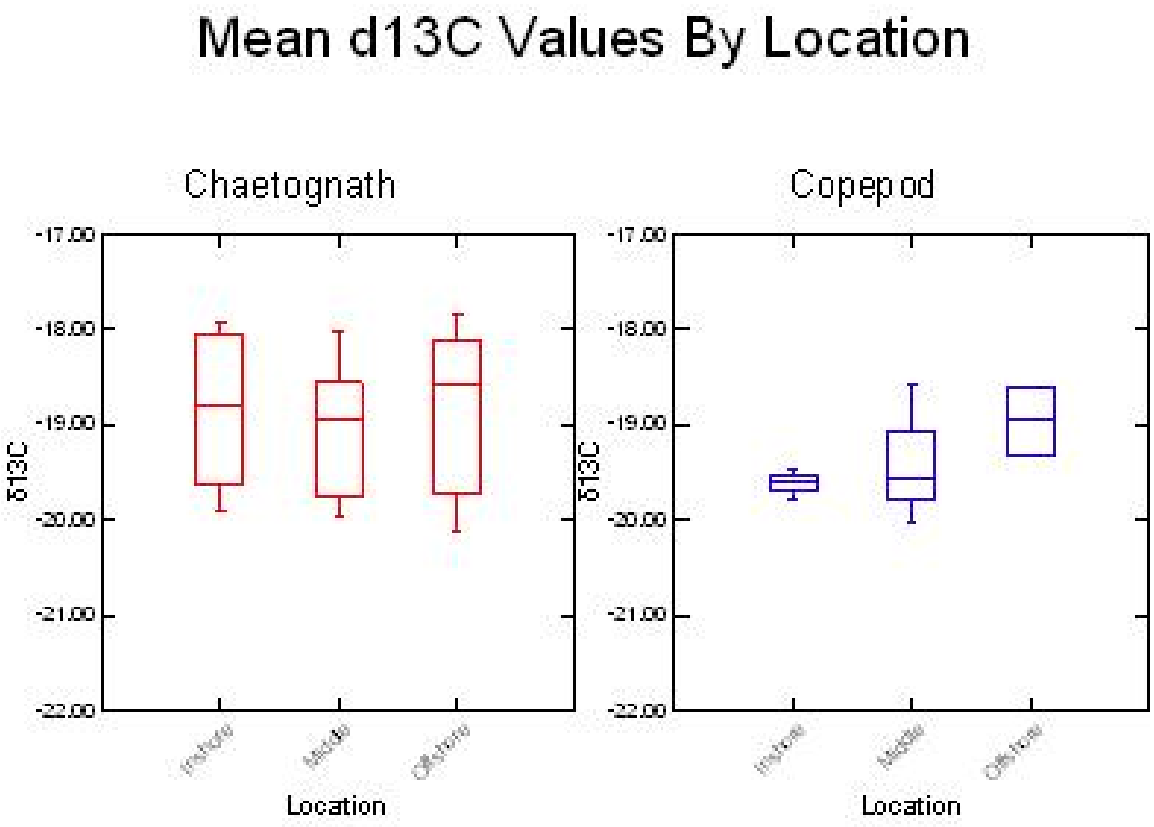

Figure 34. The $\delta^{13}C$ values (‰) by location for each taxon. The box indicates the values of the first quartile, median, and third quartile. The whiskers indicate the next values below the first quartile and above the third quartile.

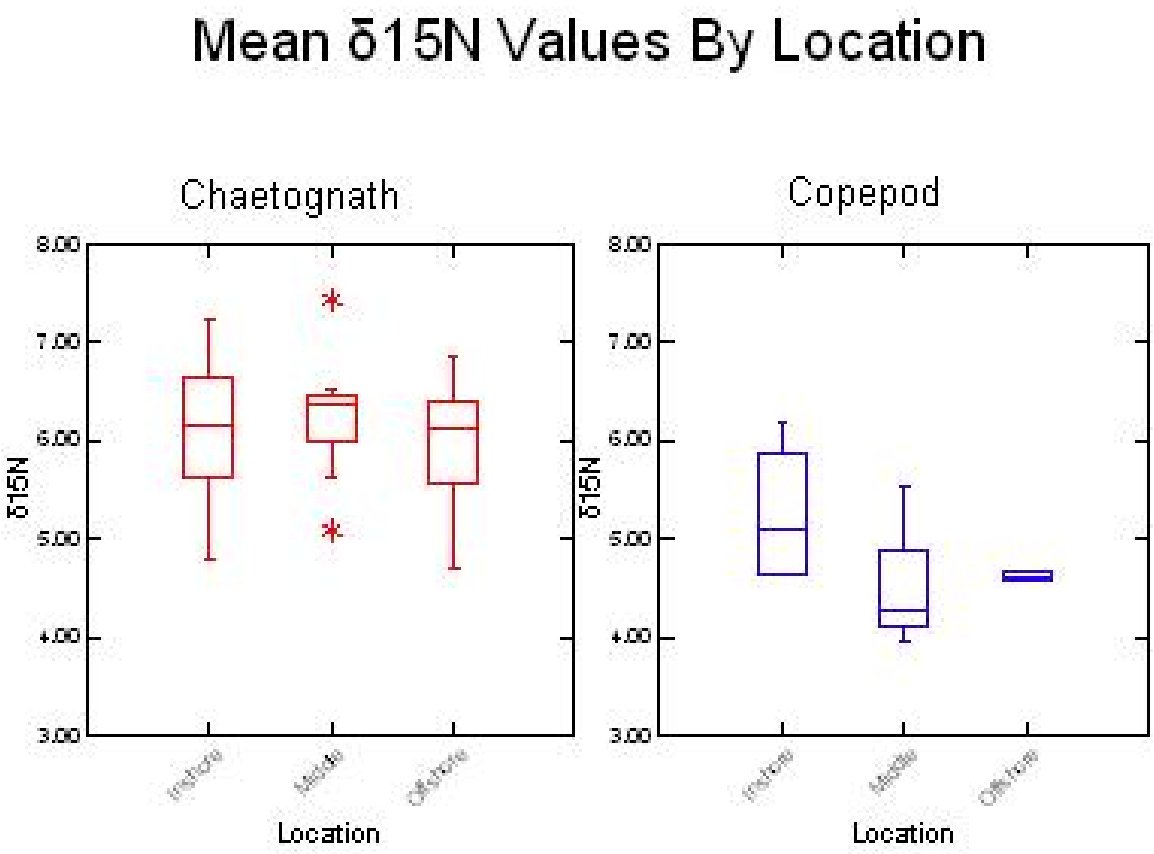

Figure 35. The $\delta^{15}N$ values (‰) by month for each taxon. The box indicates the values of the first quartile, median, and third quartile. The whiskers indicate the next values below the first quartile and above the third quartile. The stars represent the far outside values.

4.2.3.4. Density and Stable Isotope Results by Depth

Analysis of values by depth only showed the high mean density of both taxa was found at the deep tow, while the lowest mean density was found at the shallow tow. Mean calanoid copepod density (#/m^3) ranged from 8.0 (SD=6.2, n=15) to 3.2 (SD=5.1, n=15). Mean chaetognath density ranged (#/m^3) from 2.9 (SD=2.7, n=15) to 1.7 (SD=2.1, n=15).

The lowest mean $\delta^{13}C$ of both taxa was found at the deep tow while the highest mean $\delta^{13}C$ was found at the shallow tow. Mean calanoid copepod $\delta^{13}C$ (‰) ranged from -20.1 (SD=0.6, n=15) to -20.1 (SD=0.9, n=14). Mean chaetognath $\delta^{13}C$ (‰) ranged from -19.01 (SD=0.8, n=15) to -18.9 (SD=0.8, n=14). Mean calanoid copepod $\delta^{15}N$ (‰) was lowest at the deep tow and highest at the shallow tow. The $\delta^{15}N$ ranged from 5.1 (SD=0.7, n=15) to 5.3 (SD=1.0, n=14). Mean chaetognath $\delta^{15}N$ is highest at the deep tow and lowest at the shallow tow, and $\delta^{15}N$ (‰) ranged from 5.9 (SD=0.7, n=14) to 6.3 (SD=0.6, n=15) (Table 19, Figures 36 - 38). Shapiro-Wilk's test of normality indicated that calanoid copepod, chaetognath density, and chaetognath $\delta^{13}C$ were not normally distributed for at least one of the depth categories, and non-parametric methods should be used for further statistical analyses (Table 20). Mann-Whitney U test showed a significant difference in calanoid copepod density between the shallow and deep tow ($U(29) = 43.000$, $Z = 2.862$, $p=0.004$, $\alpha = 0.05$). No other variables were significantly different (Table 21).

Table 16. Shapiro-Wilk's test of normality for all taxa. N = 10 for all variables, except for Inshore copepod and chaetognath carbon and nitrogen isotope values, where N = 9. P values < 0.05 are considered not normally distributed.

Shapiro-Wilk's Test of Normality α = 0.05, p value			
	Inshore	**Middle**	**Offshore**
Copepod Density (#/m^3)	0.008	0.014	0.145
Chaetognath Density (#/m^3)	0.149	0.001	0.086
Copepod δ13C (‰)	0.438	0.825	0.161
Chaetognath δ13C (‰)	0.169	0.037	0.156
Copepod δ15N (‰)	0.652	0.476	0.054
Chaetognath δ15N (‰)	0.628	0.814	0.556

Table 17. Parametric and non-parametric ANOVA results. P values < 0.05 indicate a significant difference.

Parametric and Non-parametric ANOVA Results by Location α = 0.05			
	Test	**H/F values**	**p value**
Copepod Density (#/m^3)	Kruskal-Wallis ANOVA	(2, 30) = 2.516	0.284
Chaetognath Density (#/m^3)	Kruskal-Wallis ANOVA	(2, 30) = 6.970	0.031
Copepod δ13C (‰)	One-way ANOVA	(1, 2) = 0.026	0.974
Chaetognath δ13C (‰)	One-way ANOVA	(1, 2) = 0.297	0.746
Copepod δ15N (‰)	One-way ANOVA	(1, 2) = 1.711	0.200
Chaetognath δ15N (‰)	One-way ANOVA	(1, 2) = 0.116	0.891

Table 18. Parametric and non-parametric post-hoc analysis results. P values < 0.05 indicate a significant difference.

Post Hoc Analysis			
Test	**Dependent Variable**	**Locations**	**p value**
Multiple Comparisons	Chaetognath Density	Inshore (Offshore)	0.038

Table 19. Descriptive statistics by depth for each taxon.

Descriptive Statistics By Depth			N	Mean	Med	Min	Max	Rng	SD
Density (#/m3)	**Calanoid**	Shallow	15	3.21	1.20	0.08	19.64	19.56	5.14
	Copepod	Deep	15	7.98	5.11	1.18	22.57	21.39	6.17
	Chaet	Shallow	15	1.74	0.91	0.11	6.40	6.29	2.11
		Deep	15	2.91	1.48	0.41	8.35	7.95	2.72
$\delta^{13}C$ (‰)	**Calanoid**	Shallow	14	-20.05	-20.12	-21.34	-18.57	2.77	0.91
	Copepod	Deep	15	-20.10	-19.99	-21.31	-19.32	2.00	0.60
	Chaet	Shallow	14	-18.87	-18.72	-19.98	-17.92	2.06	0.77
		Deep	15	-18.95	-18.67	-20.13	-17.84	2.29	0.84
δ15N (‰)	**Calanoid**	Shallow	14	5.30	5.16	3.94	7.18	3.24	1.04
	Copepod	Deep	15	5.14	5.08	3.96	6.17	2.21	0.65
	Chaet	Shallow	14	5.86	5.94	4.70	6.85	2.16	0.66
		Deep	15	6.33	6.40	5.09	7.43	2.34	0.63

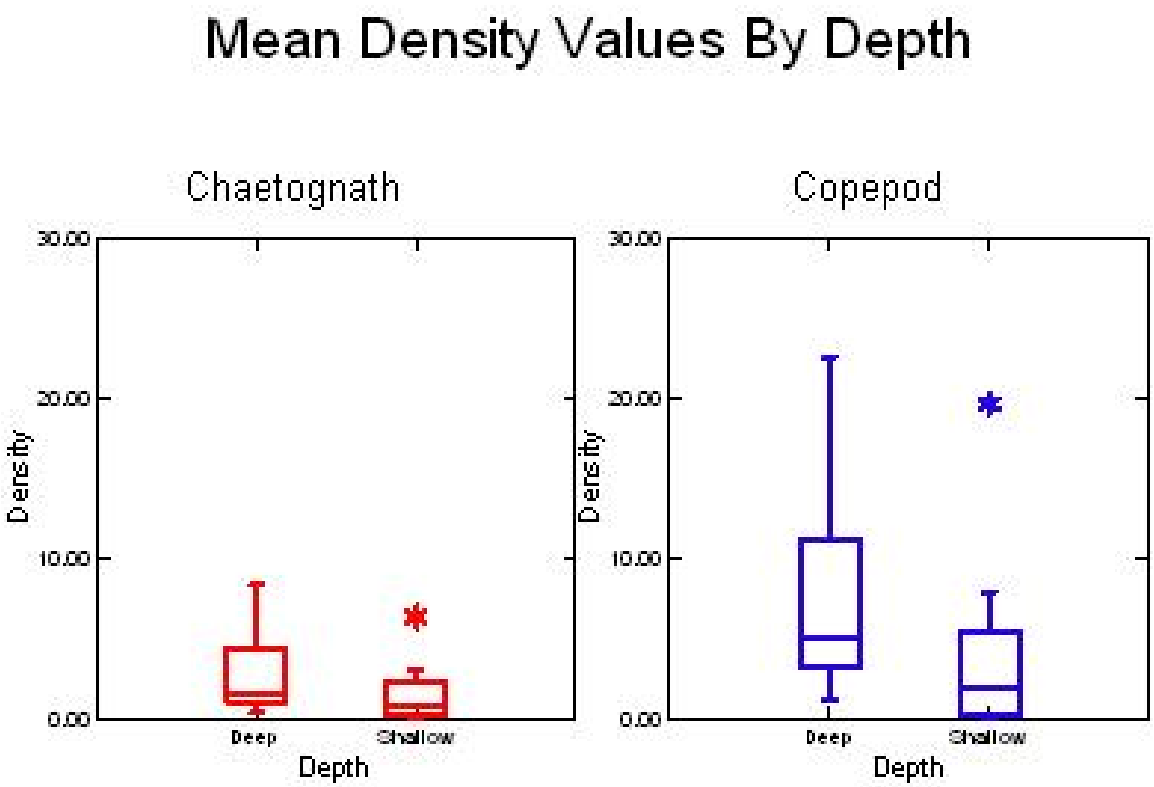

Figure 36. Density values (#/m^3) by depth for each taxon. The box indicates the values of the first quartile, median, and third quartile. The whiskers indicate the next values below the first quartile and above the third quartile. The stars represent the far outside values.

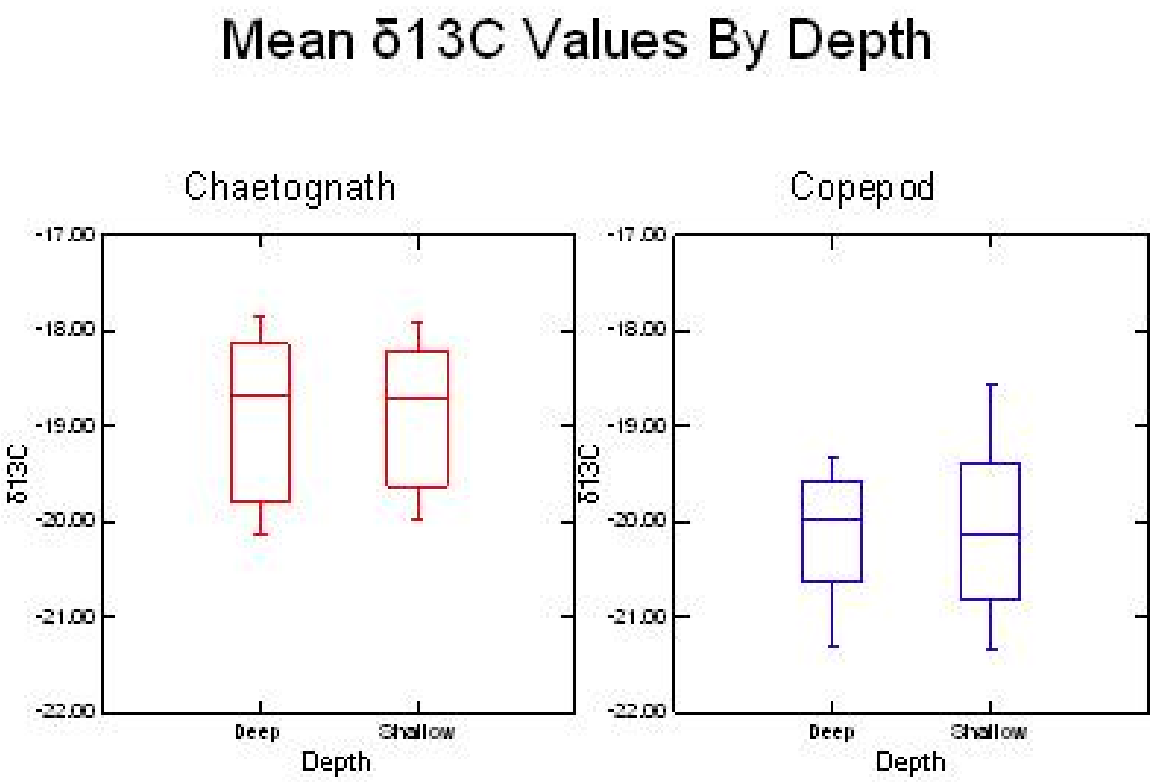

Figure 37. The $\delta^{13}C$ values (‰) by depth for each taxon. The box indicates the values of the first quartile, median, and third quartile. The whiskers indicate the next values below the first quartile and above the third quartile.

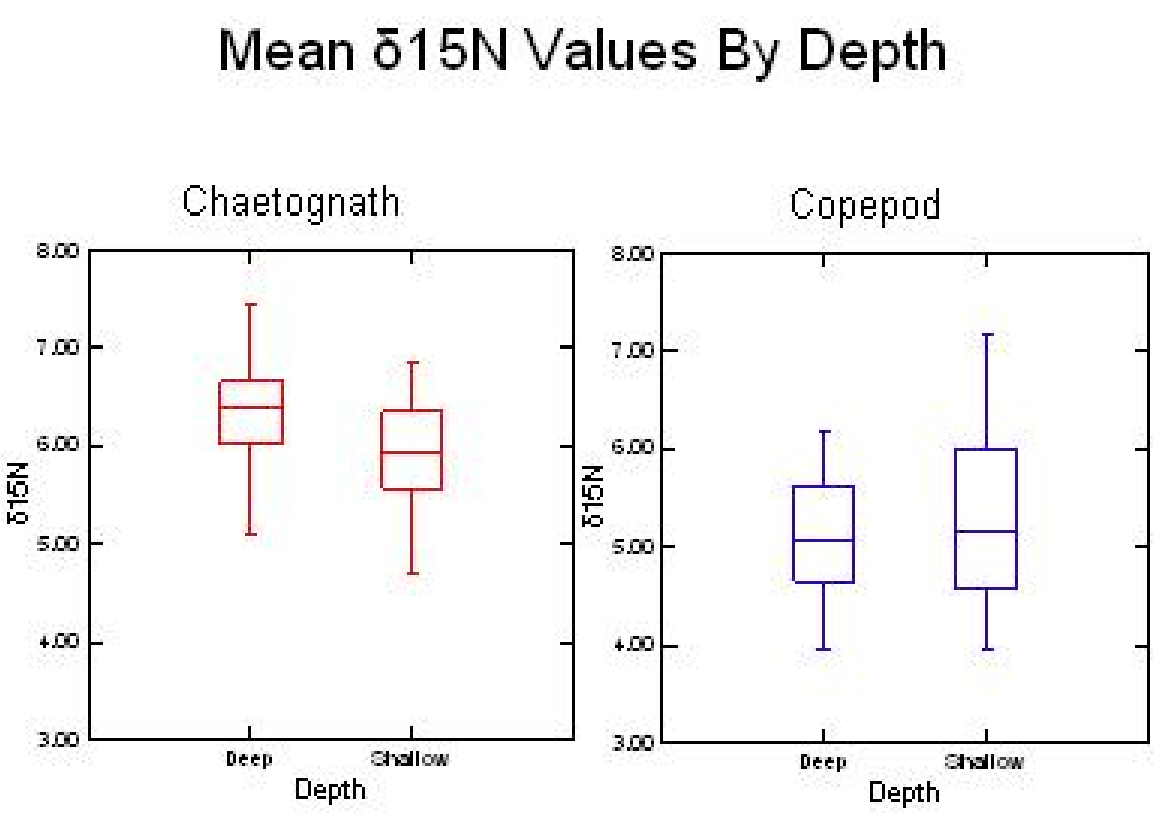

Figure 38. The $\delta^{15}N$ values (‰) by depth for each taxon. The box indicates the values of the first quartile, median, and third quartile. The whiskers indicate the next values below the first quartile and above the third quartile.

Table 20. Shapiro-Wilk's test of normality for each taxon. N = 15 for all variables, except for Shallow copepod and chaetognath carbon and nitrogen isotope values, where N = 14. P values < 0.05 are considered not normally distributed.

Shapiro-Wilk's Test of Normality		
α = 0.05, p-value		
	Shallow	**Deep**
Copepod Density (#/m^3)	0.000	0.0378
Chaetognath Density (#/m^3)	0.001	0.0026
Copepod δ13C (‰)	0.263	0.21657
Chaetognath δ13C (‰)	0.065	0.04542
Copepod δ15N (‰)	0.399	0.81475
Chaetognath δ15N (‰)	0.599	0.85482

Table 21. Parametric and non-parametric t-test results by depth for each taxon. P values < 0.05 indicate a significant difference.

Parametric and Non-parametric t-test Results by Depth				
α = 0.05, p-value				
	Test	**U/ t value**	**Z value**	**p value**
Copepod Density (#/m^3)	Mann-Whitney U	(29) = 43.000	2.862	0.004
Chaetognath Density (#/m^3)	Mann-Whitney U	(29) = 72.000	-0.458	0.098
Copepod δ13C (‰)	t-test	(28) = -0.163	-	0.872
Chaetognath δ13C (‰)	Mann-Whitney U	(28) = 94.000	-0.458	0.647
Copepod δ15N (‰)	t-test	(28) = -0.517	-	0.610
Chaetognath δ15N (‰)	t-test	(28) = 1.953	-	0.061

4.2.3.5. Density and Stable Isotope Results by Month*Location

When breaking down the month only statistics further by location, the highest mean values were distributed differently by location* month. During April, calanoid copepod and chaetognath mean densities (#/m^3) were highest Inshore, 21.1 (SD=2.1, n=2) and 7.4 (SD=1.4, n=2), respectively. During May, calanoid copepod and chaetognath mean densities (#/m^3) were highest Inshore, 6.0 (SD=5.7, n=2) and 3.7 (SD=3.9, n=2), respectively. During July, calanoid copepod and chaetognath mean densities (#/m^3) were highest at the Middle station, 5.7 (SD=7.8, n=2), and 3.3 (SD=4.0, n=2), respectively. September calanoid copepod mean density (#/m^3) was highest Offshore, 4.8 (SD=4.1, n=2). September chaetognath mean density (#/m^3) was highest Inshore, 2.3 (SD=1.2, n=2. November calanoid copepod mean density (#/m^3) was highest Offshore, 8.1 (SD=10.5, n=2). November chaetognath mean density was highest Inshore, 7.0 (SD=0.8, n=2). During April calanoid copepod and chaetognath mean $\delta^{13}C$ (‰) was highest Offshore, -20.7 (SD= 0.0, n=2) and -19.8 SD=0.1, n=2), respectively. In May, calanoid copepod and chaetognath mean $\delta^{13}C$ (‰) was highest Offshore, -20.6 (SD=0.2, n=2) and -19.4 (SD=0.3, n=2), respectively. In July, calanoid copepod and chaetognath mean $\delta^{13}C$ (‰) is highest Offshore, -19.6 (SD=0.3, n=2) and -18.5 (SD=0.2, n=2), respectively. September calanoid copepod mean $\delta^{13}C$ (‰) was highest Inshore, -19.3 (SD=0.1, n=2). September chaetognath mean $\delta^{13}C$ (‰) was highest Offshore, -18.0 (SD=0.1, n=2). November calanoid copepod mean $\delta^{13}C$ (‰) was highest Inshore, -18.9 (SD=0.5, n=2). November chaetognath mean $\delta^{13}C$ (‰) was highest at the Middle station, -18.2 (SD=0.4, n=2). During April, calanoid copepod and chaetognath mean $\delta^{15}N$ (‰) was highest Offshore, 5.8 (SD=1.8, n=2), and 6.9 (SD=0.8, n=2), respectively. May

calanoid copepod $\delta^{15}N$ was highest at the Middle station, 5.9 (SD=0.1, n=2). May chaetognath $\delta^{15}N$ (‰) was highest Inshore, 6.6 (SD=0.7, n=2). July calanoid copepod mean $\delta^{15}N$ (‰) was highest at the Middle station, 6.4 (SD=1.0, n=2). July chaetognath mean $\delta^{15}N$ (‰) was highest Inshore, 6.3 (n=1). September calanoid copepod mean $\delta^{15}N$ (‰) was highest at the Middle station, 5.2 (SD=1.4, n=2). September chaetognath mean $\delta^{15}N$ (‰) was highest Offshore, 6.5 (SD=0.1, n=2). November calanoid copepod mean $\delta^{15}N$ (‰) was highest Inshore, 5.1 (SD=0.6, n=2). November chaetognath mean $\delta^{15}N$ (‰) was highest at the Middle station, 5.7 (SD=0.2, n=2) (Table 22, Figures 39 - 41).

The ANOVA results indicated that calanoid copepod $\delta^{13}C$ was significantly different between months and locations ($F(1, 14) = 10.5$, $p<0.001$, $\alpha = 0.05$) and Kruskal-Wallis ANOVA by Ranks results indicate that chaetognath $\delta^{13}C$ was significantly different between months and locations ($H(14, 29) = 24.290$, $p=0.042$, $\alpha = 0.05$). Tukey HSD showed that there was no significant difference in calanoid copepod $\delta^{13}C$ between locations within months, but there were significant differences for locations between different months. April locations and May locations did not differ and September locations and November locations did not differ, but both April and May locations did differ from both September and November locations. The multiple comparisons post-hoc analysis is a conservative analysis and did not show any specific differences in chaetognath $\delta^{13}C$. The less conservative Tukey post-hoc test was run to determine where possible differences may lie. Chaetognath $\delta^{13}C$ showed the same trend as the calanoid copepod $\delta^{13}C$, no differences between locations within months, but differences for locations between months. April and May locations for chaetognath $\delta^{13}C$ differed from both September and November locations (Tables 23 - 24).

Table 22. Density descriptive statistics by Month and Location for each taxon.

Density Descriptive Statistics By Month*Location									
			N	**Mean**	**Med**	**Min**	**Max**	**Rng**	**SD**
Calanoid Copepod	April	In	2	21.11	21.11	19.64	22.57	2.93	2.07
		Mid	2	5.42	5.42	2.91	7.92	5.01	3.54
		Off	2	10.55	10.55	5.88	15.21	9.33	6.60
	May	In	2	5.97	5.97	1.93	10.01	8.08	5.71
		Mid	2	1.83	1.83	0.21	3.44	3.23	2.29
		Off	2	5.77	5.77	0.25	11.29	11.04	7.81
	July	In	2	2.24	2.24	0.25	4.22	3.97	2.81
		Mid	2	5.67	5.67	0.17	11.17	11.01	7.78
		Off	2	2.59	2.59	0.08	5.11	5.03	3.56
	Sept	In	2	2.70	2.70	2.42	2.98	0.56	0.40
		Mid	2	1.19	1.19	1.18	1.20	0.02	0.01
		Off	2	4.79	4.79	1.87	7.70	5.82	4.12
	Nov	In	2	4.29	4.29	3.47	5.11	1.64	1.16
		Mid	2	1.75	1.75	0.51	2.99	2.47	1.75
		Off	2	8.10	8.10	0.70	15.50	14.80	10.46
Chaetognath	April	In	2	7.38	7.38	6.40	8.35	1.96	1.38
		Mid	2	1.79	1.79	1.23	2.35	1.12	0.79
		Off	2	2.38	2.38	2.28	2.47	0.19	0.13
	May	In	2	3.65	3.65	0.91	6.39	5.48	3.87
		Mid	2	0.40	0.40	0.16	0.63	0.47	0.33
		Off	2	0.66	0.66	0.13	1.18	1.05	0.74
	July	In	2	1.10	1.10	0.24	1.97	1.73	1.22
		Mid	2	3.26	3.26	0.45	6.06	5.61	3.97
		Off	2	0.49	0.49	0.11	0.88	0.77	0.55
	Sept	In	2	2.28	2.28	1.46	3.10	1.64	1.16
		Mid	2	1.42	1.42	1.35	1.48	0.13	0.09
		Off	2	0.74	0.74	0.53	0.95	0.42	0.30
	Nov	In	2	6.96	6.96	6.39	7.54	1.15	0.81
		Mid	2	0.93	0.93	0.41	1.46	1.06	0.75
		Off	2	1.44	1.44	0.24	2.63	2.39	1.69

Table 23. $\delta^{13}C$ descriptive statistics by Month and Location for each taxon.

$\delta^{13}C$ Descriptive Statistics By Month*Location			N	Mean	Med	Min	Max	Rng	SD
Calanoid Copepod	April	In	2	-21.21	-21.21	-21.31	-21.10	0.21	0.15
		Mid	2	-20.96	-20.96	-21.34	-20.59	0.76	0.53
		Off	2	-20.68	-20.68	-20.69	-20.67	0.02	0.02
	May	In	2	-20.74	-20.74	-20.80	-20.68	0.12	0.09
		Mid	2	-20.75	-20.75	-20.83	-20.68	0.15	0.10
		Off	2	-20.61	-20.61	-20.74	-20.49	0.26	0.18
	July	In	1	-19.82	-19.82	-19.82	-19.82		
		Mid	2	-20.23	-20.23	-20.46	-19.99	0.48	0.34
		Off	2	-19.64	-19.64	-19.88	-19.40	0.48	0.34
	Sept	In	2	-19.34	-19.34	-19.43	-19.25	0.19	0.13
		Mid	2	-19.59	-19.59	-19.60	-19.58	0.02	0.02
		Off	2	-19.83	-19.83	-20.04	-19.61	0.42	0.30
	Nov	In	2	-18.94	-18.94	-19.32	-18.57	0.75	0.53
		Mid	2	-19.04	-19.04	-19.47	-18.60	0.87	0.62
		Off	2	-19.67	-19.67	-19.78	-19.55	0.23	0.16
Chaetognath	April	In	2	-19.85	-19.85	-19.86	-19.83	0.03	0.02
		Mid	2	-19.74	-19.74	-19.90	-19.58	0.32	0.23
		Off	2	-19.69	-19.69	-19.74	-19.63	0.11	0.08
	May	In	2	-20.05	-20.05	-20.13	-19.98	0.15	0.10
		Mid	2	-19.78	-19.78	-19.85	-19.72	0.13	0.09
		Off	2	-19.45	-19.45	-19.68	-19.21	0.47	0.33
	July	In	1	-18.67	-18.67	-18.67	-18.67		
		Mid	2	-18.64	-18.64	-19.17	-18.12	1.06	0.75
		Off	2	-18.51	-18.51	-18.62	-18.40	0.22	0.16
	Sept	In	2	-18.39	-18.39	-18.95	-17.84	1.12	0.79
		Mid	2	-17.99	-17.99	-18.05	-17.93	0.12	0.09
		Off	2	-17.98	-17.98	-18.03	-17.92	0.11	0.08
	Nov	In	2	-18.24	-18.24	-18.24	-18.23	0.01	0.01
		Mid	2	-18.21	-18.21	-18.48	-17.94	0.55	0.39
		Off	2	-18.39	-18.39	-18.56	-18.21	0.35	0.24

Table 24. $\delta^{15}N$ descriptive statistics by Month and Location for each taxon.

$\delta^{15}N$ Descriptive Statistics By Month*Location			N	Mean	Med	Min	Max	Rng	SD
Calanoid Copepod	April	In	2	5.63	5.63	5.06	6.19	1.13	0.80
		Mid	2	5.27	5.27	4.63	5.91	1.28	0.91
		Off	2	5.79	5.79	4.54	7.03	2.49	1.76
	May	In	2	5.36	5.36	5.23	5.49	0.27	0.19
		Mid	2	5.93	5.93	5.88	5.99	0.11	0.08
		Off	2	4.95	4.95	4.80	5.10	0.30	0.21
	July	In	1	5.08	5.08	5.08	5.08		
		Mid	2	6.43	6.43	5.67	7.18	1.51	1.06
		Off	2	4.98	4.98	4.07	5.88	1.81	1.28
	Sept	In	2	4.69	4.69	3.94	5.43	1.49	1.06
		Mid	2	5.20	5.20	4.24	6.17	1.93	1.37
		Off	2	4.45	4.45	4.26	4.64	0.38	0.27
	Nov	In	2	5.09	5.09	4.66	5.52	0.86	0.61
		Mid	2	5.06	5.06	4.57	5.56	0.99	0.70
		Off	2	4.31	4.31	3.96	4.65	0.70	0.49
Chaetognath	April	In	2	6.37	6.37	6.35	6.40	0.05	0.04
		Mid	2	6.77	6.77	6.69	6.85	0.16	0.11
		Off	2	6.86	6.86	6.30	7.43	1.13	0.80
	May	In	2	6.59	6.59	6.40	6.78	0.38	0.27
		Mid	2	6.55	6.55	5.88	7.22	1.34	0.95
		Off	2	5.92	5.92	5.61	6.22	0.62	0.43
	July	In	1	6.26	6.26	6.26	6.26		
		Mid	2	5.68	5.68	4.70	6.65	1.96	1.38
		Off	2	5.82	5.82	5.12	6.52	1.40	0.99
	Sept	In	2	5.82	5.82	5.62	6.02	0.40	0.28
		Mid	2	6.11	6.11	6.02	6.20	0.18	0.13
		Off	2	6.55	6.55	6.47	6.63	0.16	0.12
	Nov	In	2	5.64	5.64	5.28	6.00	0.72	0.51
		Mid	2	5.71	5.71	5.57	5.85	0.28	0.20
		Off	2	4.93	4.93	4.78	5.09	0.31	0.22

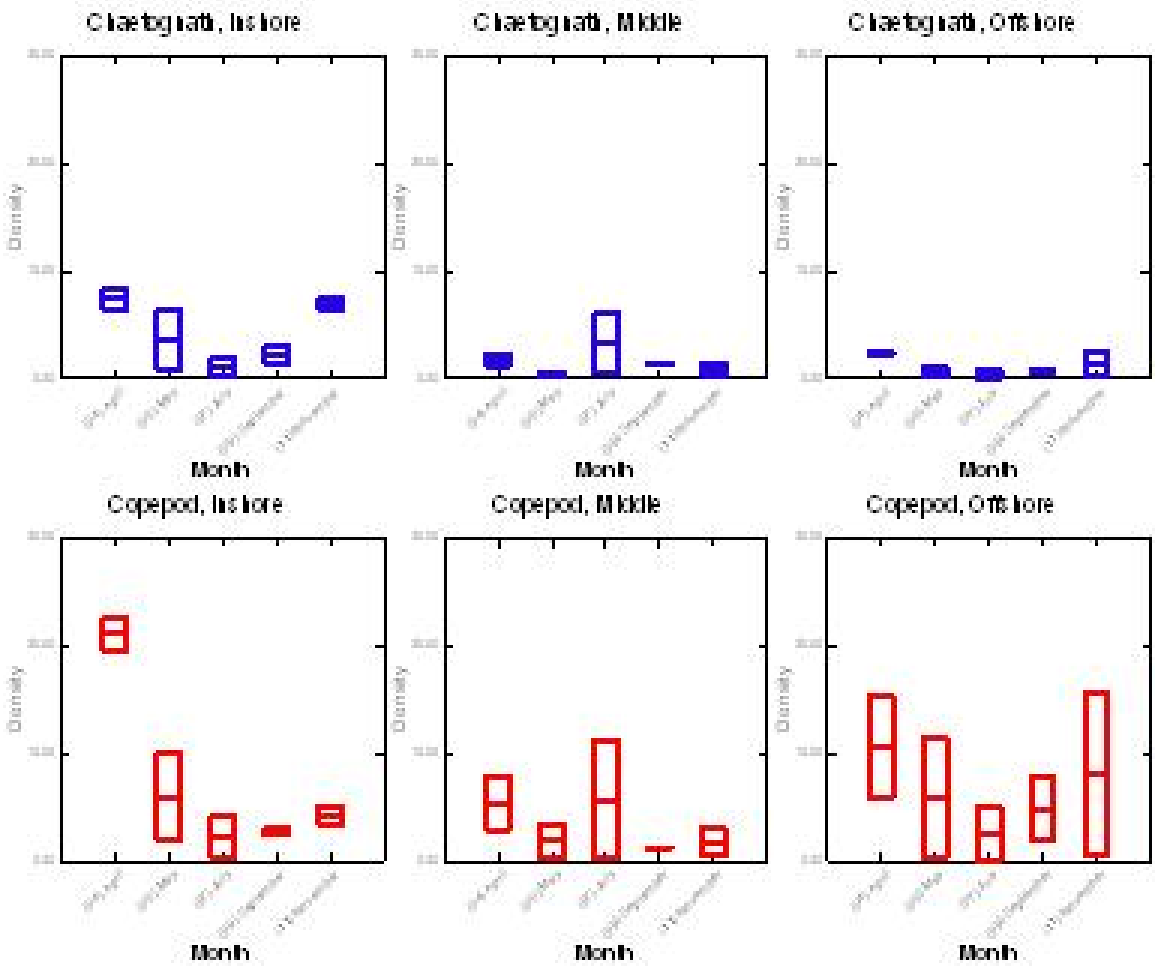

Figure 39. Calanoid copepod and chaetognath density values (#/m^3) by month and location. The box indicates the values of the first quartile, median, and third quartile. The whiskers indicate the next values below the first quartile and above the third quartile.

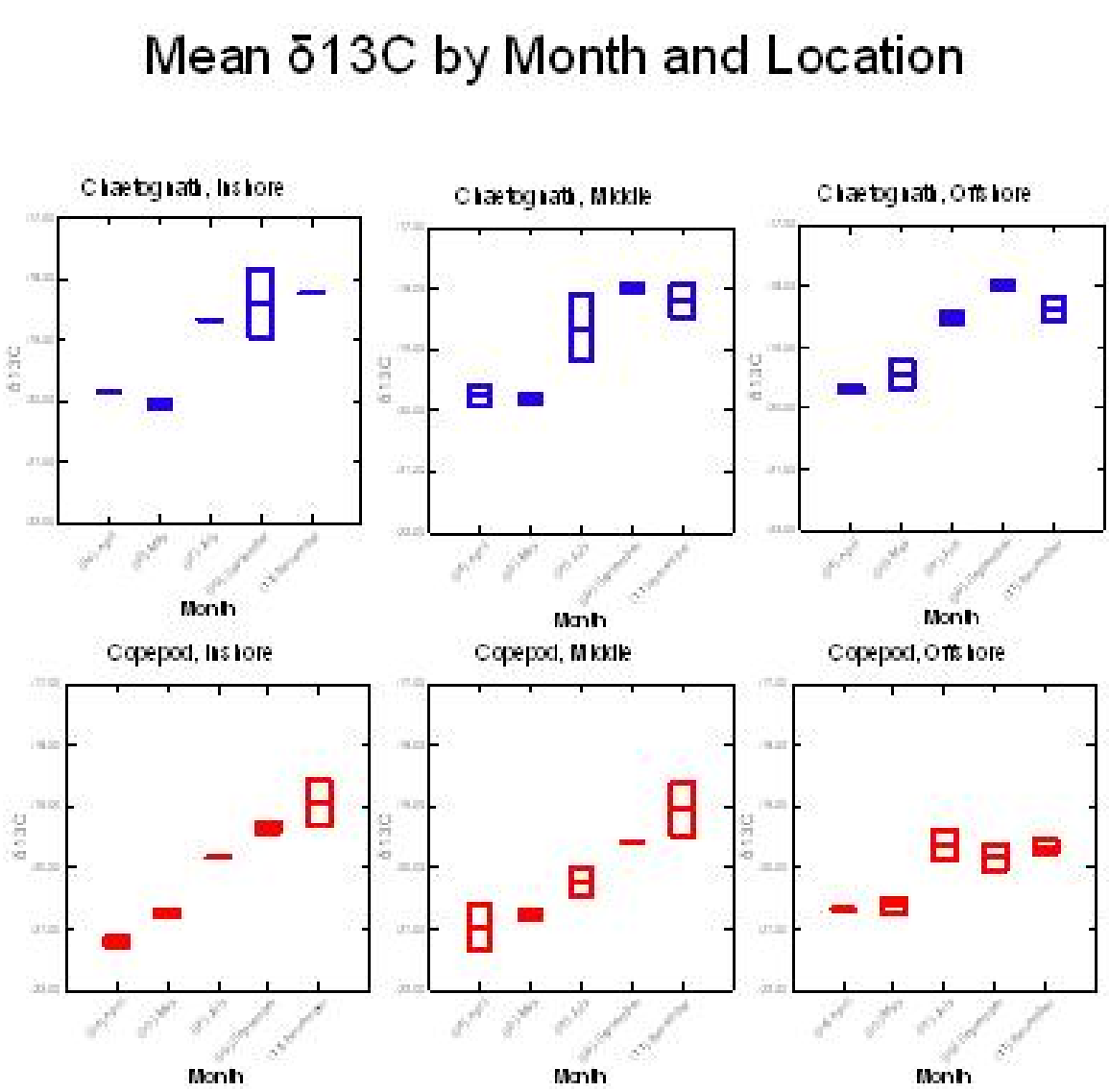

Figure 40. Calanoid copepod and chaetognath $\delta^{13}C$ values (‰) by month and location. The box indicates the values of the first quartile, median, and third quartile. The whiskers indicate the next values below the first quartile and above the third quartile.

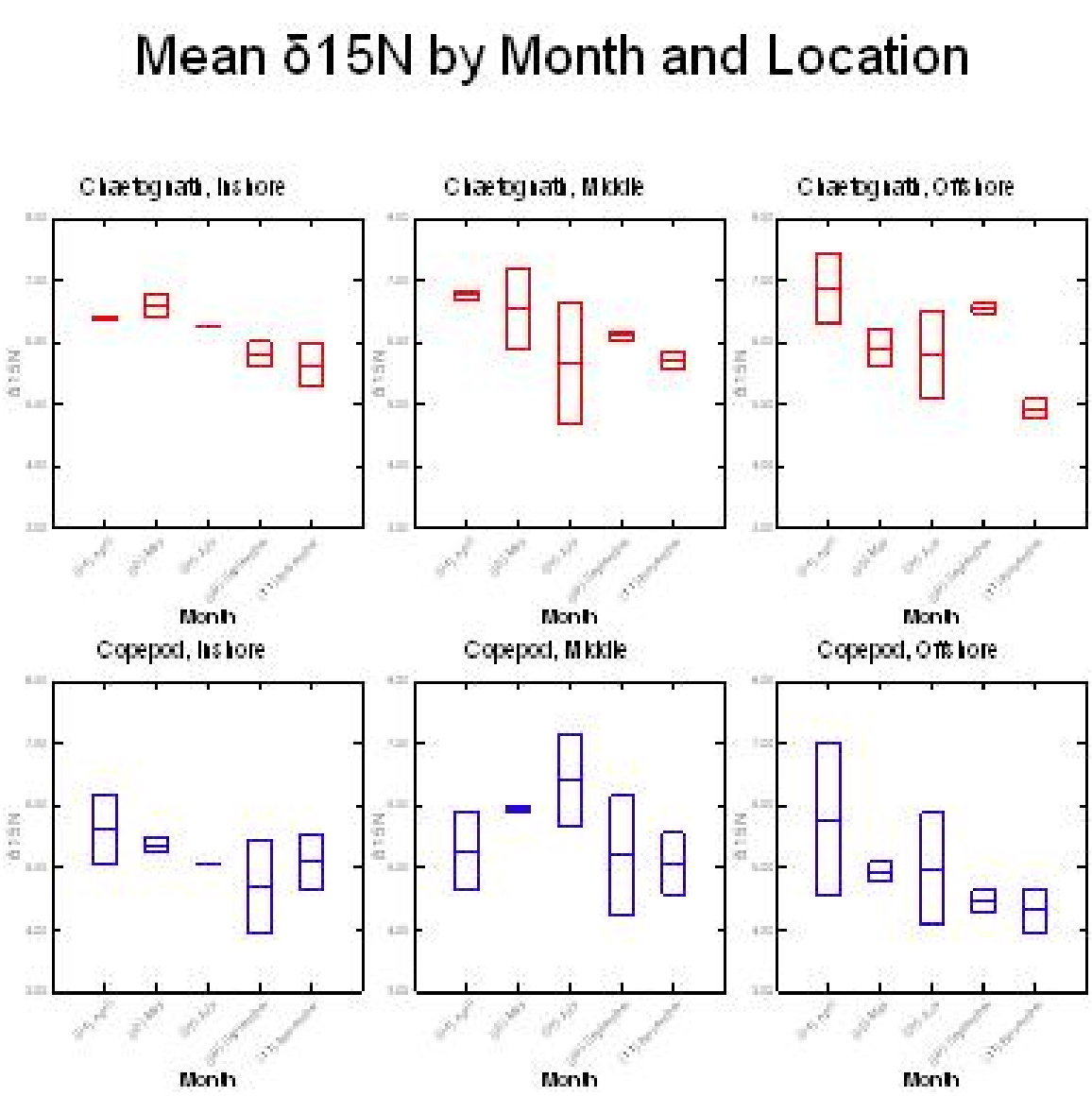

Figure 41. Calanoid copepod and chaetognath $\delta^{15}N$ values (‰) by month and location. The box indicates the values of the first quartile, median, and third quartile. The whiskers indicate the next values below the first quartile and above the third quartile.

Table 25. Parametric and nonparametric ANOVA results by month and location. P values < 0.05 indicate a significant difference.

Parametric and Non-parametric ANOVA Results by Month*Location $\alpha = 0.05$			
	Test	**H/F values**	**p value**
Copepod Density (#/m^3)	Kruskal-Wallis ANOVA	(14, 30) = 11.832	0.620
Chaetognath Density (#/m^3)	Kruskal-Wallis ANOVA	(14, 30) = 18.400	0.189
Copepod δ13C (‰)	One-way ANOVA	(1, 14) = 10.5	< 0.001
Chaetognath δ13C (‰)	Kruskal-Wallis ANOVA	(14, 29) = 24.290	0.042
Copepod δ15N (‰)	One-way ANOVA	(1, 14) = 0.755	0.697
Chaetognath δ15N (‰)	One-way ANOVA	(1, 14) = 1.496	0.230

Table 26. Parametric and nonparametric post hoc analysis results by month and location. P values < 0.05 indicate a significant difference.

Parametric and Nonparametric Post Hoc Results				
Test	**Dependent Variable**	**Month*Location**		**p value**
Tukey HSD	Calanoid Copepod $\delta^{13}C$	April Inshore	July Offshore	0.010
			Sept Inshore	0.002
			Sept Middle	0.007
			Sept Offshore	0.027
			Nov Inshore	0.000
			Nov Middle	0.001
			Nov Offshore	0.012
		April Middle	July Offshore	0.037
			Sept Inshore	0.007
			Sept Middle	0.028
			Nov Inshore	0.001
			Nov Middle	0.002
			Nov Offshore	0.044
		April Offshore	Sept Inshore	0.034
			Nov Inshore	0.004
			Nov Middle	0.007
		May Inshore	Sept Inshore	0.024
			Nov Inshore	0.003
			Nov Middle	0.005
		May Middle	Sept Inshore	0.023
			Nov Inshore	0.003
			Nov Middle	0.004
		May Offshore	Sept Inshore	0.049
			Nov Inshore	0.006
			Nov Middle	0.009
		July Middle	Nov Inshore	0.047
			Nov Middle	0.077

Table 27. Parametric and non-parametric post hoc analysis results by month and location. P values < 0.05 indicate a significant difference.

Parametric and Nonparametric Post Hoc Results				
Test	**Dependent Variable**	**Month*Location**		**p value**
Tukey HSD	Chaetognath $\delta^{13}C$	April Inshore	Sept Inshore	0.034
			Sept Middle	0.005
			Sept Offshore	0.004
			Nov Inshore	0.015
			Nov Middle	0.013
			Nov Offshore	0.032
		April Middle	Sept Middle	0.007
			Sept Offshore	0.007
			Nov Inshore	0.026
			Nov Middle	0.022
		April Offshore	Sept Middle	0.010
			Sept Offshore	0.009
			Nov Inshore	0.034
			Nov Middle	0.030
			Nov Offshore	0.072
		May Inshore	July Middle	0.042
			July Offshore	0.022
			Sept Inshore	0.012
			Sept Middle	0.002
			Sept Offshore	0.002
			Nov Inshore	0.005
			Nov Middle	0.005
			Nov Offshore	0.012
		May Middle	Sept Inshore	0.046
			Sept Middle	0.006
			Sept Offshore	0.006
			Nov Inshore	0.021
			Nov Middle	0.018
			Nov Offshore	0.044
		May Offshore	Sept Middle	0.033

4.2.3.6. Density and Stable Isotope Results by Month*Depth

When breaking down the month only statistics by depth, the highest mean calanoid copepod density (#/m^3) values were found at the deep tow for all months (April, 13.6 SD= 9.9, n = 3; May, 8.2 SD=4.2, n = 3; July, 6.8 SD=3.8, n = 3; September, 4.0 SD=3.4, n = 3; November, 7.3 SD=7.1, n = 3). Chaetognath mean densities (#/m^3) were highest at the deep tow during April, July, and November (4.0 SD=3.8, n = 3; 3.0 SD=2.7, n = 3; 3.5 SD=3.6, n = 3, respectively), while mean density (#/m^3) was highest in the shallow tow during May and September (2.7 SD=3.2, n = 3; 1.7 SD=1.3, n = 3, respectively).

Mean calanoid copepod $\delta^{13}C$ (‰) was highest at the deep tow during July (-19.9 SD=0.1, n = 3) and highest at the shallow tow during April, May, September and November (-20.9 SD=0.4, n = 3; -20.6 SD=0.1, n = 3; -19.5 SD=0.2, n = 3; -19.0 SD=0.7, n = 3, respectively). Mean chaetognath $\delta^{13}C$ (‰) was highest at the deep tow during September and November (-18.0 SD=0.1, n = 3; -18.2 SD=0.3, n = 3, respectively) and highest at the shallow tow during April, May, and July (-19.7 SD=0.1, n = 3; -19.6 SD=0.4, n=3; -18.3 SD=0.2, n = 2, respectively).

Mean calanoid copepod $\delta^{15}N$ (‰) was highest at the deep tow during May and September (5.4 SD=0.5, n = 3; 5.3 SD=1.0, n = 3, respectively) and highest at the shallow tow during April, July and November (6.4 SD=0.6, n = 3; 5.6 SD=2.2, n = 2; 4.9 SD=0.5, n = 3, respectively). Mean chaetognath $\delta^{15}N$ (‰) was highest at the deep town during April, May, July, and September (6.8 SD=0.5, n = 3; 6.7 SD=0.5, n = 3; 6.5 SD=0.2, n = 3; 6.2 SD=0.3, n = 3, respectively) and was highest at the shallow tow during November (5.4 SD=0.6, n = 3) (Table 25, Figures 42 - 44).

Table 28. Density descriptive statistics by month and depth for each taxon.

Density Descriptive Statistics By Month*Depth									
			N	Mean	Med	Min	Max	Rng	SD
Calanoid	April	Shal	3	11.15	7.92	5.88	19.64	13.76	7.42
Copepod		Deep	3	13.57	15.21	2.91	22.57	19.66	9.93
	May	Shal	3	0.80	0.25	0.21	1.93	1.72	0.98
		Deep	3	8.25	10.01	3.44	11.29	7.85	4.21
	July	Shal	3	0.17	0.17	0.08	0.25	0.17	0.09
		Deep	3	6.83	5.11	4.22	11.17	6.95	3.78
	Sept	Shal	3	1.83	1.87	1.20	2.42	1.21	0.61
		Deep	3	3.95	2.98	1.18	7.70	6.51	3.36
	Nov	Shal	3	2.11	0.70	0.51	5.11	4.60	2.60
		Deep	3	7.32	3.47	2.99	15.50	12.51	7.09
Chaet	April	Shal	3	3.68	2.35	2.28	6.40	4.12	2.36
		Deep	3	4.02	2.47	1.23	8.35	7.13	3.81
	May	Shal	3	2.74	1.18	0.63	6.39	5.76	3.18
		Deep	3	0.40	0.16	0.13	0.91	0.78	0.44
	July	Shal	3	0.27	0.24	0.11	0.45	0.34	0.17
		Deep	3	2.97	1.97	0.88	6.06	5.19	2.73
	Sept	Shal	3	1.66	1.35	0.53	3.10	2.57	1.31
		Deep	3	1.30	1.46	0.95	1.48	0.53	0.30
	Nov	Shal	3	2.70	1.46	0.24	6.39	6.15	3.26
		Deep	3	3.53	2.63	0.41	7.54	7.13	3.65

Table 29. $\delta^{13}C$ descriptive statistics by month and depth for each taxon.

$\delta^{13}C$ Descriptive Statistics By Month*Depth			N	Mean	Med	Min	Max	Rng	SD
Calanoid	April	Shal	3	-20.86	-20.69	-21.31	-20.59	0.73	0.39
Copepod		Deep	3	-21.04	-21.10	-21.34	-20.67	0.67	0.34
	May	Shal	3	-20.62	-20.68	-20.68	-20.49	0.20	0.11
		Deep	3	-20.79	-20.80	-20.83	-20.74	0.09	0.04
	July	Shal	2	-19.93	-19.93	-20.46	-19.40	1.07	0.75
		Deep	3	-19.89	-19.88	-19.99	-19.82	0.17	0.09
	Sept	Shal	3	-19.49	-19.60	-19.61	-19.25	0.36	0.21
		Deep	3	-19.68	-19.58	-20.04	-19.43	0.60	0.32
	Nov	Shal	3	-18.98	-18.60	-19.78	-18.57	1.21	0.69
		Deep	3	-19.45	-19.47	-19.55	-19.32	0.24	0.12
Chaet	April	Shal	3	-19.68	-19.63	-19.83	-19.58	0.25	0.13
		Deep	3	-19.83	-19.86	-19.90	-19.74	0.16	0.08
	May	Shal	3	-19.64	-19.72	-19.98	-19.21	0.77	0.39
		Deep	3	-19.88	-19.85	-20.13	-19.68	0.45	0.23
	July	Shal	2	-18.26	-18.26	-18.40	-18.12	0.28	0.20
		Deep	3	-18.82	-18.67	-19.17	-18.62	0.55	0.31
	Sept	Shal	3	-18.27	-17.93	-18.95	-17.92	1.03	0.59
		Deep	3	-17.97	-18.03	-18.05	-17.84	0.21	0.12
	Nov	Shal	3	-18.31	-18.23	-18.48	-18.21	0.27	0.15
		Deep	3	-18.25	-18.24	-18.56	-17.94	0.62	0.31

Table 30. $\delta^{15}N$ descriptive statistics by month and depth for each taxon.

$\delta^{15}N$ Descriptive Statistics By Month*Depth			**N**	**Mean**	**Med**	**Min**	**Max**	**Rng**	**SD**
Calanoid Copepod	April	Shal	3	6.38	6.19	5.91	7.03	1.13	0.59
		Deep	3	4.74	4.63	4.54	5.06	0.52	0.28
	May	Shal	3	5.39	5.49	4.80	5.88	1.08	0.55
		Deep	3	5.44	5.23	5.10	5.99	0.89	0.48
	July	Shal	2	5.63	5.63	4.07	7.18	3.11	2.20
		Deep	3	5.55	5.67	5.08	5.88	0.80	0.41
	Sept	Shal	3	4.27	4.24	3.94	4.64	0.70	0.35
		Deep	3	5.29	5.43	4.26	6.17	1.91	0.96
	Nov	Shal	3	4.91	4.65	4.57	5.52	0.95	0.53
		Deep	3	4.72	4.66	3.96	5.56	1.60	0.80
Chaet	April	Shal	3	6.50	6.35	6.30	6.85	0.56	0.31
		Deep	3	6.84	6.69	6.40	7.43	1.03	0.53
	May	Shal	3	5.96	5.88	5.61	6.40	0.79	0.40
		Deep	3	6.74	6.78	6.22	7.22	1.00	0.50
	July	Shal	2	4.91	4.91	4.70	5.12	0.42	0.30
		Deep	3	6.48	6.52	6.26	6.65	0.39	0.20
	Sept	Shal	3	6.15	6.20	5.62	6.63	1.01	0.51
		Deep	3	6.17	6.02	6.02	6.47	0.45	0.26
	Nov	Shal	3	5.45	5.57	4.78	6.00	1.23	0.62
		Deep	3	5.41	5.28	5.09	5.85	0.76	0.39

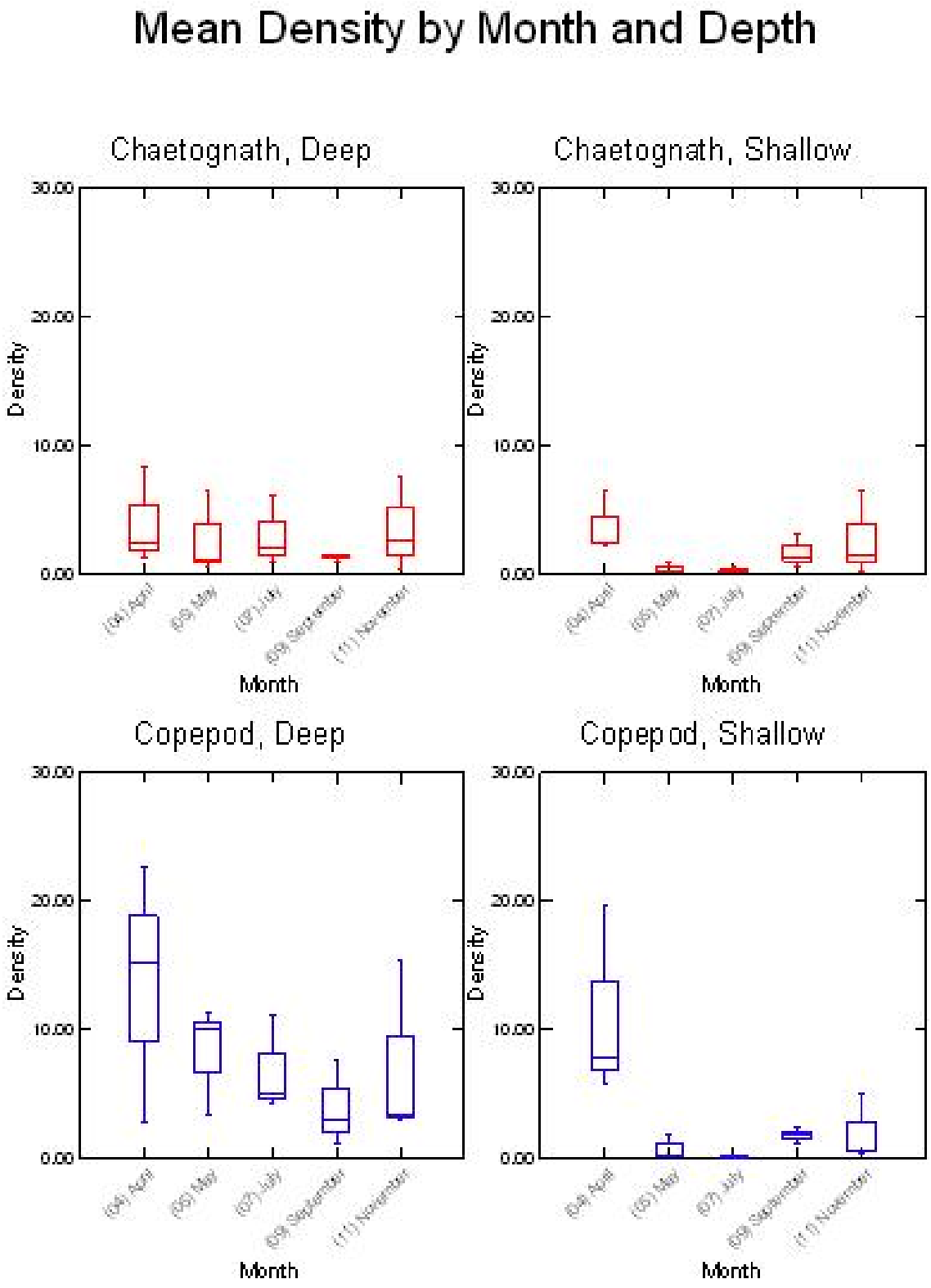

Figure 42. Calanoid copepod and chaetognath density values (#/m^3) by month and depth. The box indicates the values of the first quartile, median, and third quartile. The whiskers indicate the next values below the first quartile and above the third quartile.

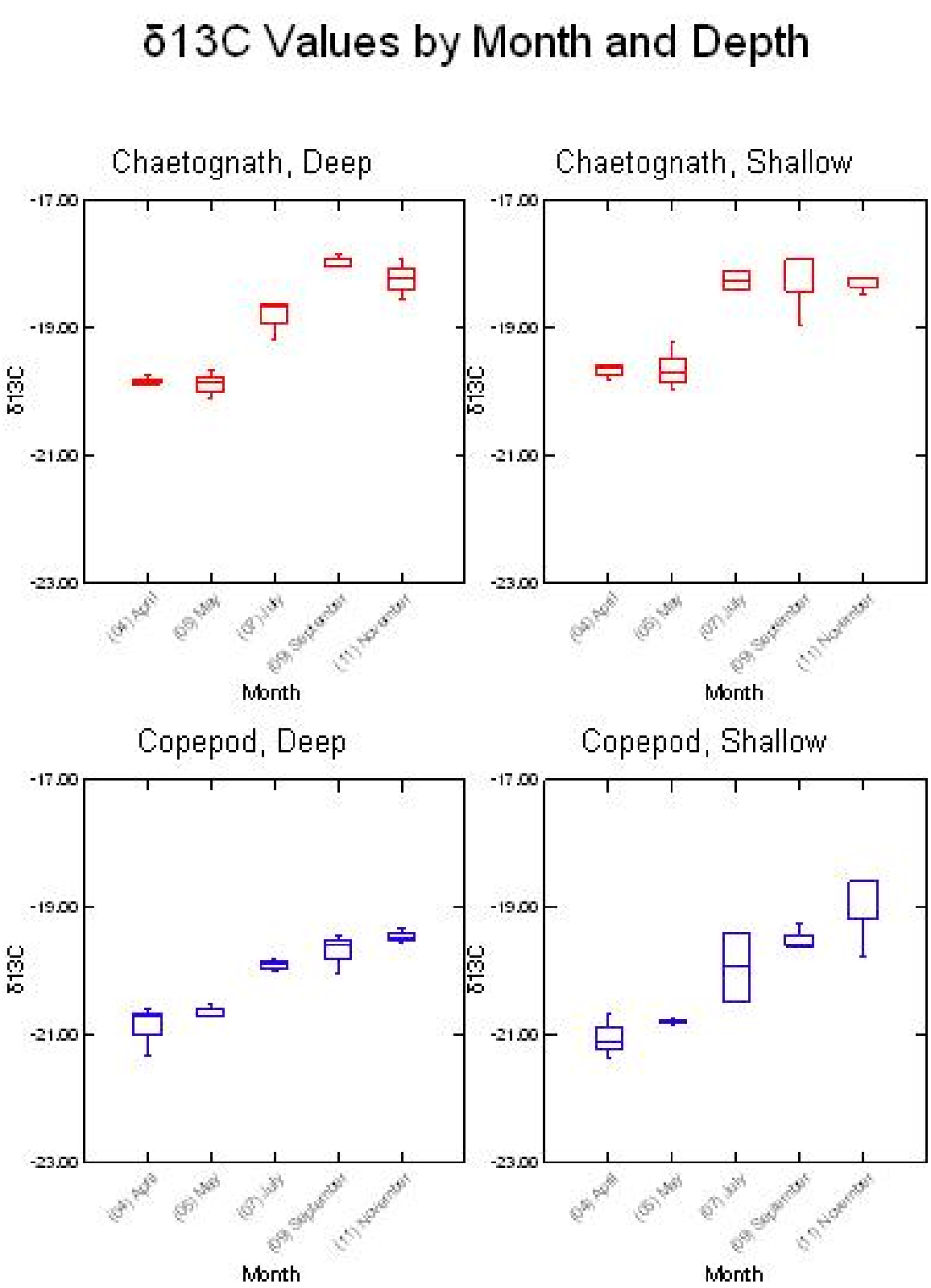

Figure 43. Calanoid copepod and chaetognath $\delta^{13}C$ values (‰) by month and depth. The box indicates the values of the first quartile, median, and third quartile. The whiskers indicate the next values below the first quartile and above the third quartile.

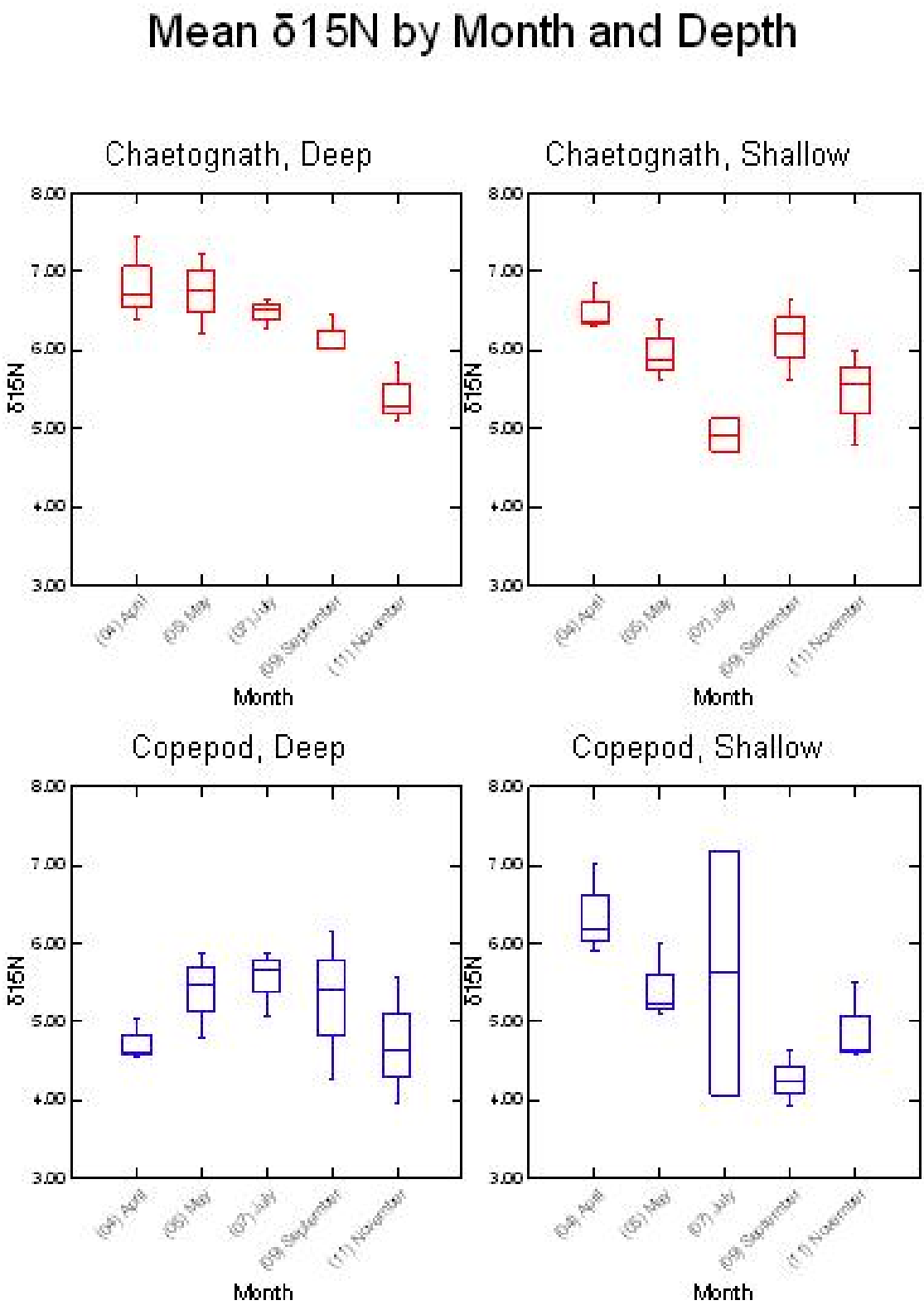

Figure 44. Calanoid copepod and chaetognath $\delta^{15}N$ values (‰) by month and depth. The box indicates the values of the first quartile, median, and third quartile. The whiskers indicate the next values below the first quartile and above the third quartile.

The ANOVA results indicated that calanoid copepod $\delta^{13}C$ and chaetognath $\delta^{15}N$ were significantly different between months and depth ($F(1, 9) = 11.72$, $p<0.001$, and $F(1,9) = 5.717$, $p = 0.001$, $\alpha = 0.05$, respectively). Kruskal-Wallis ANOVA by Ranks results indicated that calanoid copepod density and chaetognath $\delta^{13}C$ were significantly different between months and depth ($H (9, 30) = 20.561$, $p=0.0415$, $H(9, 29) = 23.798$, $p=0.005$, $\alpha = 0.05$, respectively). The multiple comparisons and Tukey HSD did not show any significant differences in calanoid copepod densities, so an even less conservative test, the Fisher FSD, was used to determine where specific differences may lie. The shallow tow in April was significantly different from the shallow tows in May, July, September and November. The deep tow in April was significantly different from the shallow tow in May, July, September, and November, as well as different from the deep tow in September. Tukey HSD showed that calanoid copepod $\delta^{13}C$ was significantly different for the shallow April, deep April, shallow and May tows compared to both September and November shallow and deep tows. The shallow April tow was also significantly different from the deep July tow. The deep May tow was significantly different from the September and November shallow tow, as well as the November deep tow. Tukey HSD showed that chaetognath $\delta^{13}C$ was significantly different in April and May, shallow and deep, compared to July, September, and November, shallow and deep tows. Tukey HSD for chaetognath $\delta^{15}N$ showed that April and May deep tows were significantly different from July shallow, and November shallow and deep tows. April shallow was significantly different from July shallow, and July shallow was significantly different from July deep (Tables 26 - 27).

Table 31. Parametric and non-parametric ANOVA results by month and depth for each taxon. P values < 0.05 indicate a significant difference.

Parametric and Nonparametric ANOVA Results by Month*Depth $\alpha = 0.05$			
	Test	**H/F values**	**p value**
Copepod Density (#/m^3)	Kruskal-Wallis ANOVA	(9, 30) = 20.561	0.015
Copepod Density (#/m3)**	One-way ANVOA	(1, 9) = 2.44635	0.046
Chaetognath Density (#/m^3)	Kruskal-Wallis ANOVA	(9, 30) = 13.783	0.130
Copepod δ13C (‰)	One-way ANVOA	(1, 9) = 11.72	< 0.001
Chaetognath δ13C (‰)	Kruskal-Wallis ANOVA	(9, 29) = 23.798	0.005
Copepod δ15N (‰)	One-way ANVOA	(1, 9) = 1.781	0.139
Chaetognath δ15N (‰)	One-way ANVOA	(1, 9) = 5.717	0.001

Table 32. Parametric and non-parametric post-hoc analysis results of calanoid copepods by month and depth. P values < 0.05 indicate a significant difference.

Parametric and Nonparametric Post Hoc Results				
Test	**Dependent Variable**	**Month*Location**		**p value**
Fisher LSD	Calanoid Copepod Density	April-Shallow	May-Shallow	0.021
			July-Shallow	0.015
			Sep-Shallow	0.035
			Nov-Shallow	0.040
		April-Deep	May-Shallow	0.006
			July-Shallow	0.004
			Sep-Shallow	0.010
			Sep-Deep	0.030
			Nov-Shallow	0.012
Tukey HSD	Calanoid Copepod $\delta^{13}C$	April-Shallow	July-Deep	0.024
			Sep-Shallow	0.001
			Sep-Deep	0.005
			Nov-Shallow	0.000
			Nov-Deep	0.001
		April-Deep	Sep-Shallow	0.005
			Sep-Deep	0.018
			Nov-Shallow	0.000
			Nov-Deep	0.003
		May-Shallow	Sep-Shallow	0.008
			Sep-Deep	0.031
			Nov-Shallow	0.000
			Nov-Deep	0.006
		May-Deep	Sep-Shallow	0.027
			Nov-Shallow	0.001
			Nov-Deep	0.020

Table 33. Parametric and non-parametric post-hoc analysis results of chaetognaths by month and depth. P values < 0.05 indicate a significant difference.

Parametric and Nonparametric Post Hoc Results				
Test	**Dependent Variable**	**Month*Location**		**p value**
Tukey HSD	Chaetognath $\delta^{13}C$	April-Shallow	July-Shallow	0.001
			July-Deep	0.049
			Sep-Shallow	0.001
			Sep-Deep	0.000
			Nov-Shallow	0.001
			Nov-Deep	0.000
		April-Deep	July-Shallow	0.001
			July-Deep	0.013
			Sep-Shallow	0.000
			Sep-Deep	0.000
			Nov-Shallow	0.000
			Nov-Deep	0.000
		May-Shallow	July-Shallow	0.002
			Sep-Shallow	0.001
			Sep-Deep	0.000
			Nov-Shallow	0.001
			Nov-Deep	0.001
		May-Deep	July-Shallow	0.000
			July-Deep	0.009
			Sep-Shallow	0.000
			Sep-Deep	0.000
			Nov-Shallow	0.000
			Nov-Deep	0.000
Tukey HSD	Chaetognath δ^{15N}	April-Shallow	July-Shallow	0.018
		April-Deep	July-Shallow	0.003
			Nov-Shallow	0.021
			Nov-Deep	0.017
		May-Deep	July-Shallow	0.005
			Nov-Shallow	0.038
			Nov-Deep	0.030
		July-Shallow	July-Deep	0.020

4.2.3.7. Density and Stable Isotope Results by Location*Depth

When breaking down the location only statistics by depth, the highest mean calanoid copepod density (#/m^3) and mean chaetognath density (#/m^3) values were found at the deep tow for all locations (Copepod: Inshore, 8.7 SD=8.3, n = 5; Middle, 4.3 SD=3.9, n = 5; Offshore, 11.0 SD=4.6, n = 5; Chaet: Inshore, 5.1 SD=3.2, n = 5; Middle, 2.0 SD=2.3, n = 5, Offshore, 1.6 SD=0.9, n = 5). Calanoid copepod mean $\delta^{13}C$ (‰) was highest in the shallow tow Inshore and Offshore (-19.9 SD=1.2, n = 4; -20.0 SD=0.6, n = 5, respectively). Mean calanoid copepod $\delta^{13}C$ (‰) is highest in the deep tow at the Middle station (-20.1 SD=0.6, n = 5). Chaetognath mean $\delta^{13}C$ (‰) was highest in the shallow tow at the Middle and Offshore stations (-18.8 SD=0.8, n = 5; -18.7 SD=0.7, n = 5, respectively). Mean chaetognath $\delta^{13}C$ (‰) was highest in the deep tow Inshore (-19.0 SD=1.0, n = 5). The mean calanoid copepod $\delta^{15}N$ (‰) was highest in the shallow tow at the Middle station (5.6 SD=1.2, n = 5) and the mean calanoid copepod $\delta^{15}N$ (‰) was lowest in the deep tow Inshore and Offshore (5.1 SD=0.3, n = 4; 5.1 SD=1.1, n= 5). The highest mean chaetognath $\delta^{15}N$ (‰) values were found at the deep tow for all locations (Inshore, 6.1 SD=0.6, n = 5; Middle, 6.5 SD=0.6, n = 5; Offshore, 6.3 SD=0.8, n = 5) (Table 28, Figures 45 - 47). Kruskal-Wallis ANOVA by Ranks showed that calanoid copepod density values were significantly different ($H(5, 30) = 12.933$, $p = 0.024$, $\alpha = 0.05$). Multiple comparisons and Tukey HSD showed no significant differences, so the Fisher LSD post-hoc test was used. Fisher LSD showed a significant difference between the shallow tow at the Middle station and the deep tow at the Offshore station ($p = 0.017$, $\alpha = 0.05$). There was also a significant difference between the shallow Offshore tow and the deep Offshore tow ($p = 0.146$, $\alpha = 0.05$) (Tables 29 - 30).

Table 34. Descriptive statistics by location and depth for each taxon.

Descriptive Statistics By Location*Depth				N	Mean	Med	Min	Max	Rng	SD
Den #/m^3	Cope	In	Shal	5	5.87	2.42	0.25	19.64	19.39	7.89
			Deep	5	8.65	4.22	2.98	22.57	19.59	8.28
		Mid	Shal	5	2.00	0.51	0.17	7.92	7.76	3.34
			Deep	5	4.34	2.99	1.18	11.17	9.99	3.92
		Off	Shal	5	1.76	0.70	0.08	5.88	5.80	2.41
			Deep	5	10.96	11.29	5.11	15.50	10.39	4.57
	Chaet	In	Shal	5	3.41	3.10	0.24	6.40	6.16	2.92
			Deep	5	5.14	6.39	1.46	8.35	6.90	3.21
		Mid	Shal	5	1.16	1.35	0.16	2.35	2.19	0.87
			Deep	5	1.96	1.23	0.41	6.06	5.66	2.33
		Off	Shal	5	0.66	0.24	0.11	2.28	2.18	0.92
			Deep	5	1.62	1.18	0.88	2.63	1.75	0.86
δ^{13}C (‰)	Cope	In	Shal	4	-19.93	-20.03	-21.10	-18.57	2.53	1.22
			Deep	5	-20.11	-19.82	-21.31	-19.32	2.00	0.86
		Mid	Shal	5	-20.17	-20.46	-21.34	-18.60	2.74	1.08
			Deep	5	-20.06	-19.99	-20.68	-19.47	1.21	0.56
		Off	Shal	5	-20.04	-19.78	-20.74	-19.40	1.34	0.62
			Deep	5	-20.13	-20.04	-20.69	-19.55	1.14	0.46
	Chaet	In	Shal	4	-19.25	-19.39	-19.98	-18.23	1.75	0.82
			Deep	5	-18.95	-18.67	-20.13	-17.84	2.29	1.00
		Mid	Shal	5	-18.77	-18.48	-19.72	-17.93	1.79	0.83
			Deep	5	-18.98	-19.17	-19.90	-17.94	1.97	0.95
		Off	Shal	5	-18.68	-18.40	-19.63	-17.92	1.71	0.72
			Deep	5	-18.93	-18.62	-19.74	-18.03	1.71	0.75
δ^{15}N (‰)	Cope	In	Shal	4	5.15	5.08	4.66	5.49	0.83	0.33
			Deep	5	5.22	5.37	3.94	6.19	2.25	0.94
		Mid	Shal	5	5.58	5.67	4.63	6.17	1.54	0.58
			Deep	5	5.58	5.91	4.24	7.18	2.94	1.19
		Off	Shal	5	4.69	4.54	3.96	5.88	1.93	0.74
			Deep	5	5.10	4.65	4.07	7.03	2.96	1.14
	Chaet	In	Shal	4	6.09	6.17	5.62	6.40	0.79	0.36
			Deep	5	6.15	6.26	5.28	6.78	1.50	0.56
		Mid	Shal	5	5.84	5.88	4.70	6.85	2.16	0.80
			Deep	5	6.49	6.65	5.85	7.22	1.38	0.56
		Off	Shal	5	5.69	5.61	4.78	6.63	1.85	0.78
			Deep	5	6.35	6.47	5.09	7.43	2.34	0.84

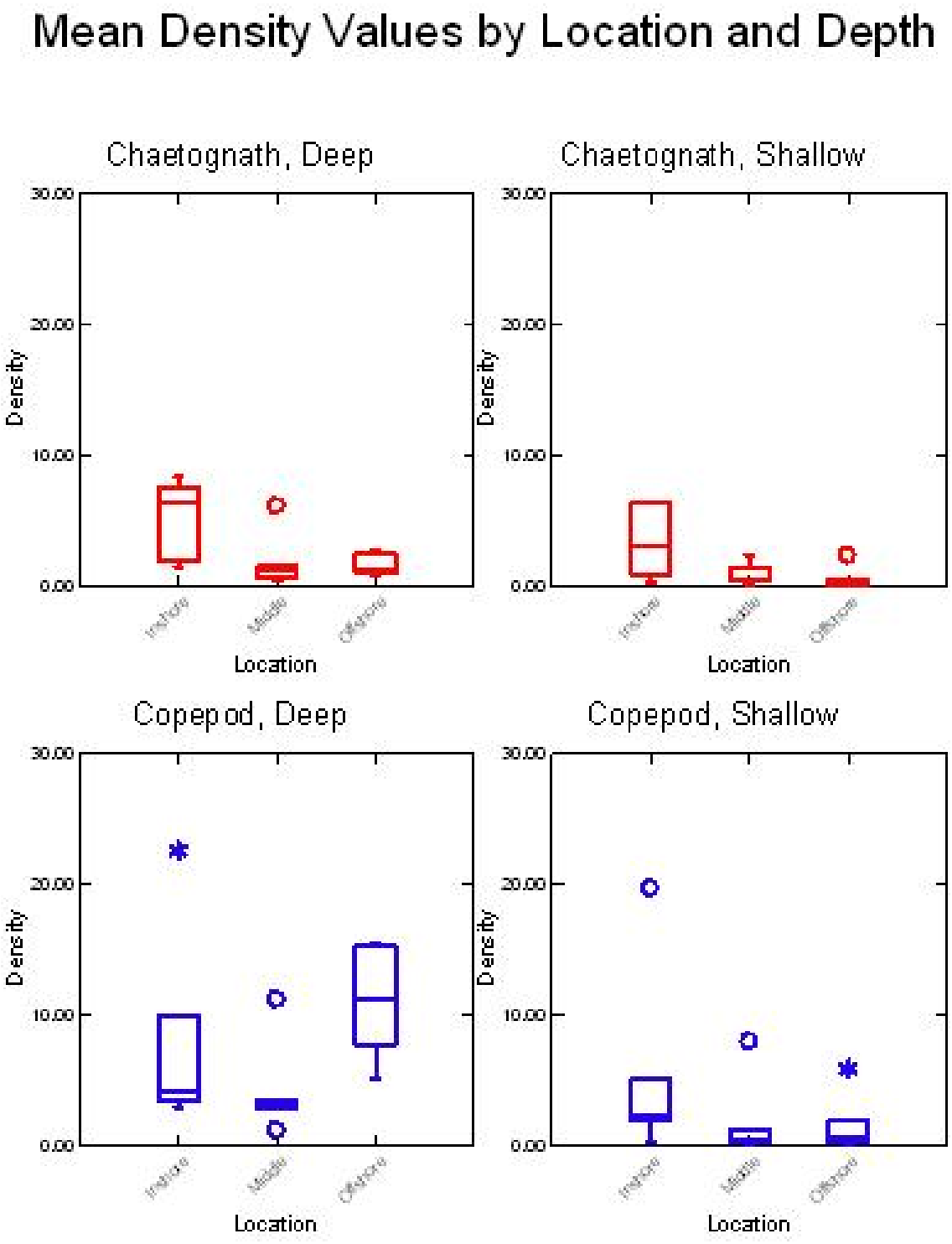

Figure 45. Calanoid copepod and chaetognath density values (#/m^3) by location and depth. The box indicates the values of the first quartile, median, and third quartile. The whiskers indicate the next values below the first quartile and above the third quartile. The stars represent the far outside values. Open circles represent the outliers.

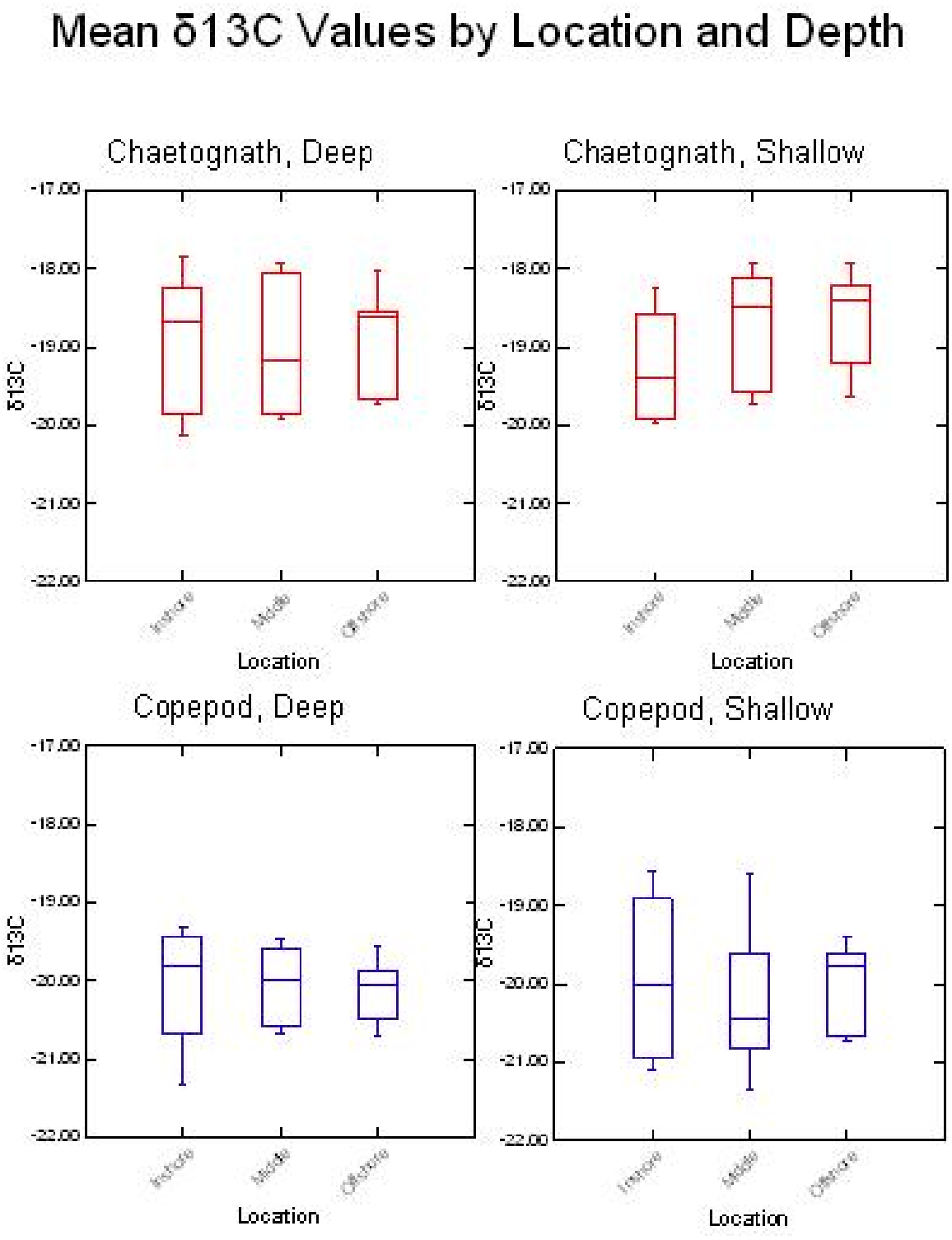

Figure 46. Calanoid copepod and chaetognath $\delta^{13}C$ values (‰) by location and depth. The box indicates the values of the first quartile, median, and third quartile. The whiskers indicate the next values below the first quartile and above the third quartile. The stars represent the extreme values. Open circles (when present) represent the outliers.

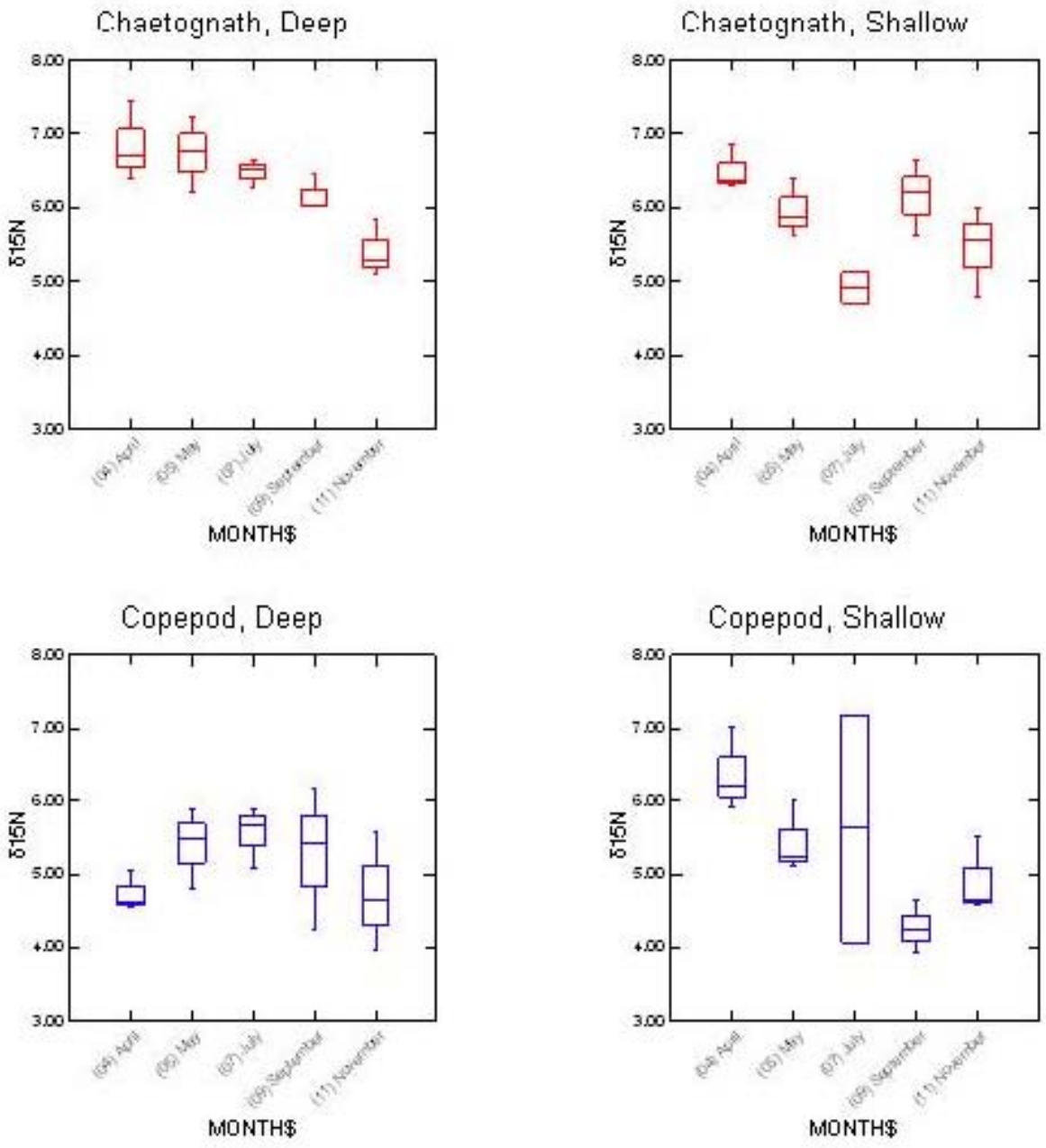

Figure 47. Calanoid copepod and chaetognath $\delta^{15}N$ (‰) values by location and depth. The box indicates the values of the first quartile, median, and third quartile. The whiskers indicate the next values below the first quartile and above the third quartile.

Table 35. Parametric and non-parametric ANOVA results by location and depth for each taxon. P values < 0.05 indicate a significant difference.

Parametric and Non-parametric ANOVA Results by Location*Depth $\alpha = 0.05$			
	Test	**H/F value**	**p value**
Copepod Density (#/m^3)	Kruskal-Wallis ANOVA	(5, 30) = 12.933	0.024
Copepod Density (#/m3)**	One-way ANVOA	(1, 5) = 2.198	0.088
Chaetognath Density (#/m^3)	Kruskal-Wallis ANOVA	(5, 30) = 10.585	0.060
Copepod δ13C (‰)	One-way ANVOA	(1, 5) = 0.04	0.999
Chaetognath δ13C (‰)	One-way ANVOA	(1, 5) = 0.24	0.941
Copepod δ15N (‰)	One-way ANVOA	(1, 5) = 0.735	0.605
Chaetognath δ15N (‰)	One-way ANVOA	(1, 5) = 0975	0.454

Table 36. Parametric and non-parametric post-hoc analysis results by location and depth for each taxon. P values < 0.05 indicate a significant difference.

Parametric and Non-parametric Post-Hoc Analysis				
Test	**Dependent Variable**	**Location*Location**		**p value**
Fisher LSD	Calanoid Copepod Density	Middle-Shallow	Offshore-Deep	0.017
		Offshore Shallow	Offshore-Deep	0.015

4.2.3.8. Density and Stable Isotope Results by Current

Using the previously analyzed ADCP data, descriptive statistics were calculated for density and stable isotopes in each of the currents. For both calanoid copepod and chaetognath densities, the highest densities (#/m^3) were found in the SSCC and the lowest were found in the FC. (Copepod: SSCC, 11.9 (SD=9.9, n = 3), FC, 2.9 (SD=4.1, n = 15); Chaetognath, 5.4 (SD=0.4, n = 3), FC, 1.3 (SD=1.6, n = 15)). For both calanoid copepod and chaetognath $\delta^{13}C$ values, the lowest were found in the SSCC and the highest in the FC (Copepod: SSCC, -20.5 (SD=1.0, n = 3), FC -19.9 (SD=0.8, n = 14); Chaetognath: SSCC -19.3 (SD=1.3, n = 3), FC -18.7 (SD=0.7, n = 14)). Calanoid copepod $\delta^{15}N$ was highest in the SSCC (5.3 SD=0.2, n = 3) and lowest in the Interm (5.2 SD=0.8, n = 12). Chaetognath $\delta^{15}N$ was highest in the SSCC (6.4 SD=0.4, n = 3) and lowest in the FC (5.8 SD=1.6, n = 14) (Table 31, Figures 48 - 50).

The Kruskal-Wallis ANOVA by Ranks indicated that both calanoid copepod density and chaetognath density showed significant differences by current ($H(2, 29) = 8.402$, $p = 0.015$, $H(2. 29) = 7.427$, $p = 0.024$, $\alpha = 0.05$, respectively) (Tables 32 - 33). The multiple comparisons analysis showed a significant difference in calanoid copepod density between the FC and the Interm ($p = 0.04$, $\alpha = 0.05$). The multiple comparisons analysis did not show any significant difference for chaetognath density, so the less conservative Tukey HSD post-hoc analysis was used. Results showed there was a significant difference between the FC and the SSCC ($p = 0.04$, $\alpha = 0.05$).

Table 37. Descriptive statistics by current for each taxon.

Descriptive Statistics By Current			**N**	**Mean**	**Med**	**Min**	**Max**	**Rng**	**SD**
Dens	Copepod	FC	15	2.87	1.20	0.08	15.50	15.42	4.06
(#/m^3)		Interm	12	7.45	5.58	1.18	19.64	18.46	5.84
		SSCC	3	11.85	10.01	2.98	22.57	19.59	9.92
	Chaet	FC	15	1.32	0.88	0.11	6.39	6.28	1.63
		Interm	12	2.82	1.91	0.41	7.54	7.13	2.47
		SSCC	3	5.40	6.39	6.02	6.78	0.76	0.38
δ^{13}C	Copepod	FC	14	-19.88	-19.80	-20.83	-18.57	2.26	0.75
(‰)		Interm	12	-20.21	-20.27	-19.25	-21.34	2.09	0.71
		SSCC	3	-20.47	-20.68	-21.31	-19.43	1.88	0.96
	Chaet	FC	14	-18.69	-18.52	-19.98	-17.92	2.06	0.65
		Interm	12	-19.08	-19.38	-19.90	-17.94	1.96	0.80
		SSCC	3	-19.28	-19.86	-20.13	-17.84	2.29	1.25
δ^{15}N	Copepod	FC	14	5.22	5.09	3.96	7.18	3.22	1.01
(‰)		Interm	12	5.18	5.18	3.94	6.19	2.25	0.79
		SSCC	3	5.32	5.46	5.06	5.49	0.43	0.23
	Chaet	FC	14	5.79	5.94	4.70	6.63	1.93	1.63
		Interm	12	6.39	6.41	5.38	7.43	2.15	0.64
		SSCC	3	6.40	6.40	6.02	6.78	0.76	0.38

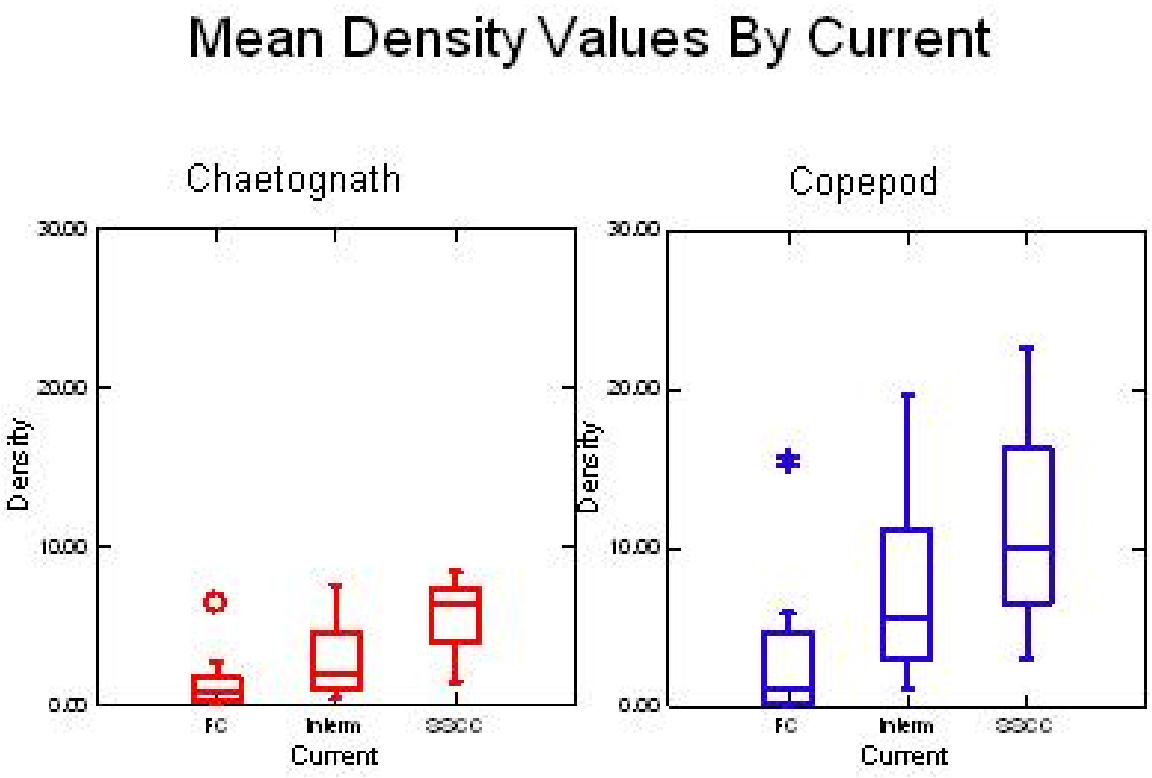

Figure 48. Density values (#/m^3) by current for each taxon. The box indicates the values of the first quartile, median, and third quartile. The whiskers indicate the next values below the first quartile and above the third quartile. The stars represent the far outside values. Open circles represent the outliers.

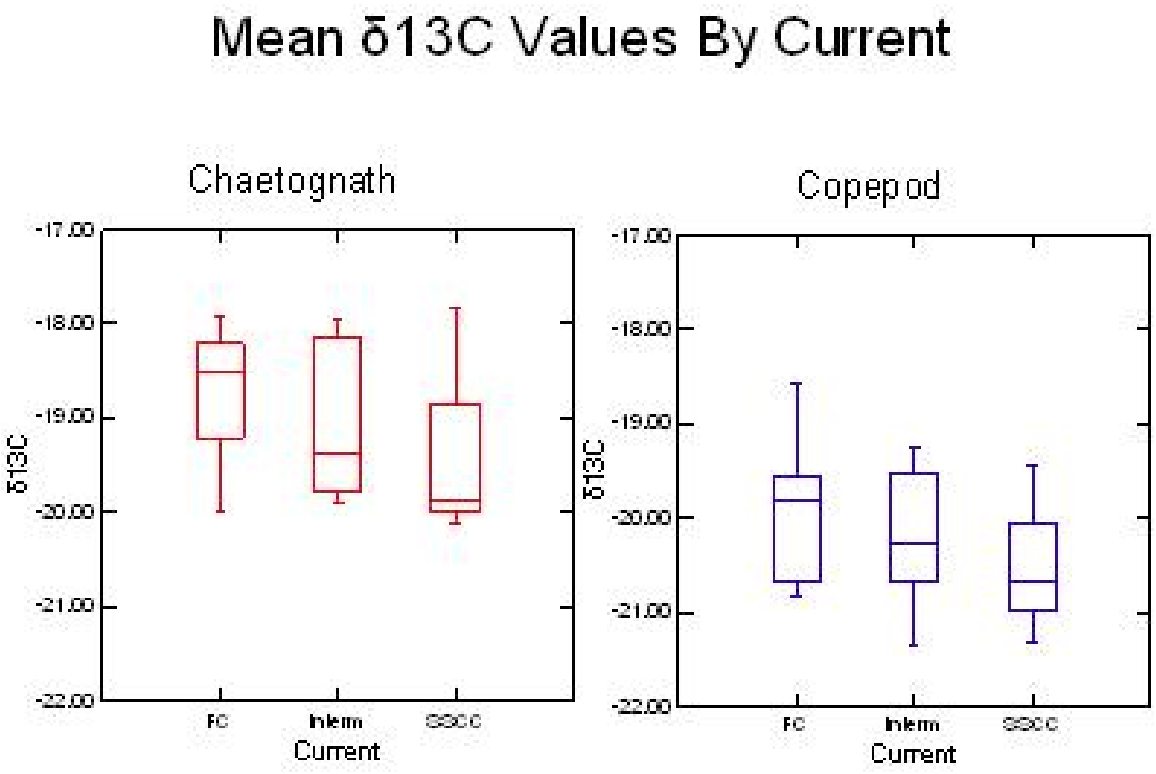

Figure 49. The $\delta^{13}C$ values (‰) by current for each taxon. The box indicates the values of the first quartile, median, and third quartile. The whiskers indicate the next values below the first quartile and above the third quartile.

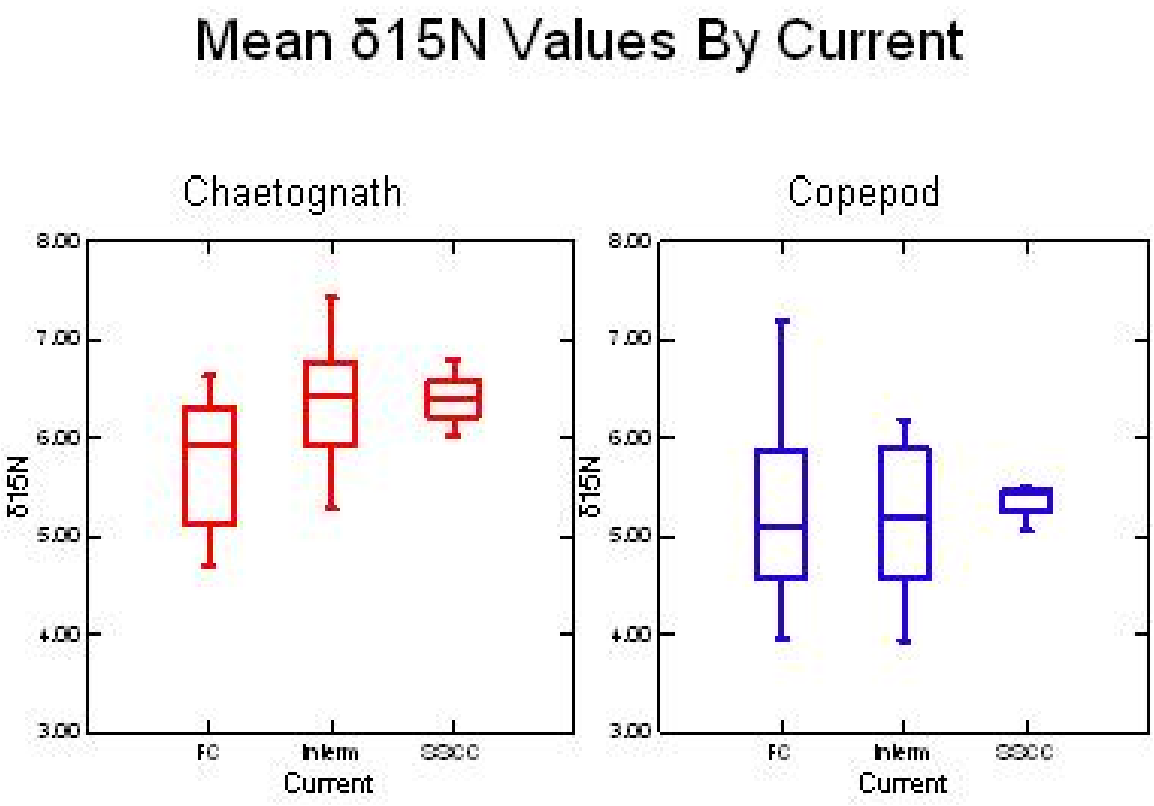

Figure 50. The $\delta^{15}N$ values (‰) by current for each taxon. The box indicates the values of the first quartile, median, and third quartile. The whiskers indicate the next values below the first quartile and above the third quartile.

Table 38. Parametric and non-parametric ANOVA results by current for each taxon. P values < 0.05 indicate a significant difference.

Parametric and Non-parametric ANOVA Results by Current $\alpha = 0.05$			
	Test	**H/F values**	**p value**
Copepod Density (#/m^3)	Kruskal-Wallis ANOVA	(2, 29) = 8.402	0.015
Chaetognath Density (#/m^3)	Kruskal-Wallis ANOVA	(2, 28) = 7.427	0.024
Copepod δ13C (‰)	One-Way ANOVA	(2, 28) = 1.099	0.348
Chaetognath δ13C (‰)	Kruskal-Wallis ANOVA	(2, 28) = 1.661	0.436
Copepod δ15N (‰)	One-Way ANOVA	(2, 28) = 0.032	0.969
Chaetognath δ15N (‰)	One-Way ANOVA	(2, 28) = 3.304	0.053

Table 39. Parametric and non-parametric post hoc results by current for each taxon. P values < 0.05 indicate a significant difference.

Parametric and Non-parametric Post-Hoc Results by Current			
Test	**Dependent Variable**	**Current**	**p value**
Multiple Comparisons	Calanoid Copepod Density	FC (Interm)	0.040
Tukey HSD	Chaetognath Density	FC (SSCC)	0.040

4.2.3.9. Density and Stable Isotope Results by Water Mass

Using the previously analyzed CTD data, descriptive statistics were calculated for density and stable isotopes in each of the water masses. Calanoid copepod density was highest in the Other water mass and lowest in the YW (5.1 SD=4.4, n = 4, 3.3 SD=5.0, n = 6, respectively. Chaetognath density was highest in the YW and lowest in the CEW (2.3 SD=2.8, n = 9, 1.5 SD=1.0, n = 5, respectively. Calanoid copepod $\delta^{13}C$ values were highest in the YW and lowest in the Other water mass (-19.4 SD=0.6, n = 8, -19.7 SD=0.4, n = 4, respectively). Chaetognath $\delta^{13}C$ values were highest in the CEW and lowest in the Other water mass (-18.1SD=0.5, n = 5, -18.5 SD=0.6, n = 4, respectively). Calanoid copepod $\delta^{15}N$ was highest in the Other water mass and lowest in the CEW (5.8 SD=0.3, n = 4, 4.0 SD=0.6, n = 5, respectively). Chaetognath $\delta^{15}N$ was highest in the Other water mass and lowest in the YW (6.3 SD=0.4, n = 4, 5.4 SD=0.6, n = 8, respectively) (Table 34, Figures 51 - 53).

One-way ANOVA results indicated that chaetognath $\delta^{15}N$ values differed by water mass ($F(2, 16) = 6.870$, $p = 0.008$, $\alpha = 0.05$) (Table 35 and 36). The Tukey HSD pos-hoc results indicated that there was a significant difference between the YW and Other water masses, and the YW and CEW water masses ($p = 0.021$, $p = 0.023$, $\alpha = 0.05$, respectively) (Tables 35 - 36).

Table 40. Descriptive statistics by water mass for each taxon.

Descriptive Statistics by Water Mass									
			N	**Mean**	**Med**	**Min**	**Max**	**Rng**	**SD**
Density #/m^3	Copepod	YW	9	3.33	0.70	0.08	15.50	15.42	4.96
		CEW	5	3.23	2.42	1.20	7.70	6.49	2.58
		Other	4	5.11	4.05	1.18	11.17	9.99	4.35
	Chaet	YW	9	2.34	1.46	0.11	7.54	7.43	2.78
		CEW	5	1.48	1.35	0.53	3.10	2.57	0.98
		Other	4	2.21	1.18	0.41	6.06	5.66	2.61
δ^{13}C ‰	Copepod	YW	8	-19.44	-19.48	-20.46	-18.57	1.90	0.63
		CEW	5	-19.59	-19.60	-20.04	-19.25	0.79	0.29
		Other	4	-19.73	-19.73	-19.99	-19.47	0.52	0.24
	Chaet	YW	8	-18.36	-18.32	-18.67	-18.12	0.55	0.19
		CEW	5	-18.13	-17.93	-18.95	-17.84	1.12	0.46
		Other	4	-18.45	-18.34	-19.17	-17.94	1.24	0.57
δ^{15}N ‰	Copepod	YW	8	4.96	4.66	3.96	7.18	3.22	1.03
		CEW	5	4.50	4.26	3.94	5.43	1.49	0.58
		Other	4	5.82	5.78	5.56	6.17	0.61	0.27
	Chaet	YW	8	5.35	5.20	4.70	6.26	1.57	0.56
		CEW	5	6.19	6.20	5.62	6.63	1.01	0.40
		Other	4	6.26	6.27	5.85	6.65	0.81	0.39

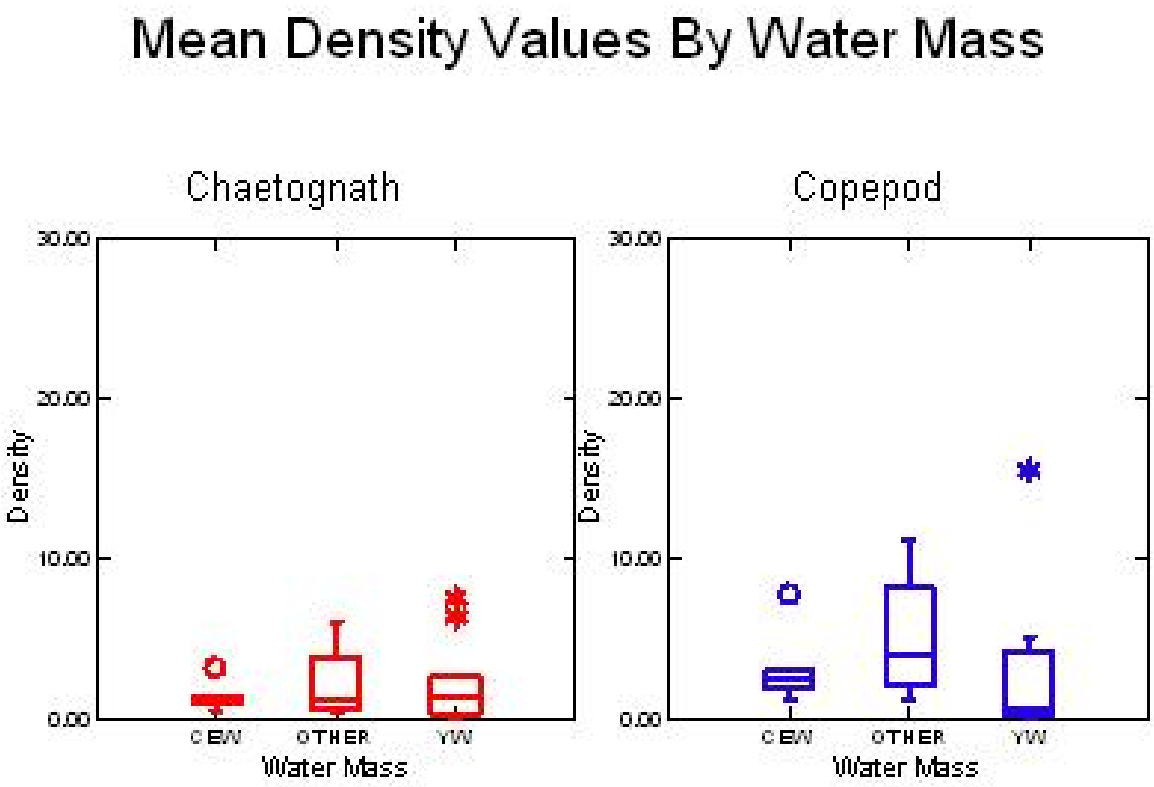

Figure 51. Density values (#/m^3) by water mass for each taxon. The box indicates the values of the first quartile, median, and third quartile. The whiskers indicate the next values below the first quartile and above the third quartile. The stars represent the far outside values. Open circles represent the outliers.

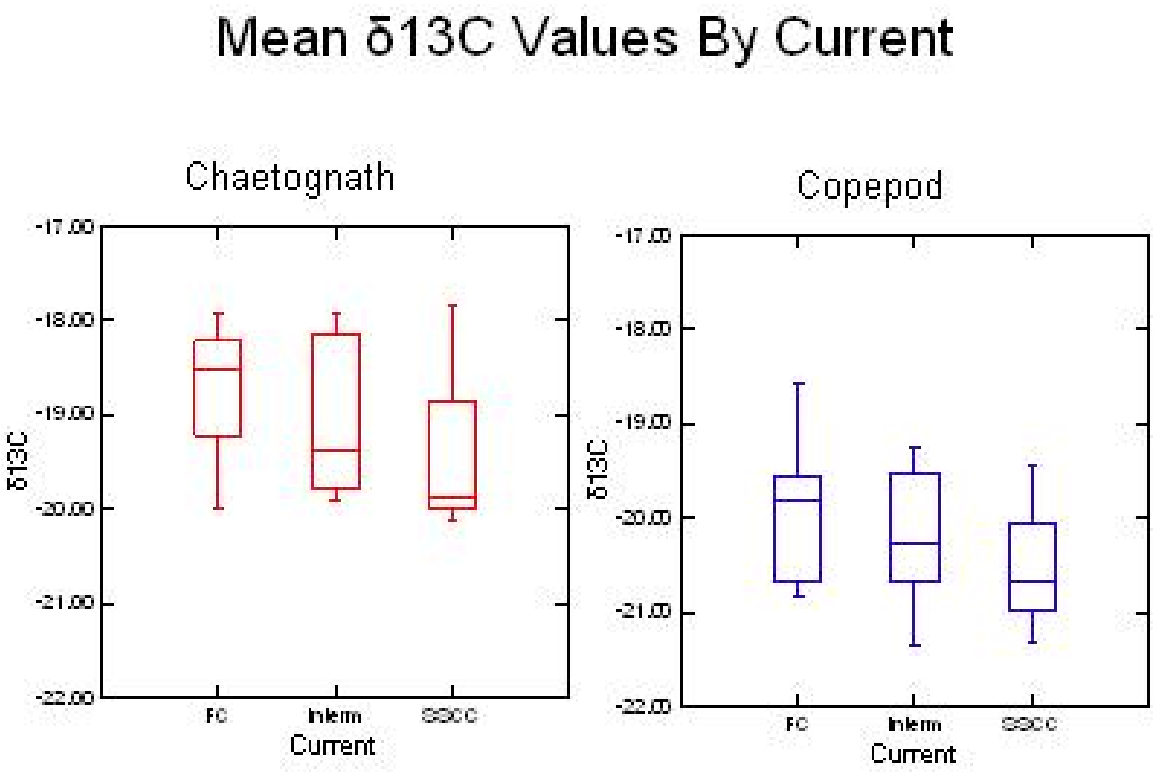

Figure 52. The $\delta^{13}C$ values (‰) by water mass for each taxon. The box indicates the values of the first quartile, median, and third quartile. The whiskers indicate the next values below the first quartile and above the third quartile. The stars represent the far outside values. Open circles represent the outliers.

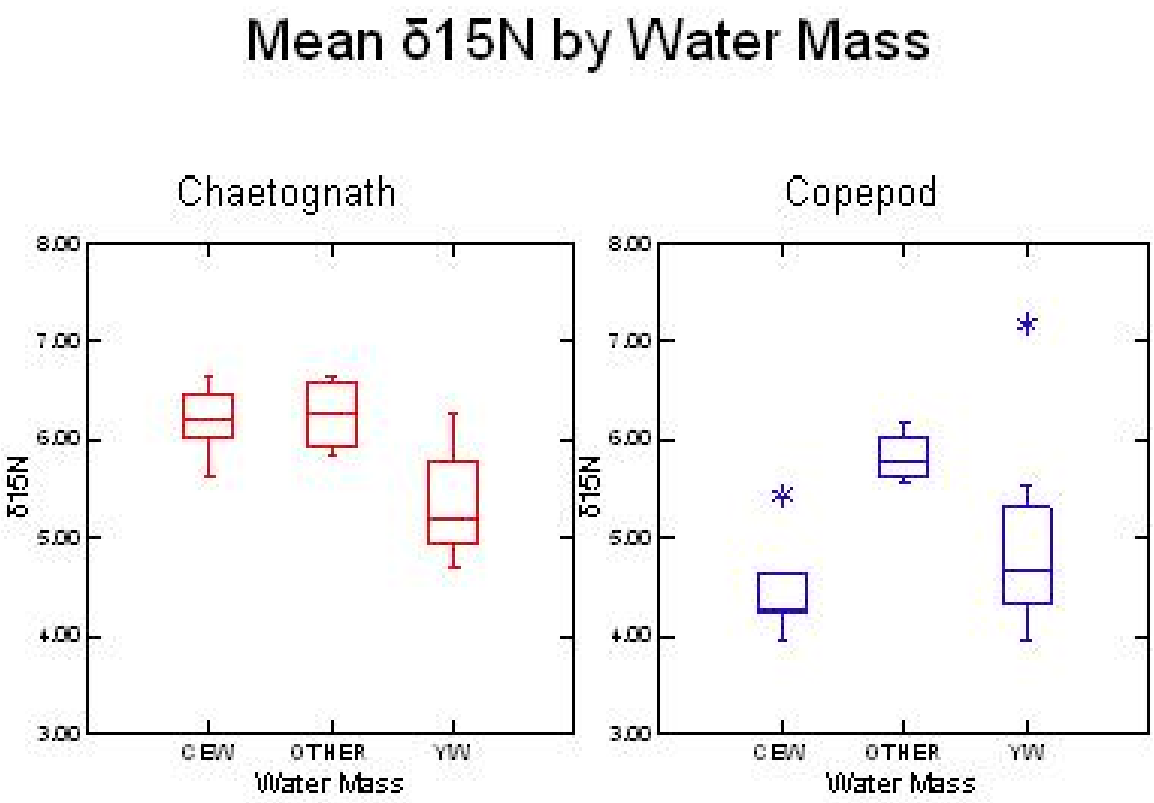

Figure 53. The $\delta^{15}N$ values (‰) by water mass for each taxon. The box indicates the values of the first quartile, median, and third quartile. The whiskers indicate the next values below the first quartile and above the third quartile. The stars represent the far outside values. Open circles represent the outliers.

Table 41. Parametric and non-parametric ANOVA results by water mass for each taxon. P values < 0.05 indicate a significant difference.

Parametric and Non-parametric ANOVA Results by Water Mass $\alpha = 0.05$			
	Test	**H/F values**	**p value**
Copepod Density (#/m^3)	Kruskal-Wallis ANOVA	(2, 18) = 1.530	0.465
Chaetognath Density (#/m^3)	Kruskal-Wallis ANOVA	(2, 18) = 0.019	0.99
Copepod δ13C (‰)	One-way ANOVA	(2, 16) = 0.490	0.62
Chaetognath δ13C (‰)	Kruskal-Wallis ANOVA	(2, 17) = 3.615	0.153
Copepod δ15N (‰)	One-way ANOVA	(2, 16) = 3.084	0.078
Chaetognath δ15N (‰)	One-way ANOVA	(2, 16) = 6.870	0.008

Table 42. Parametric and nonparametric post hoc results by current for each taxon. P values < 0.05 indicate a significant difference.

Parametric and Non-Parametric Post-Hoc Results by Water Mass			
Test	**Dependent Variable**	**Water Mass**	**p value**
Tukey HSD	Chaetognath δ^{15}N	YW (Other)	0.021
		YW (CEW)	0.023

5. Discussion

5.1. Preservation Effect

This study addressed the effect of multiple types of common preservation methods on the carbon and nitrogen stable isotope ratios of common zooplankton species. All the preservation media used were carbon based and did not contain a nitrogen group (Ethanol: C_2H_6O; Formalin: $H_2C(OH)_2$ (aqueous formaldehyde)). The preservation methods that utilized only ethanol showed significant increase in calanoid copepod and chaetognath $\delta^{13}C$ values when compared to the control preservation method (frozen). Alcohol has been used as a lipid extractor since the first methods of lipid extraction were described by Folch et al. (1957) and then again by Bligh and Dyer (1959). The increase in $\delta^{13}C$ in both taxa for both treatments involving ethanol can be explained by lipid loss. Tissues and organisms high in lipid content will have a more negative (depleted) $\delta^{13}C$ than those low in lipid (DeNiro and Epstein, 1978, Tieszen et al., 1983). When the organisms were preserved in ethanol, the lipids are extracted and the $\delta^{13}C$ values become more positive (enriched). This was in accordance with the results reported by Syvaranta et al. (2008) who studied calanoid copepods, cyclopoid copepods, and cladocera, the results by Sweeting et al. (2004) who examined the muscle tissue of Atlantic cod, and also the results summarized by Kelly et al. (2006) who studied the effects on the muscle tissue of the Arctic char.

In a study by Kelly et al. (2006), the stable isotope analysis indicated that the $\delta^{13}C$ of the formalin used for preservation was very much depleted (-58.5‰). The $\delta^{13}C$ of individual formalin samples varies depending on the manufacturer (-37.8‰ to -52.5‰) as Edwards et al. (2002) found, but depleted in regards to many organisms' tissue $\delta^{13}C$.

The aldehyde group in the $\delta^{13}C$ depleted formalin binds to the nitrogen group in protein, glycoprotein, nucleic acid, and phospholipids, leading to depletion in the overall $\delta^{13}C$ tissue values. Organisms higher in these biochemical components should show a greater depletion in $\delta^{13}C$ as more $\delta^{13}C$ depleted formalin attaches to the nitrogen groups by cross-linking the polymers of formalin and protein (Helander, 1994, Kiernan, 2000). The results did not show a decrease in $\delta^{13}C$ values so it is possible that neither formalin, attaching to these biochemical components, nor the presence of excess preservation media on the organisms occurred. This indicates that formalin fixation does not have a large effect on the $\delta^{13}C$ values of calanoid copepods and chaetognaths along the southeast continental shelf of Florida during the fall, and the observed standard deviation was most likely due to the natural variation in zooplankton $\delta^{13}C$ values.

Non-quantified observation of the sample indicated that copepods were the majority of the sample, so initial expectations were that the bulk zooplankton preservation trends were going to follow the same trends as the calanoid copepod treatment trends. The observed decrease in $\delta^{13}C$ values of the bulk zooplankton sample due to formalin treatment may be attributed to other organisms in the sample that may have different biochemical composition that allows for formalin binding. Also, the method used to collect the bulk sample after treatment may have allowed residual formalin to remain in the sample prior to analysis. Individual calanoid copepods and chaetognaths were picked and rinsed prior to analysis, while the bulk sample was pipetted into a dish and rinsed as a whole, possibly diluting the formalin rather than rinsing it off.

Analysis of the treatment effects on $\delta^{15}N$ values showed that all treatments led to an increase in $\delta^{15}N$ compared to the control, with only a significant increase in

chaetognath $\delta^{15}N$ values. The most common lipid types found in zooplankton are triacylglycerols, wax esters, diacylglycerol ethers, and phospholipids (Lee and Hirota, 1973). Of these lipids, the phospholipid is the only group that contains a nitrogen group. Protein, glycoprotein, nucleic acid, and phospholipids are the major categories of biochemical components that have a nitrogen group. Similar to the $\delta^{13}C$ values, the greatest changes were observed between the control and the treatments involving ethanol (ethanol only and formalin/ethanol combination). As previously stated, alcohol is a lipid extracting agent. Most lipids, except for phospholipids, do not contain a nitrogen group. If the ethanol treatments were extracting phospholipids from the zooplankton, then the trend would be for the $\delta^{15}N$ to become depleted, not enriched. Perhaps ethanol treatments affect the $\delta^{15}N$ of one or more of the biochemical components by removing the isotopically light components preferentially over the heavier ones, similar to the concept that heavier isotopes are incorporated into tissues and light isotopes are preferentially discarded by respiration and egestion.

The effect of treatments was highly variable in this study and it is possible that the effect varies due to the biochemical components of the zooplankton present at the time of acquisition. Especially because of the observed changes in $\delta^{15}N$, it can be hypothesized that isotopic shifts in the study were due to biochemical extraction, as the preservation media was carbon based and did not contain a nitrogen group. In order to determine with relative accuracy the magnitude and direction of the isotopic change due to preservation, the ratios of specific biochemical components must be determined before preservation begins. Biochemical composition is known to change due to many factors, including food availability, prey selection (herbivorous, carnivorous, and omnivorous), reproductive

cycle, geographic location, and seasonal changes that affect these factors (Lee and Hirota, 1973, Sargent et al., 1981, Bhat and Wagh, 1992, Choe et al, 2003). Stable isotope analysis should be done on specific lipids, wax esters, proteins, and other biochemical components over various seasons to determine which component(s) are isotopically altered.

5.2. Physical Analysis of Currents and Water Masses

Analysis of ADCP data indicated that there was a fast moving, northward flowing current present along the transect for all months of the study, which was assumed to be the Florida Current. The western boundary of this current meandered from month to month along the 10 km wide transect, which is characteristic of the Florida Current (Lee et al., 1981, Zantopp et al., 1987) . A subsurface counter current of unknown origin was also present in the ADCP data, but this current was not present during all months sampled. Counter currents have been previously documented but at depths of 500-800m, not 50-200m, as observed in this study (Duing and Johnson, 1971, Stepien, 1980). The CTD data collected during some of the months indicated that two specific water masses were present: Continental Edge Water and Yucatan Water. Continental Edge Water is located on the continental margin and Yucatan Water is located on the Insular margin in the Straits of Florida, and both water masses occupy the water column from surface to the bottom. The boundary between these two water masses is delineated by the western boundary of the Florida Current (Bsharah, 1957, Wennekens, 1959). Data from this study supported this premise, as Continental Edge Water occupied the entire transect during September, when the western edge of the Florida Current was at the Offshore station. Yucatan Water occupied the entire transect during July and November when the western

boundary of the Florida Current was at the Inshore station. During September, the SSCC was present at the Inshore station and the temperature and salinity profiles identify this water as Continental Edge Water, identical to the northward flowing water around it. This indicated that this particular counter current was not a spin-off eddy of the Florida Current because it did not exhibit characteristics of Yucatan Water, which is found in the Florida Current at this latitude.

5.3. Biological Analysis of Currents and Water Masses

Regardless of the current, water mass or location sampled, the monthly variation in density for both calanoid copepods and chaetognaths was an overwhelming factor. Highest overall densities were found in April and May, while the lowest overall densities were found in July and September. Summer is generally a nutrient-limited time for phytoplankton growth in tropical and subtropical waters (Pasciak and Gavis, 1974, 1975), but passing spin-off eddies of the Florida Current may provide nutrients for a short-lived phytoplankton bloom, and subsequent zooplankton bloom (Lee et al., 1981, Yoder et al., 1981).

Both calanoid copepods and chaetognaths are continuous spawners in tropical waters, so food availability is a major factor in determining zooplankton blooms. There is a possibility that zooplankton samples collected during this study may have been from isolated zooplankton blooms, giving larger than expected density values and possible explanation for seasonal variation. Zooplankton are known to have an inherent patchy distribution both horizontally and vertically and, therefore, multiple year sampling must be done in order to determine if this observed trend was a seasonal trend or if they were

anomalous events (Omori and Hammer, 1982; Legendre and Demers, 1984; Daley and Smith, 1993.)

Overall, the highest densities of calanoid copepods and chaetognaths were found at the Inshore station, and were lower at the Middle and Offshore stations. These findings are in accordance with the premise that production is higher in the near shore waters and substantially diminishes just 10 km offshore (Turner et al, 1979b), as the Inshore station was location 6.5 km offshore and the Middle station was located 12.5 km offshore.

Calanoid copepod and chaetognath densities in this study have demonstrated typical patterns of tropical/subtropical, coastal production trends. Further discussion of these patterns in conjunction with the previously defined physical results will provide a detailed suggestion of the biological characteristics specific to the southern Straits of Florida.

Calanoid copepod and chaetognath density was highest in the SSCC and lowest in the Florida Current. When the Subsurface Counter Current was not present, the density values were highest in the Intermediate water when compared to the Florida Current. Upon initial investigation, it was hypothesized that the greater density of zooplankton in the Subsurface Counter Current was caused by entrapment from the shelf in a passing eddy, based on previous observations in other studies that focused on the eddies produced by the meandering Florida Current (Hopkins et al., 1981; Mauchline, 1998), but when combining the information from ADCP data and CTD data, it was concluded that the Subsurface Counter Current was not part of a passing eddy. The Subsurface Counter Current has temperature and salinity properties of the Continental Edge Water around it, and not properties of Yucatan water, which is characteristic of the Florida Current.

Water flowing through the Straits of Florida has been known to reach temperatures as low as 7^{o}C, and have origins in the South Atlantic (Wennekens, 1959). It is possible that the cold water that was found during the deep tow at the Middle station during July, September and November (OTHER water mass) may be this South Atlantic cold water. Further analysis of these waters needs to be done to determine their actual origin. There is some intrusion of Western Atlantic water into the Straits of Florida but most occurs through the Old Bahama Channel, north of the sampling stations, so it is unlikely that the cold water that is observed has Western North Atlantic origins. High densities of especially calanoid copepods (chaetognaths were a little more variable) were observed in the Other water mass, but analysis of densities by location and also by depth indicated that the highest densities occurred at the deep tow for all stations during all months. Therefore, the high densities of calanoid copepods and chaetognaths observed in the Other water mass are characteristic of the deep water at the sampling location, and not specific to a particular water mass.

5.4. Stable Isotope Analysis of Currents and Water Masses

The preservation study proved that the stable isotope values obtained cannot be used because the formalin/ethanol treatment altered the stable isotope ratios. If carbon isotopes had been usable, pelagic zooplankton would have expected to have a depleted ^{13}C value while the more coastal organisms would have been enriched, as found by Perry et al. (1999). If colder and deeper water was being transported into the Straits of Florida (the OTHER water mass), the δ^{13}C values of the zooplankton would be expected to be depleted relative to the Continental Edge Water and the Yucatan Water. If the Subsurface Counter Current was entraining coastal populations, those δ^{13}C values should have been

more enriched compared to the Florida Current, and possibly the Intermediate water, as well.

Even though the $\delta^{15}N$ values were not as altered as much as the $\delta^{13}C$ values, no correction factor could be determined and therefore, these samples could not be used to help identify currents and water masses because it is unclear why the $\delta^{15}N$ values increase, as they were expected to decrease., The $\delta^{15}N$ values, in combination with the $\delta^{13}C$ values, were going to be used to distinguish different foraging patterns within different currents and water masses. In combination with calanoid copepod and chaetognath densities, the $\delta^{15}N$ values would have given some insight as to how feeding habits changed with varying prey availability. Copepods have been shown to be selective feeders that prey upon organisms with higher protein content (Cowles, 1988). Varying types of prey may show different $\delta^{15}N$ values based on their biochemical content. The $\delta^{15}N$ values would also have been utilized to identify the source of nitrogen, either recently upwelled nitrate or regenerated ammonia. Organisms that utilized nitrate will have higher $\delta^{15}N$ values than organisms that utilize ammonia.

6. Conclusions

6.1. Preservation Effect

Originally, a preservation study was going to be conducted using frozen zooplankton samples that were collected at the same time as the preserved samples, but there were too many variables that could have skewed the results. The ring net towed just below the surface would collect different populations with possible different species composition. Secondly, the samples to compare were collected at different locations, with some populations being influenced by coastal waters and some populations being

influenced by Florida Current waters. Finally, the density found in each ring net sample was not high enough to produce repetitive samples. Preservation of the zooplankton in formalin and ethanol rendered the use of the samples, specifically $\delta^{13}C$, useless to identify different currents or water masses. In the preservation study, zooplankton samples collected from an area just south of the sampling transect yielded results that indicated it was not possible to provide a universal correction factor to previously sampled and preserved zooplankton. Further studies need to be done to determine which biochemical components are affected most by the preservation media. Variations in biochemical composition due to season, food availability, and reproductive cycle indicate that a correction factor may vary based on different biochemical ratios, and may not be species' specific.

6.2. Currents and Water Masses

Variation in the calanoid copepod and chaetognath densities from month to month was vast, with the lowest densities being found during late summer, but there was a still a distinct differences between individual currents and water masses. The Florida Current had lower densities of both taxa than the Intermediate water and the Subsurface Counter Current. The higher densities of both taxa in the Subsurface Counter Current and the Intermediate water could have come from deep water populations being transported with the Florida Current or cross shelf flow from more coastal regions.

The presence of the Subsurface Counter Current in association with an onshore meander of the Florida Current is harder to explain, but it might be independent of the Florida Current. Water mass formation in the Caribbean and Gulf of Mexico and intrusions of Western North Atlantic water masses influence the water masses found in

the Straits of Florida. The temperature-salinity data used in this study gave a basic idea of the water masses found at the E-W transect. Using carbon stable isotopes, dissolved oxygen levels, nutrient levels, and potential density will provide additional information about the water masses present in the Straits of Florida. Greater plankton densities, found in waters with low $\delta^{13}C_{(sw)}$ levels in conjunction with high levels of nutrients (nitrate and phosphate), could indicate a plankton bloom due to upwelled, deep water. Measuring nitrate and ammonia levels will determine if production in the water masses is new production or regenerated production. Zooplankton sampling and isotopic analysis during each month, and multiple year sampling regimes will help to determine if the results from this study are anomalous and if the trends seen here dictate a seasonal pattern. Also, identification of calanoid copepod and chaetognath species will aid in determining whether they are deep water populations, upwelled during onshore flow, or if they are coastal populations being pulled from the coastal waters. Overall, the physical data in this project identified two distinct water masses off the coast of southeast Florida, Continental Edge Water and Yucatan Water. The vertical boundary of these two water masses is the western front of the Florida Current, with the Continental Edge Water occupying the continental margin and the Yucatan water occupying the insular margin of the Straits of Florida. The physical data also confirmed that the aperiodic flow reversal (Subsurface Counter Current) was not an extension of the Florida Current, but an independent southward flow. Zooplankton density information confirmed that the lowest densities are found in the Florida Current (Yucatan Water) and high densities are found in the coastal waters (Continental Edge Water), including the Subsurface Counter Current.

7. References

1. Ashjian, C.J. 1993. Trends in copepod species abundances across and along a Gulf Stream meander: evidence for entrainment and detrainment of fluid parcels from the Gulf Stream. Deep-Sea Research 40: 461-482.
2. Atkinson, L.P., T. Berger, P. Hamilton, E. Waddell, K. Leaman, and T.N. Lee. 1995. Current meter observations in the Old Bahama Channel. *Journal of Geophysical Research* 100: 8555-8560.
3. Albers, C.S., G. Kattner, and W. Hagen. 1996. The compositions of wax esters, triacylglycerols and phospholipids in Arctic and Antarctic copepods: evidence of energetic adaptations. *Marine Chemistry* 55: 347-358.
4. Alcaraz, M., E. Saiz, and A. Calbet. 1994. Small-scale turbulence and zooplankton metabolism: effects of turbulence on heartbeat rates of planktonic crustaceans. *Limnology and Oceanography* 36(6): 1465-1470.
5. Alvarino, A. 1994. "Chaetognatha". In Adiyodi, K.G., and R.G. Adiyodi (eds). *Reproductive Biology of Invertebrates*. Wiley. 456 pp.
6. Arrington, D.A., and K.O Winemiller. 2002. Preservation effects on stable isotope analysis of fish muscle. *Transactions of the American Fisheries Society* 131: 337-342.
7. Baier, C.T., and J.E. Purcell. 1997. Trophic interactions of chaetognaths, larval fish, and zooplankton in the South Atlantic Bight. *Marine Ecology Progress Series* 146: 43-53.

8. Bender, M.L. 1990. The $\delta^{18}O$ of dissolved O_2 in seawater: A unique tracer of circulation and respiration in the Deep Sea. *Journal of Geophysical Research* 95: 22243-22252.

9. Bostock et al. 2010. Bostock, H.C., B.N. Opdyke, M.J.M. Williams. 2010. Characterizing the intermediate depth waters of the Pacific Ocean using $\delta^{13}C$ and other geochemical tracers. *Deep Sea Research I* 57: 847-859.

10. Bsharah, L. 1957. Plankton of the Florida Current.V. Environmental conditions, standing crop, seasonal and diurnal changes at a station forty miles east of Miami. *Bulletin of Marine Science: Gulf and Caribbean*, 7(3): 201-249.

11. Bishop, S.S., J.A. Yoder, and G.-A. Paffenhofer. 1980. Phytoplankton and nutrient variability along a cross-shelf transect off Savannah, Georgia, U.S.A. *Estuarine Coastal Marine Science* 11: 359-368.

12. Bhat, K.L., and A.B. Wagh. 1992. Biochemical composition of zooplankton of Bombay High (oil platform) area in the Arabian Sea. *Indian Journal of Marine Science* 21: 220-223.

13. Bligh, E.G., and W.J. Dyer. 1959. A rapid method for total lipid extraction and purification. *Canadian Journal of Biochemistry and Physiology* 37: 911-917.

14. Bosley, K.L., and S.C. Wainright. 1999. Effects of preservatives and acidification on the stable isotope ratios (^{15}N:^{14}N, ^{13}C:^{12}C) of two species of marine animals. *Canadian Journal of Fisheries and Aquatic Sciences* 56: 2181-2185.

15. Bowman, T.E. 1979. The distribution of calanoid copepods off the southeastern United States between Cape Hatteras and southern Florida. *Smithsonian Contributions to Zoology* 96: 1-64.

16. Brooks, I.H. 1979. Fluctuations in the transport of the Florida Current at periods between tidal and two weeks. *Journal of Physical Oceanography* 9: 1048-1053.

17. Buskey, E.J., K.H. Dunton, and P.L. Parker. 1999. Variations in stable carbon isotope ratio of the copepod *Acartia tonsa* during the onset of the Texas Brown Tide. *Estuaries* 22: 995-1003.

18. Carabel, S., E. Godinez-Dominguez, P. Verisimo, L. Fernandez, and J. Freire. 2006. An assessment of sample processing methods for stable isotope analyses of marine food webs. *Journal of Experimental Marine Biology and Ecology* 336: 254-261.

19. Casanova, J.P. 1999. Chaetognatha. In: Boltovskoy, D. ed. *South Atlantic zooplankton.* Vol. 2. Backhuys, Leiden, The Netherlands, 1353-1374.

20. Chavez, F.P., and R.T. Barber. 1987. An estimate of new production in the equatorial Pacific. *Deep-Sea Research* 34(7): 1229-1243.

21. Choe, N., D. Deibel, R.J. Thompson, S.H. Lee, and V.K. Bushell. 2003. Seasonal variation in the biochemical composition of the chaetognath *Parasagitta elegans* from the hyperbenthic zone of Conception Bay, Newfoundland. *Marine Ecology Progress Series* 251: 191-200.

22. Colling, A. 2004. Ocean Circulation, 2nd Edition. The Open University, Milton Keynes, England. 286pp.

23. Cowles, T.J., R.J. Olson, and S.W. Chisholm. 1988. Food selection by copepods: discrimination of the basis of food quality. *Marine Biology* 100: 41-49.

24. Daly, K.L., and W.O. Smith, Jr. 1993. Physical-biological interactions influencing marine plankton production. *Annual Review Ecology Systematics* 24: 55-585.

25. DeNiro, M.J., and S. Epstein. 1978. Influence of diet on the distribution of carbon isotopes in animals. *Geochimica et Cosmochimica Acta* 42: 495-506.

26. DeNiro, M.J., and S. Epstein. 1981. Influence of diet on the distribution of nitrogen isotopes in animals. *Geochimica et Cosmochimica Acta* 45: 341-351.

27. DiMarco, S.F., W.D. Nowlin, Jr., and R.O. Reid. 2005. A statistical description of the velocity fields from upper ocean drifters in the Gulf of Mexico. Geophysical Monograph Series 161: 101-110.

28. Diel, S., and K. Tand. 1992. Does the spawning of *Calanus finmarchicus* in high latitudes follow a reproducible pattern? *Marine Biology* 113: 21-31.

29. Duiing, W., and D. Johnson. 1971. Southward flow under the Florida Current. *Science* 173: 428-430.

30. Duplessy, J-C, N.J. Shackelton, R.K. Matthews, W. Prell, W.F. Ruddiman, M. Caralp, and C.H. Hendy. 1984. ^{13}C record of benthic foraminifera in the last interglacial ocean: Implications for the carbon cycle and the global deep water circulation. *Quaternary Research* 21: 225-243.

31. Edwards, M.S., T.F. Turner, and Z.D. Sharp. 2002. Short- and long-term effects of fixation and preservation on stable isotope values ($\delta^{13}C$, $\delta^{15}N$, $\delta^{34}S$) of fluid-preserved museum specimens. *Copeia* 2002: 1106-1112.

32. Feuchtmayr, H., and J. Grey. 2003. Effect of preparation and preservation procedures on carbon and nitrogen stable isotope determinations from zooplankton. *Rapid Communications in Mass Spectrometry* 17: 2605-2610.

33. Folch, J., M. Lees, and G.H.Sloan Stanley. 1957. A simple method for the isolation and purification of total lipids from animal tissues. *Journal of Biological Chemistry* 226: 497-509.

34. Frost, B.W. 1987. Grazing control of phytoplankton stock in the open subarctic Pacific Ocean: a model assessing the role of mesozooplankton, particularly the large calanoid copepods *Neocalanus* spp. *Marine Ecology Progress Series* 39: 49-68.

35. Fry, B. 2006. *Stable Isotope Ecology*. Springer Science and Business Media, LLC. New York. 308 pp.

36. Fry, B., and C. Arnold. 1982. 13C/12C turnover during growth of brown shrimp (*Penaeus aztecus*). Oecologia 54: 200-204.

37. Fry, B., and R.B. Quinones. 1994. Biomass spectra and stable isotope indicators of trophic level in zooplankton of the northwest Atlantic. *Marine Ecology Progress Series* 112: 201-204.

38. Fuglister, F.C. 1946. Average monthly surface temperatures and the years maxima and minima of monthly surface temperatures for the area west of the 60th meridian. Complete report on the hydrography of the western Atlantic. Woods Hole Oceanographic Institution Technical Report 2: 1-4.

39. Haines, E.B., and W.M. Dunstan. 1975. The distribution and relation of particulate organic material and primary productivity in the Georgia Bight, 1973-1974. *Estuarine and Coastal Marine Science* 3: 431-441.

40. Heinrikh, A.K. 1962. The life histories of plankton animals and seasonal cycles of plankton communities in the oceans. *Journal du Conseil International pour l'Exploration de la Mer* 27: 15-24.

41. Helander, K.G. 1994. Kinetic studies of formaldehyde binding in tissue. Biotechnic and Histochemistry 66: 177-179.

42. Hirons, A.C., D.M. Schell, and B.P. Finney. 2001. Temporal records of $\delta^{13}C$ and $\delta^{15}N$ in North Pacific pinnipeds: inferences regarding environmental change and diet. *Oecologia* 129: 591-601.

43. Hobson, K.A., H.L. Gibbs, and M.L. Gloutney. 1997. Preservation of blood and tissue samples for stable-carbon and stable-nitrogen isotope analysis. *Canadian Journal of Zoology* 75: 1720-1723.

44. Hobson, K.A., and H.E. Welch. 1992. Determination of trophic relationships within a high Arctic marine food web using $\delta^{13}C$ and $\delta^{15}N$ analysis. *Marine Ecology Progress Series* 84: 9-18.

45. Hopkins, T.L., D.M. Milliken, L.M. Bell, E.J. McMichael, J.F. Heffernan, and R.V. Cano. 1981. The landward distribution of oceanic plankton and micronekton over the west Florida continental shelf related to their vertical distribution. *Journal of Plankton Research* 3(4): 645-633.

46. Humes, A.G. 1994. How many copepods? *Hydrobiologia* 292/293: 1-7.

47. Iles, T.D., and M. Sinclair. 1982. Atlantic herring: Stock discreteness and abundance. *Science* 215(4533): 627-633.

48. Johns, W.E., T.L. Townsend, D.M. Fratantoni, and W.D. Wilson. 2002. On the Atlantic inflow to the Caribbean Sea. *Deep-Sea Research* 49: 211-243.

49. Johnson, W.S., and D.M. Allen. 2005. *Zooplankton of the Atlantic and Gulf Coasts: A Guide to Their Identification and Ecology.* The Johns Hopkins University Press, 379 pp.

50. Kaehler, S., and E.A. Pakhomov. 2001. Effects of storage and preservation on the $\delta^{13}C$ and $\delta^{15}N$ signatures of selected marine organisms. *Marine Ecology Progress Series* 219: 299-304.

51. Kattner G, Hagen W, Lee RF, Campbell R, Deibel D, Falk-Petersen S, Graeve M, Hansen BW, Hirche HJ, Jonasdottir SH, Madsen ML, Mayzaud P, Muller-Navarra D, Nichols PD, Paffenhofer GA, Pond D, Saito H, Stubing D, Virtue P. 2007. Perspectives on marine zooplankton lipids. *Canadian Journal of Fisheries and Aquatic Science* 64:1628-1639.

52. Kelly, B., J.B. Dempson, and M. Power. 2006. The effects of preservation on fish tissue stable isotope signatures. *Journal of Fish Biology* 69: 1595-1611.

53. Kiernan, J.A. 2000. Formaldehyde, formalin, paraformaldehyde and glutaraldehyde: what they are and what they do. *Microscopy Today* 1: 8-12.

54. Kroopnick, P. 1985. The distribution of carbon-13 in the world oceans, *Deep-Sea Research* 32: 57–84.

55. Laws, E.A., G.R. DiTullio, and D.G. Redalje. 1987. High phytoplankton growth and production rates in the North Pacific Subtropical gyre. *Limnology and Oceanography* 32: 905-918.

56. Leaman, K.D., E. Johns, and T. Rossby. 1989. The average distribution of volume transport and potential vorticity with temperature at three sections across the Gulf Stream. *Journal of Physical Oceanography* 19: 36-51.

57. Leaman, K.D., R.L. Molinari, and P.S. Vertes. 1987. Structure and variability of the Florida Current at 27°N: April 1982-July 1984. *Journal of Physical Oceanography* 17: 565-583.

58. Leaman, K.D., P.S. Vertes, L.P. Atkinson, T.N. Lee, P. Hamilton, and E. Waddell. 1995. Transport, potential vorticity, and current/temperature structure across Northwest Providence and Santaren Channels and the Florida Current off Cay Sal Bank. *Journal of Geophysical Research* 100: 8561-8569.

59. Lee, R.F., and J. Hirota. 1973. Wax esters in tropical zooplankton and nekton and the geographical distribution of wax esters in marine copepods. *Limnology and Oceanography* 18: 227-239.

60. Lee, T.N., L.P. Atkinson, and R. Legeckis. 1981. Observations of a Gulf Stream frontal eddy on the Georgia continental shelf, April 1977. *Deep-Sea Research* 28A: 347-378.

61. Lee, T.N., K. Leaman, and E. Williams. 1995. Florida Current meanders and gyre formation in the southern Straits of Florida. *Journal of Geophysical Research*. 100(C5): 8607-8620.

62. Lee, T.N., F.A. Schott, and R. Zantopp. 1985. Florida Current: low-frequency variability as observed with moored current meters during April 1982 to June 1983. *Science* 227: 298-302.

63. Legendre, L., and S. Demers. 1984. Towards dynamic biological oceanography and limnology. *Canadian Journal of Fisheries and Aquatic Sciences* 41: 2-19.

64. Li, W.K.W. 2002. Macroecological patterns of phytoplankton in the northwestern North Atlantic Ocean. *Nature*. 419: 154-157.

65. Longhurst, A. 1995. Seasonal cycles of pelagic production and consumption. *Progress in Oceanography* 36: 77-167.

66. Lonsdale, D.J., E.M. Cosper, W.-S. Kim, M. Doall, A. Divadeenam, and S.H. Jonasdottir. 1996. Food web interactions in the plankton of Long Island bays, with preliminary observations on brown tide effects. Marine Ecology Progress Series 134: 247-263.

67. Lynch-Stieglitz, J. and R.G. Fairbanks, 1994. A conservative tracer for glacial ocean circulation from carbon isotope and palaeo-nutrient measurements in benthic foraminifera. *Letters to Nature* 369: 308- 310.

68. Mann, K.H., and J.R.N. Lazier. 2005. *Dynamics of Marine Ecosystems: Biological-Physical Interactions in the Oceans.* Blackwell Publishing. 496 p.

69. Mauchline, J. 1998. The Biology of calanoid copepods. In *Advances in Marine Biology*. Vol. 33, pp 1-710, J.H.S. Blaxter, A.J. Southward, P.A. Tyler, eds. Academic Press.

70. McConnaughey, T., and C.P. McRoy. 1979. Food-web structure and the fractionation of carbon isotopes in the Bering Sea. *Marine Biology* 53: 257-262.

71. Michener, R.H., and L.S. Kaufman. (2007). Stable isotope ratios as tracers in marine food webs: an update. In: K. Lajtha and R.H. Michener (eds.). *Stable Isotopes in Ecology and Environmental Science*. Blackwell Scientific, Boston. 316pp.

72. Minagawa, M., and E. Wada. 1984. Stepwise enrichment of ^{15}N along food chains: further evidence and the relation between $\delta^{15}N$ and animal age. *Geochimica et Cosmochimica Acta* 48: 1135-1140.

73. Molinari, R.L., W.D. Wilson, and K. Leaman. 1985. Volume and heat transports of the Florida Current: April 1982 through August 1983. *Science* 227: 295-297.

74. Mullin, M.M., G.H. Rau, and R.W. Eppley. 1984. Stable nitrogen isotopes in zooplankton: some geographic and temporal variations in the North Pacific. *Limnology and Oceanography* 29: 1267-1273.

75. Niebauer, H.J., and W.O. Smith, Jr. 1989. A numerical model of mesoscale physical-biological interactions in the Fram Strait Marginal Ice Zone. *Journal of Geophysical Research* 94(C11): 16151-16175.

76. Omori, M., and W.M. Hammer. 1982. Patchy distribution of zooplankton: behavior, population assessment and sampling problems. *Marine Biology* 72: 193-200.

77. Parr 1938. Parr, A.E. 1938. Further observations on the hydrography of the Eastern Caribbean and adjacent Atlantic waters. *Bulletin of the Bingham Oceanographic Collection* 6(4): 1-29.

78. Pasciak, W.J., and J. Gavis. 1974. Transport limitation of nutrient uptake in phytoplankton. *Limnology and Oceanography*. 19(6): 881-888.

79. Pasciak, W.J., and J. Gavis. 1975. Transport limitation of nutrient uptake rates in *Ditylum brightwellii*. *Limnology and Oceanography* 20(4): 604-607.

80. Perry, R.I., P.A. Thompson, D.L. Mackas, P.J. Harrison, and D.R. Yelland. 1999. Stable carbon isotopes as pelagic food web tracers in adjacent shelf and slope regions off British Columbia, Canada. *Canadian Journal of Fisheries and Aquatic Sciences* 56: 2477-2486.

81. Phleger 1951. Pheleger, F.B., and F.L. Parker. 1951. Ecology of the foraminimfer in the northwest Gulf of Mexico. *Geological Society of America, Memoirs,* 46:1-88.

82. Piontkovski, S.A., T.D. O'Brien, S.F. Umani, E.G. Krupa, T.S. Stuge, K.S. Balymbetov, O.V. Grishaeva, and A.G. Kasymov. 2006. Zooplankton and the North Atlantic Oscillation: a basin-scale analysis. *Journal of Plankton Research* 28(11): 1039-1046.

83. Platt, T., W.G. Harrison, M.R. Lewis, W.K.W. Li, S. Scethyendranath, R.E. Smith, and A.F. Vezina. 1989. Biological production of the oceans: the case for a consensus. *Marine Ecology Progress Series* 52: 77-88.

84. Pomeroy, L.R. 1974. The ocean's food web, a changing paradigm. *BioScience* 24(9): 499-504.

85. Ponsard, S., and M. Amlou. 1999. Effects of several preservation methods on the isotopic content of *Drosophila* samples. *C.R. Academy of Sciences Paris, Life Sciences* 322: 35-41.

86. Rau, G.H., A.J. Mearns, D.R. Young, R.J. Olson, H.A. Schafer, and I.R. Kaplan. 1983. Animal $^{13}C/^{12}C$ correlates with trophic level in pelagic food webs. *Ecology* 64: 1314-1318.

87. Rau, G.H., R.E. Sweeney, and I.R. Kaplan. 1982. Plankton C-13/C-12 ratio changes with latitude: differences between northern and southern oceans. *Deep-Sea Research* 29(8A): 1035-1039.

88. Ryther, J.H. 1969. Photosynthesis and fish production in the sea. *Science* 166(3901): 72-76.

89. Sarakinos, H.C., M.L. Johnson, and M.J. Vander Zanden. 2002. A synthesis of tissue-preservation effects on carbon and nitrogen stable isotope signatures. *Canadian Journal of Zoology* 80: 381-387.

90. Sargent, J.R., R.R. Gatten, and R.J. Henderson. 1981. Marine wax esters. *Pure and Applied Chemistry* 53: 867-871.

91. Savidge, G. 1981. Studies of the effects of small-scale turbulence on phytoplankton. *Journal of Marine Biological Association* 61: 477-488.

92. Schaefer, M.B. 1965. The potential harvest of the sea. *Transactions of the American Fisheries Society* 94(2): 123-128.

93. Schell, D.M., B.A. Barnett, and K.A. Vinette. 1998. Carbon and nitrogen isotope ratios in zooplankton of the Bering, Chukchi and Beaufort Seas. *Marine Ecology Progress Series* 126: 11-23.

94. Schmitz, W.J. Jr., and W.S. Richardson. 1968. On the transport of the Florida Current. *Deep-Sea Research* 15: 679-693.

95. Schmitz, W.J., Jr., and P.L. Richardson. 1991. On the sources of the Florida Current. *Deep Sea Research* 38: S389-S409.

96. Schmitz, W.J. Jr., and M.S. McCartney. 1993. On the North Atlantic Circulation. *Reviews of Geophysics* 31(1): 29-49.

97. Schmitz, W.J. Jr., J.R. Luyten, and R.W. Schmitt. 1993. On the Florida Current T/S envelope. *Bulletin of Marine Science* 53: 1048-1065.

98. Schott, F., and R. Zantopp. 1985. Florida Current: Seasonal and interannual variability. *Science* 227: 308-311.

99. Schott, F.A., T.N. Lee, and R. Zantopp. 1988. Variability of structure and transport of the Florida Current in the period range of days to seasonal. *Journal of Physical Oceanography* 18: 1209-1230.

100. Sheinbaum, J., J. Candela, A. Badan, and J. Ochoa. 2002. Flow structure and transport in the Yucatan Channel. *Geophysical Research Letters* 29(3): 1040-1043.

101. Sholto-Douglas, A.D., J.G. Field, A.G. James, and N.J. van der Merwe. 1991. $^{13}C/^{12}C$ and $^{15}N/^{14}N$ isotope ratios in the Southern Benguela Ecosystem: indicators of food web relationships among different size-classes of plankton and pelagic fish; differences between fish muscle and bone collagen tissues. *Marine Ecology Progress Series* 78: 23-31.

102. Silva et al., 2009. Silva, N., N. Rojas, and A. Fedele. 2009. Water masses in the Humbolt Current System: Properties, distribution, and the nitrate deficit as a chemical water mass tracer for Equatorial Subsurface Water off Chile. *Deep-Sea Research II* 56: 1004-1020.

103. Steele, J.H. 1989. The ocean 'landscape'. *Landscape Ecology* 3: 185-192.

104. Stepien, J.C. 1980. The occurrence of chaetognaths, pteropods and euphausiids in relation to deep flow reversals in the Straits of Florida. *Deep-Sea Research* 27A: 987-1011.

105. Stommel, H. 1966. *The Gulf Stream: A Physical and Dynamical Description*. 2nd Edition. University of California Press, Berkley, CA. 248 p.

106. Sverdrup, H.V., M.W. Johnson, and R.H. Fleming. 1946. *The Oceans*. Prentice-Hall, Inc., N.Y. 1087 pp.

107. Sweeting, C.J., N.V.C. Polunin, and S. Jennings. 2004. Tissue and fixative dependent shifts of $\delta^{15}N$ and $\delta^{15}N$ in preserved ecological material. *Rapid Communications in Mass Spectrometry* 18: 2597-2592.

108. Syvaranta, J., S. Vesala, M. Rask, J. Ruuhijarvi, and R.I. Jones. 2008. Evaluating the utility of stable isotope analyses of archived freshwater sample materials. *Hydrobiologia* 600: 121-130.

109. Thomas, W.H., and C.H. Gibson. 1990. Effects of small-scale turbulence on microalgae. *Journal of Applied Phycology* 2: 71-77.

110. Thomas, W.H., and C.H. Gibson. 1992. Effects of quantified small-scale turbulence on the dinoflagellate, *Gymnodimium sanguineum (splendens)*: contrast with *Gonyaulax (Lingulodinium) polyedra* and fishery implications. *Deep-Sea Research* 39: 1429-37.

111. Tieszen, L.L., T.W. Boutton, K.G. Tesdahl, and N.A. Slade. 1983. Fractionation and turnover of stable carbon isotopes in animal tissues: implications for δ13C analysis of diet. *Oecologia* 57(1/2): 32-37.

112. Turner, R.E., S.W. Woo, and H.R. Jitts. 1979a. Estuarine influences on a continental shelf plankton community. *Science* 206: 218-220.

113. Turner, R.E., S.W. Woo, and H.R. Jitts. 1979b. Phytoplankton production in a turbid, temperate salt marsh estuary. *Estuarine and Coastal Marine Science* 9: 603-613.

114. Wang, J., and C.N.K. Mooers. 1997. Three-dimensional perspectives of the Florida Current: transport, potential vorticity, and related dynamical properties. *Dynamics of Atmospheres and Oceans* 27: 135-149.

115. Wennekens, M.P. 1959. Water mass properties of the Straits of Florida and related waters. *Bulletin of Marine Science of the Gulf and Caribbean* 9(1): 1-52.

116. Vander Zanden, M.J., and J.B. Rasmussen. 2001. Variation in $\delta^{15}N$ and $\delta^{13}C$ trophic fractionation: implications for aquatic food web studies. *Limnology and Oceanography* 46: 2061-2066.

117. Vander Zanden, M.J., J.M. Casselman, and J.B. Rasmussen. 1999. Stable isotope evidence for the food web consequences of species invasions in lakes. *Nature* 401: 464-467.

118. Vander Zanden, J.M., S. Chandra, B.C. Allen, J.E. Reuter, and C.R. Goldman. 2003. Historical food web structure and restoration of native aquatic communities in the Lake Tahoe (California-Nevada) Basin. *Ecosystems* 6: 274-288.

119. Yoder, J.A., L.P. Atkinson, T.N. Lee, H.H. Kim, and C.R. McClain. 1981. Role of Gulf Stream frontal eddies in forming phytoplankton patches on the outer southeastern shelf. *Limnology and Oceanography* 26(6): 1103-1110.

120. Zantopp, R.J., K.D. Leaman, and T.N. Lee. 1987. Florida Current meanders: A close look in June-July 1984. *Journal of Physical Oceanography* 17: 584-595.